



Flood Hydroclimatology in the Upper Mississippi and Missouri River Basins

Final Draft

J. Rolf Olsen
Eugene Z. Stakhiv

**Planning and Policy Studies Division
Institute for Water Resources
U.S. Army Corps of Engineers
Alexandria, VA**



January 2000

Flood Hydroclimatology in the Upper Mississippi and Missouri River Basins

Final Draft

J. Rolf Olsen
Eugene Z. Stakhiv

**Planning and Policy Studies Division
Institute for Water Resources
U.S. Army Corps of Engineers
Alexandria, VA**

January 2000

Acknowledgements

We thank Dr. Nicholas Matalas and Prof. Jery Stedinger of Cornell University for their exceptionally valuable contributions, advice, and comments on our study, and their detailed review of this report. The support of Dr. S. K. Nanda made this research possible. We appreciate the contribution of the staff of the Institute for Water Resources who assisted in this study: Dr. Philip Chao, William Werick, and Dr. David Moser. We also thank Dr. Dave Goldman of the Hydrologic Engineering Center for his review and comments.

Table of Contents

Acknowledgements	i
Table of Contents	iii
List of Figures	v
List of Tables	ix
Executive Summary	xi
1 Introduction	1
1.1 Characteristics of Major Floods in Large Basins	2
1.2 Mississippi and Missouri Basin Characteristics	5
1.3 References	8
2 Climatic Influences on Floods	11
2.1 Precipitation Patterns	11
2.2 Streamflow Seasonality	13
2.2.1 Snowmelt Floods	14
2.2.2 Rainfall Floods	15
2.3 Flood Records and Dates	15
2.4 Hydrometeorological Causes of Extreme Floods	19
2.4.1 1993 Flood	19
2.4.2 1952 Flood	22
2.4.3 1965 Flood	22
2.4.4 1973 Flood	22
2.4.5 1951 Flood	23
2.5 Analysis of Rainfall and Snowmelt Floods	24
2.6 Summary	29
2.7 References	30
3 Climate Variability and Mississippi and Missouri Floods	33
3.1 Introduction	33
3.2 El Niño/Southern Oscillation (ENSO)	33
3.3 Studies of ENSO and Midwestern Hydroclimatology	35
3.3.1 Precipitation	36
3.3.2 Streamflow	39
3.3.3 Floods	44
3.4 Pacific Ocean Climate Patterns	46
3.4.1 North Pacific Patterns	46
3.4.2 Other Pacific Ocean Patterns	48
3.4.3 Spring Climate Patterns	49
3.5 North Atlantic Oscillation	50
3.6 Relationship between Climate Patterns and Mississippi River Flow	51
3.7 Climate Patterns and Mississippi and Missouri Floods	54
3.8 Summary	56
3.9 References	57

4	Climate Change and Upper Mississippi and Missouri Basin Flooding	59
4.1	Mechanisms of Anthropogenic Climate Change	59
4.2	Climate Modeling and Prediction	61
4.3	General Circulation Models and Regional Hydrologic Models.....	61
4.4	GCMs Used in Climate Simulations.....	62
4.5	Missouri River Basin	64
4.6	Changes in Climate Patterns	66
4.7	Summary	67
4.8	References.....	73
5	Climate Trends.....	77
5.1	Temperature	77
5.2	Precipitation	77
5.3	Snow Cover and Depth	79
5.4	Precipitation Extremes	79
5.5	Streamflow	81
5.6	Streamflow Extremes.....	82
5.7	Summary	83
5.8	References.....	85
6	Trends in Mississippi and Missouri River Floods	87
6.1	Trend Analysis of Mississippi and Missouri River Floods.....	87
6.2	Other Results Reporting Trends.....	98
6.3	Present-to-Past and Past-to-Present Trend Analysis for Basins.....	102
6.4	Possible Causes of Trends	108
6.4.1	Trends in Precipitation.....	108
6.5	Summary	111
6.6	References.....	113
7	Climate Variability and Flood Frequency Analysis	115
7.1	Need for Flood Frequency Analysis.....	115
7.2	Climate Variability, Non-Stationarity, and Temporal Dependence.....	118
7.3	Trends and Possible Future Flood Risk	120
7.4	References.....	126
8	Conclusions.....	129
	Appendix A: Data Sources.....	133
	Appendix B: Abbreviations and Acronyms	135
	Appendix C: Nonparametric Trend Analysis at Selected Sites	137
	Appendix D: Assessment of Trend.....	139
	Appendix E: Climate Figures.....	165

List of Figures

Figure 1.2: Streamflow gages and locations used in the Upper Mississippi, Lower Missouri and Illinois Flow Frequency Study.	4
Figure 1.3: Spatial and temporal scales of selected atmospheric and hydrologic conditions related to flooding (Hirschboeck, 1988).	5
Figure 1.4: Size of drainage area at each gage site for the Missouri River.	7
Figure 1.5: Size of drainage area at each gage site for the Mississippi River.	7
Figure 1.6: Relative size of flood peaks during three major floods (using unregulated flow data).	8
Figure 1.8: Average annual flood for each gage on the Mississippi River (using unregulated flow data).	9
Figure 1.9: Change in average annual flood per change in drainage area for gages on the Missouri River and two gages on the Mississippi River (using unregulated flow data)...	10
Figure 1.10: Change in average annual flood per change in drainage area for gages on the Mississippi River (using unregulated flow data).	10
Figure 2.1: Major meteorological influences on the weather and climate of the Upper Mississippi and Lower Missouri basin (Rodenhuis, 1996).	12
Figure 2.2: Monthly distribution of annual peak floods for five gage sites on the Mississippi River (1900 to 1996).	16
Figure 2.3: Monthly distribution of annual peak floods for four gage sites on the Missouri River and for St. Louis on the Mississippi River (1930 to 1996).	18
Figure 2.4: Weather patterns that led to the 1993 Mississippi floods (Wahl <i>et al.</i> , 1993)	21
Figure 2.5: The peak flow at sites along the Mississippi River for five large flood events. The 1965 and 1969 are snowmelt floods while the other floods were caused by rainfall.	24
Figure 2.6: Mean annual snowfall in inches, Upper Mississippi River Basin, 1931-1952 (UMRCBS, 1972).	25
Figure 2.7: Normal annual precipitation, inches, Upper Mississippi River Basin, 1931-1960 (UMRCBS, 1972).	25
Figure 2.8: The hydrograph for the Mississippi River at Keokuk for water year 1965. ..	26
Figure 2.9: The hydrograph for the Mississippi River at Keokuk for water year 1993. ..	26
Figure 2.10: The hydrograph for the Mississippi River at St. Louis for water year 1965.	27
Figure 2.11: The hydrograph for the Mississippi River at St. Louis for water year 1993.	27
Figure 2.12: A plot of the largest flows for three different periods in a water year sorted by size.	28

Figure 2.13: A plot of the March-April flood versus the May-September flood for each water year.	29
Figure 3.1: 12-month moving averages of the Southern Oscillation Index (SOI) and an index of tropical Pacific sea surface temperature anomalies from the Japan Meteorological Agency. Large negative SOI and positive SST indices indicate El Niño events.	34
Figure 3.2: An example of a plot of a first harmonic and a harmonic dial.	38
Figure 3.3: The phase and magnitude of precipitation vectors of the 24-month aggregate composite of ENSO events are plotted as a harmonic dial with the direction indicating the phase and the length the magnitude.	38
Figure 3.4: The phase and magnitude of the 24-month aggregate composite of ENSO events are plotted as a harmonic dial with the direction indicating the phase and the length the magnitude.	41
Figure 3.5: (a) An ENSO aggregate composite for the North Central region of the United States.	42
Figure 3.6: (a) A La Niña aggregate composite for the North Central region of the United States.	43
Figure 3.7: Annual floods (1950-1996) for the Mississippi River at St. Louis and tropical Pacific sea surface temperature anomalies.	44
Figure 3.8: Annual floods (1868-1996) for the Mississippi River at St. Louis and tropical Pacific sea surface temperature anomalies.	45
Figure 3.9: El Niño floods and other floods plotted with the Log-Pearson III distribution fitted to the peak annual floods for the Mississippi River at Hannibal, Missouri.	46
Figure 3.10: The annual average Pacific Decadal Oscillation from 1900 to 1998 (International Pacific Halibut Commission, University of Washington).	48
Figure 3.11: The average annual winter North Atlantic Oscillation Index from 1864 to 1995 (Climate Research Unit, University of East Anglia).	51
Figure 3.12: Annual average flow for each water year from 1874 to 1996 of the Mississippi River at Clinton, Iowa. LOESS is a technique to smooth the data (Baldwin and Lall, 1998).	53
Figure 3.13: The superposition of the interannual (3.1-3.6 year) period and the interdecadal (8.3-12.5 year) period for Mississippi River flow at Clinton, Iowa (Baldwin and Lall, 1998).	53
Figure 3.14: Superposition of the decadal (0.1 cycle per year) and interannual (0.28 cpy) frequencies for the Mississippi River at Clinton, Iowa and an index of ENSO (NIN) times North Atlantic Oscillation. The dotted lines highlight the 1988 low flow and the 1993 flood (Baldwin and Lall, 1998).	54
Figure 4.1: Average temperature changes in degrees Celsius for the Missouri Basin for four GCMs.	68

Figure 4.2: Average percentage change in precipitation for the Missouri Basin for four GCMs.....	68
Figure 4.3: Average percentage change in potential evapotranspiration for the Missouri Basin for four GCMs.	69
Figure 4.5: Observed versus simulated flows for the Missouri River at Omaha, Nebraska, and Hermann, Missouri (Lettenmaier <i>et al.</i> , 1996).....	70
Figure 4.6: Change in average monthly streamflow for the Missouri River at Omaha as projected by four GCMs (Decade 3 for transient GCMs).....	71
Figure 4.7: Change in average monthly streamflow for the Missouri River at Herman as projected by four GCMs (Decade 3 for transient GCMs).....	72
Figure 5.1: Trend in temperature from 1900 to 1994 in degrees C per century (Karl <i>et al.</i> , 1996).	78
Figure 5.2: Trend in precipitation from 1900 to 1994 in % change per century (Karl <i>et al.</i> , 1996).	78
Figure 5.3: Number of stream gages, out of a total of 395, with statistically significant ($p < 0.05$) trends for the 50-year period 1944-1993 (Lins and Slack, 1999).	84
Figure 5.4: Trends in the annual maximum flow for various regions of the United States (Lins and Slack, 1999).	84
Figure 6.1: Annual floods for the Mississippi River at Clinton.....	92
Figure 6.2: Annual floods for the Missouri River at Nebraska City.....	92
Figure 6.3: Annual floods for the Missouri River at Hermann and trendline.....	93
Figure 6.4: Annual floods for the Mississippi River at Hannibal and trendline.	93
Figure 6.5: Annual floods for the Illinois River at Meredosia.....	94
Figure 6.6: Annual floods for the Mississippi River at St. Louis and trendline.	94
Figure 6.7: Comparison of the U.S. Geological Survey and U.S. Army Corps of Engineers flood records for St. Louis	99
Figure 6.8: The average monthly precipitation for March and April for five stations in the Iowa River basin.	110
Figure 6.9: The average monthly precipitation for May and June for five stations in the Iowa River basin.	111
Figure 6.10: The average monthly precipitation for March and April for five stations in the Des Moines River basin.	112
Figure 6.11: The average monthly precipitation for May and June for five stations in the Des Moines River basin.	113
Figure 7.1: Different distributions for flood risk at St. Louis obtained by using the entire 1861-1996 record, and by correcting for trend and then estimating the specific	

distribution of floods for the years 1923, 2000, and 2050. The dotted vertical line corresponds to the 1 percent chance risk level..... 123

Figure 7.2:A graph showing a log Pearson III (corrected for low outliers) for the Mississippi River at St. Louis using the full period of record, the first half of the record, and the second half of the record. 124

List of Tables

Table 2.1: Monthly distribution of the five largest annual peak floods for five gage sites on the Mississippi River (1900 to 1996).....	17
Table 2.2: Monthly distribution of the five largest annual peak floods for four gage sites on the Missouri River and for St. Louis on the Mississippi River (1930 to 1996).....	18
Table 2.3: The two largest floods of record for ten locations along the Missouri and Mississippi Rivers (observed peak flow).....	19
Table 3.1: Definitions of El Niño years used by various researchers.....	36
Table 3.2: Terms with the most significance in multiple regression using 97-year (1900-1996) record.	55
Table 3.3: Terms with the most significance in multiple regression using 47-year (1950-1996) record.	56
Table 4.1: Summary of the coupled ocean-atmosphere GCMs used in IPCC transient climate change experiments (Lettenmaier, <i>et al.</i> , 1998)	63
Table 5.1: Changes in annual maximum precipitation for various durations at 304 Midwestern stations (significance level = 95%) (Angel and Huff, 1997).	80
Table 6.1: Linear Trend Analyses for Upper Mississippi Basin Gages	91
Table 6.2: Mississippi River (USACE Records)	95
Table 6.3: Missouri River (USACE Records). Drainage areas below Gavins Point Dam are in parenthesis.....	96
Table 6.4: Upper Mississippi River below Confluence w/ Missouri (USACE Records)	96
Table 6.5: Missouri River Tributaries (USGS Gage Records).....	97
Table 6.6: Mississippi River Tributaries (USGS Gage Records)	97
Table 6.7: Variations in Flood Potential with Time reported by Knox (1983).....	98
Table 6.8: Statistical significance of trends in annual flood for several tributaries of the Mississippi River (Goldman, 1999).....	100
Table 6.9: Correlation and significance level for trend in average monthly flows for four stations in Iowa.	102
Table 6.10: Past-to-present and present-to-past trend analysis for Hermann.....	104
Table 6.11: Past-to-present and present-to-past trend analysis for Keokuk.....	105
Table 6.12: Past-to-present and present-to-past trend analysis for Hannibal	106
Table 6.13: Past-to-present and present-to-past trend analysis for St. Louis	107
Table 6.14: Precipitation trend analysis for Keosauqua, Iowa.....	109

Table 6.15: Trends in average monthly precipitation of five precipitation gages in the Iowa River basin (1895-1994).	110
Table 6.16: Trends in average monthly precipitation of five precipitation gages in the Des Moines River basin (1895-1994).	111
Table 7.1: Estimates of 10%, 1%, and 0.2% chance exceedance flood at St. Louis. [Based upon a LP3 fit to the record using log-space moments. No low-outlier correction was made. At-site skew employed.].....	123
Table 7.2: The percentage difference between the 10%, 1%, and 0.2% chance exceedance flood for the entire period of record and quantiles corrected for trend and estimated for the years 1923, 2000, and 2050.....	124
Table 7.3: Estimates of 10%, 1%, and 0.2% chance exceedance flood at St. Louis using a LP3 (corrected for low outliers) using the full period of record, the first half of the record, and the second half of the record.	125
Table 7.4: The percentage difference between the estimates of the 10%, 1%, and 0.2% chance exceedance flood using the first and second half of the record and the estimate using the full period of record.....	125

Executive Summary

This inquiry supports the Upper Mississippi River System Flow Frequency Study and considers how climate variability and climate change may affect the probability of large floods. The study area includes the Mississippi River upstream of the confluence with the Ohio River and the Missouri River downstream of Gavins Point Dam.

Objective 1

Study the relationship between global-scale climate patterns and hydrologic variability for the Upper Mississippi and Missouri Rivers.

Finding

A simple regression analysis reported here found that climate indices such as the El Niño/Southern Oscillation (ENSO), the Pacific Decadal Oscillation (PDO), and the North Atlantic Oscillation (NAO) explain only a small percentage of the variability in the annual maximum floods.

Conclusion

As long as the future intensity and frequency of El Niño events over time resemble the historical value, flood frequency analysis can account for the climate variability associated with these events. However, there is some speculation that ENSO events may become more frequent and intense as a result of global warming.

Objective 2

Study how climate change associated with global warming may affect future flooding on the Upper Mississippi and Missouri Rivers.

Finding

The results of General Circulation Models used to project future climate are mixed and at this time there is little evidence that flood frequencies will increase as a result of global warming.

Objective 3

Study whether there are contemporary climate trends that are affecting floods on the Upper Mississippi River and Missouri River.

Findings

The literature reports evidence of historical trends of increasing temperatures and precipitation in the Upper Midwest since 1900. Analysis of unimpaired flow data constructed by the U.S. Army Corps of Engineers found statistically significant upward trends in many gage records along the Upper Mississippi and Missouri Rivers. The most likely cause of the trends is natural climate variability.

Conclusions

Trends in the Upper Mississippi basin challenge the traditional assumption that flood series are independent and identically distributed random variables and suggest that flood risk may be changing over time. As a result, it is not clear how to accommodate this shift within traditional flood frequency analysis. In the absence of viable alternatives, the use of traditional Bulletin 17B procedures are warranted until better methods are developed. Research is needed on how to incorporate interdecadal variation in flood risk into flood frequency analysis so that state and federal water agencies can move to adopt procedures that appropriately reflect such variations.

Flood Hydroclimatology in the Upper Mississippi and Missouri Rivers Basin

1 Introduction

Large floods are caused by many interacting factors and particularly unusual combinations of meteorological and hydrological factors. This inquiry will examine some of the underlying climatic factors that have contributed to large floods in the Upper Mississippi and Lower Missouri basin (Figure 1.1). It will also examine how climate variability and climate change may affect extreme flooding events in this basin, and what the implications are for traditional Corps analytical methods and design criteria.

This inquiry is intended to support the objectives of the **Upper Mississippi River System Flow Frequency Study**. This study was designed to improve stage and discharge frequency relationships for the Upper Mississippi, Lower Missouri, and Illinois Rivers. The study area includes the Mississippi River upstream of the confluence with the Ohio River and the Missouri River downstream of Gavins Point Dam. The drainage area above Gavins Point Dam is highly regulated by six major reservoirs and is not included in the study. The streamflow gages used in the project are shown in Figure 1.2.

This report is organized as follows. Chapter 2 will discuss precipitation patterns for the region. The floods of record for the northern part of the basin have been snowmelt floods, while the record floods downstream have been caused by persistent and intense precipitation. The major floods will be analyzed. Chapter 3 will look at global climate patterns and discuss what link if any they have with floods on the Mississippi and Missouri Rivers. Chapter 4 discusses models of future climate and the implications for determining future flood frequencies in the region. Chapter 5 is a review of climate

trends in the region, including temperature, precipitation, snow cover, and streamflow. Chapter 6 examines trends in floods on the Upper Mississippi, Illinois, and Lower Missouri Rivers. The final section discusses the implications of climate variability and change on flood frequency analysis for the Upper Mississippi and Lower Missouri Rivers.

1.1 Characteristics of Major Floods in Large Basins

Figure 1.3 shows the spatial and temporal scale of various types of flooding from small downpours that fill a drainage ditch to large-scale circulation anomalies on a global scale (Hirschboeck, 1988). The temporal domain is related to the length of time that a flood-producing atmospheric phenomenon is positioned over a basin or the period of time that a series of flood-producing events affects a basin. The upper spatial limit in Figure 1.3 is about 10^6 km^2 and corresponds to the area of the Mississippi River basin. The duration of flooding usually exceeds the duration of the atmospheric input, as shown by the shift toward a longer duration for flooding events.

Floods on very large basins like the Upper Mississippi and Missouri Rivers are caused by larger scale and longer duration atmospheric phenomena. Hirschboeck (1988) discusses several types of these events. Floods resulting from the seasonal accumulation and subsequent melting of snow can occur in any size basin including basins as large as the Mississippi River. Another type of larger scale hydroclimatic activity that can lead to flooding are anomalous circulation patterns such as the ones that produced flooding in the Mississippi basin in 1973 and 1993. Sea surface temperature anomalies such as El Niño/Southern Oscillation (ENSO) and long-period oceanic oscillations are types of global scale hydroclimatic perturbations that seem to cause hydrologic variability including wet periods and dry periods.

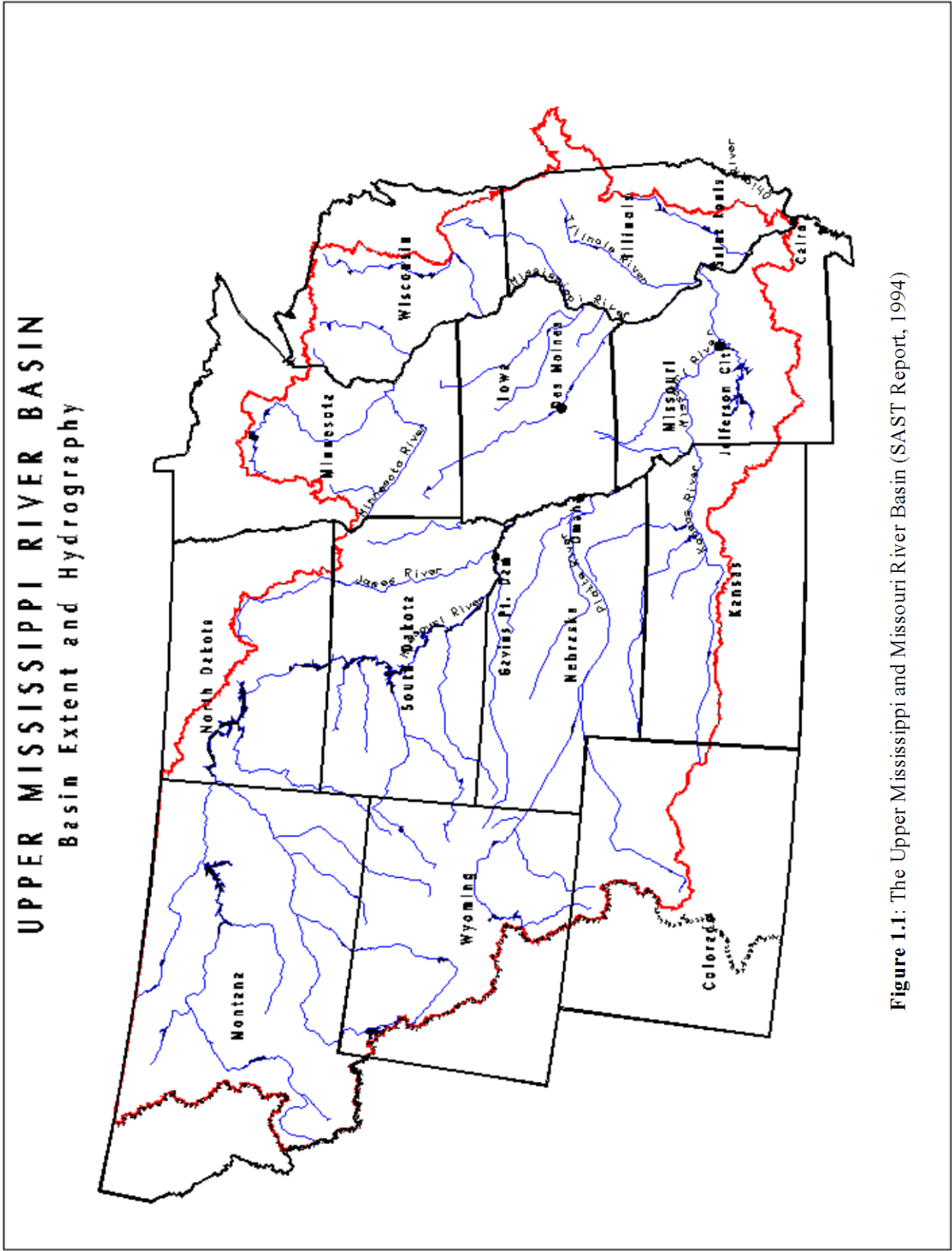


Figure 1.1: The Upper Mississippi and Missouri River Basin (SAST Report, 1994)

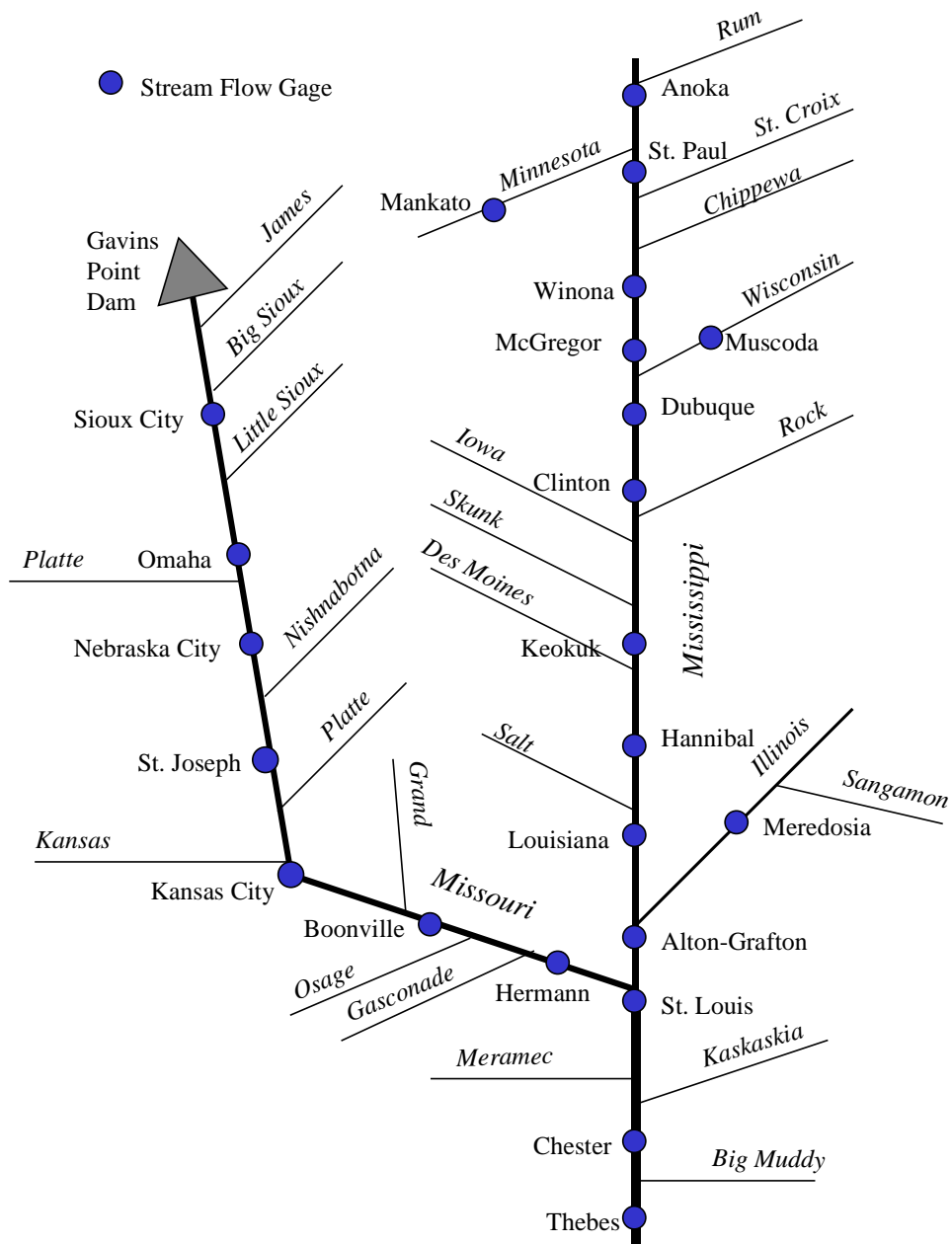


Figure 1.2: Streamflow gages and locations used in the Upper Mississippi, Lower Missouri and Illinois Flow Frequency Study.

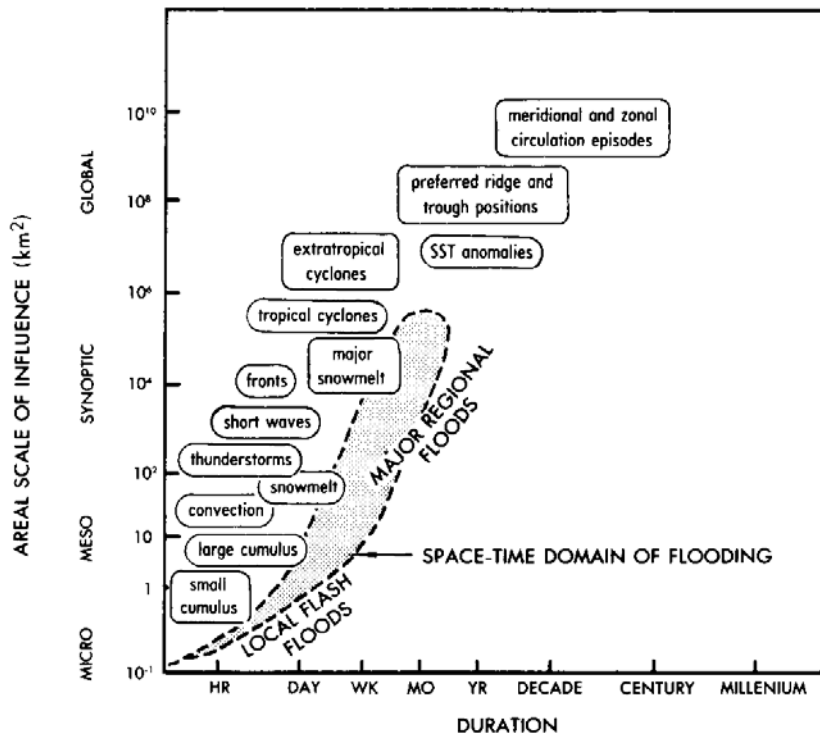


Figure 1.3: Spatial and temporal scales of selected atmospheric and hydrologic conditions related to flooding (Hirschboeck, 1988)

1.2 *Mississippi and Missouri Basin Characteristics*

The Missouri River drains about 73 percent of the Upper Mississippi River basin but from 1940-1998 accounted for only about 43 percent of the total annual streamflow. Figures 1.4 and 1.5 show the relative sizes of the drainage areas for each gage. The Missouri River basin is generally a drier region than the Upper Mississippi basin. Using the observed daily flow from 1940 to 1998, the average for the Missouri River at Hermann, Missouri was 85,000 cubic feet per second (cfs), while the average for the Mississippi River at Alton-Grafton, Illinois (upstream of the Missouri confluence) was 111,000 cfs. During major floods, however, the Missouri produces a larger percentage of the flood peak discharge downstream of the confluence of the two rivers than the Mississippi. Figure 1.6 shows the relative size of flood peaks during the 1993, 1995, and

1973 floods using unregulated flow data. During the 1993 flood, the unregulated peak flood for the Missouri River at Hermann was 970,000 cfs (750,000 cfs observed peak) and 616,000 for the Mississippi River at Alton.

Figures 1.7 and 1.8 show the average annual flood for each gage using unregulated flow data for 1937-1995. The average annual flood measured at the Hermann gage on the Missouri River is about 350,000 cfs, whereas that value is 550,000 cfs for St. Louis, downstream of the confluence of the two rivers. The average annual flood for the Upper Mississippi River above the confluence at Alton is about 300,000 cfs.

Figures 1.9 and 1.10 show the change in average annual unregulated flood (1937-1995) per change in drainage area for the two rivers. The change in drainage area is the increase in drainage area for each gage from the immediate upstream gage, while the change in average annual flood is the difference from the immediate upstream gage. The drainage area for Sioux City includes the area above Gavins Point Dam. These figures show that the Missouri River upstream of Kansas City is relatively dry, while the area directly upstream of Boonville and Hermann are fairly wet. The incremental areas with the largest runoff per square mile (such as those above Hannibal, Louisiana, Hermann, and Boonville gages) correspond to the regions with the greatest annual rainfall (UMRCBS, 1972). The Mississippi is relatively “wetter” than most of the Missouri River. Using the change at St. Louis as an indicator, the Mississippi has about twice the peak annual flood discharge per unit of drainage area.

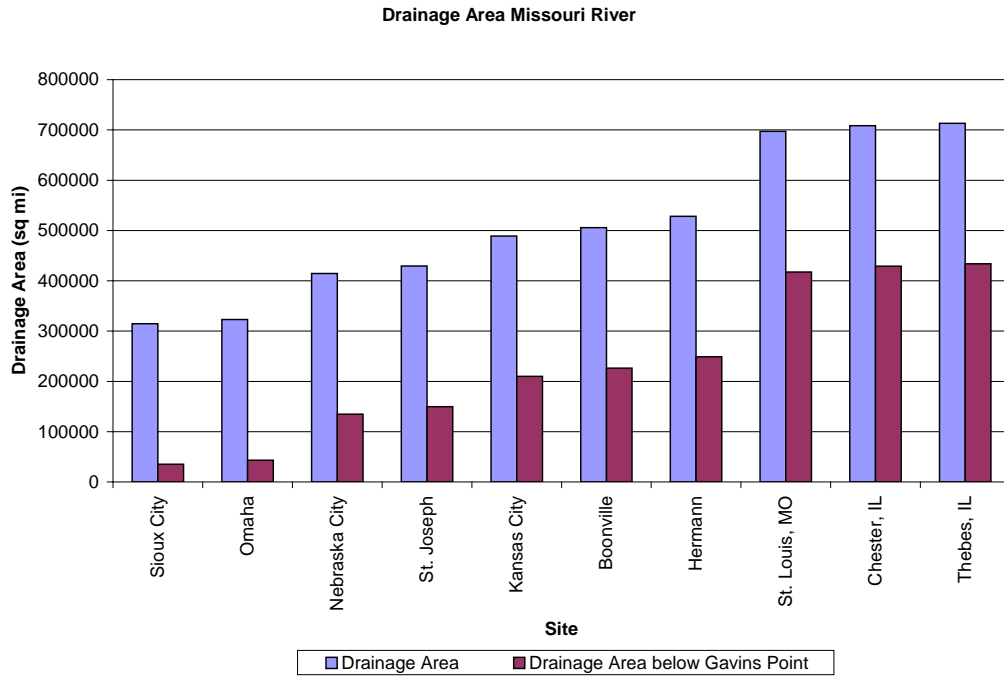


Figure 1.4: Size of drainage area at each gage site for the Missouri River.

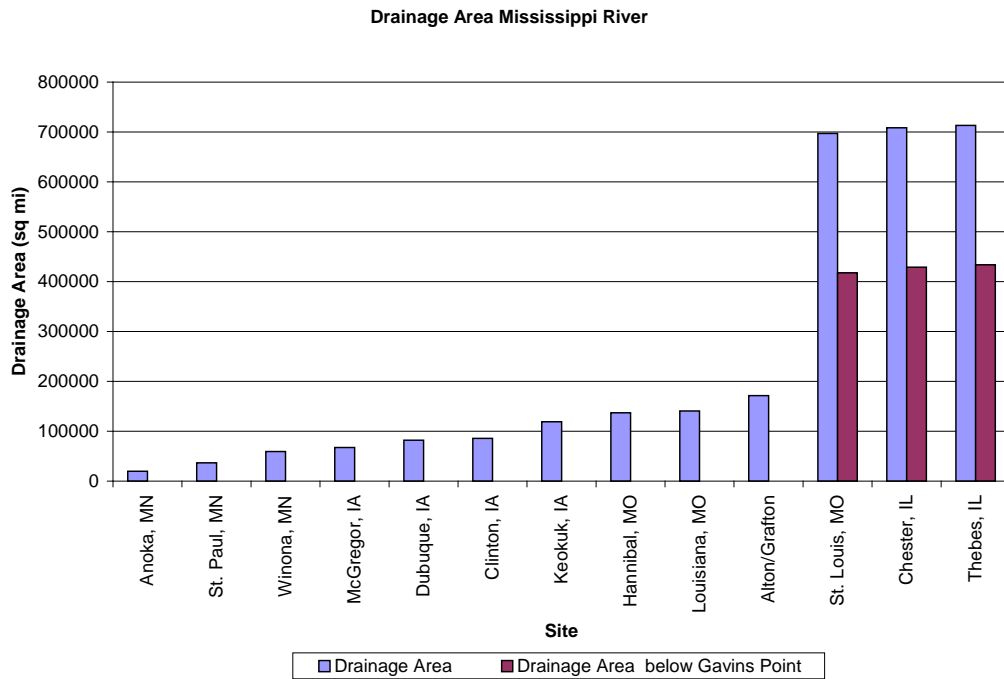


Figure 1.5: Size of drainage area at each gage site for the Mississippi River.

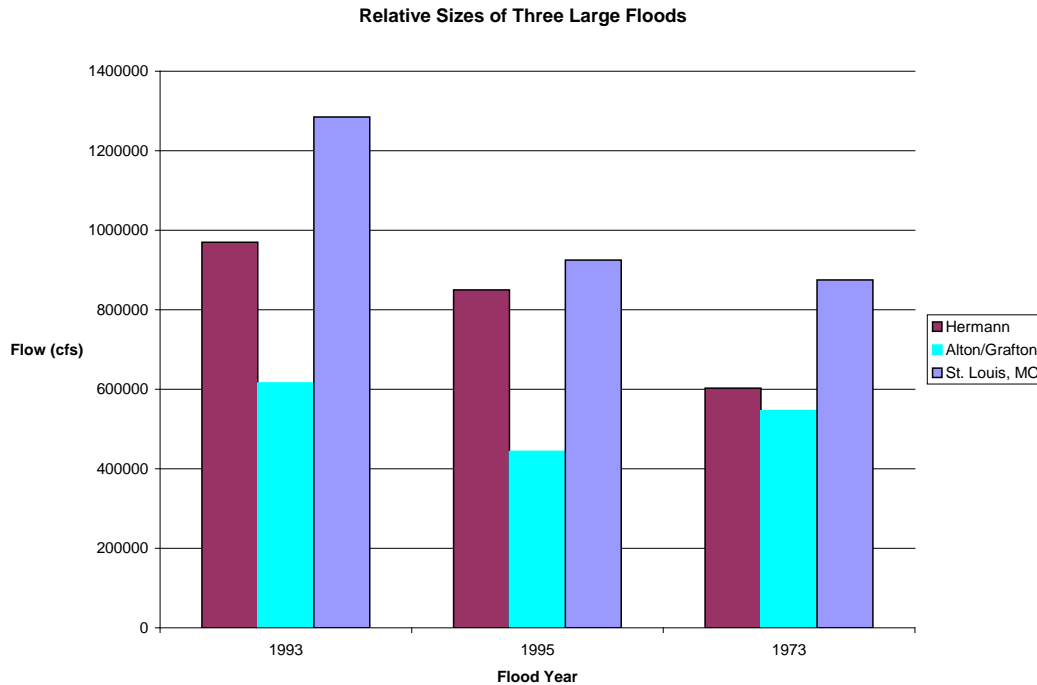


Figure 1.6: Relative size of flood peaks during three major floods (using unregulated flow data).

1.3 References

Hirschboeck, Katherine K., 1988. "Flood Hydroclimatology." in V.R. Baker *et al.*, ed., *Flood Geomorphology*. John Wiley: New York.

Hydrologic Engineering Center, U.S. Army Corps of Engineers, 1998. *An Investigation of Flood Frequency Estimation Methods for the Upper Mississippi Basin*, Draft Report.

Scientific Assessment and Strategy Team (SAST Report), 1994. *Science for Floodplain Management into the 21st Century*. Preliminary Report of the Scientific Assessment and Strategy Team Report of the Interagency Floodplain Management Review Committee To the Administration Floodplain Management Task Force (SAST Report).

Upper Mississippi River Comprehensive Basin Study Coordinating Committee (UMRCBS), 1972. *Upper Mississippi River Comprehensive Basin Study*.

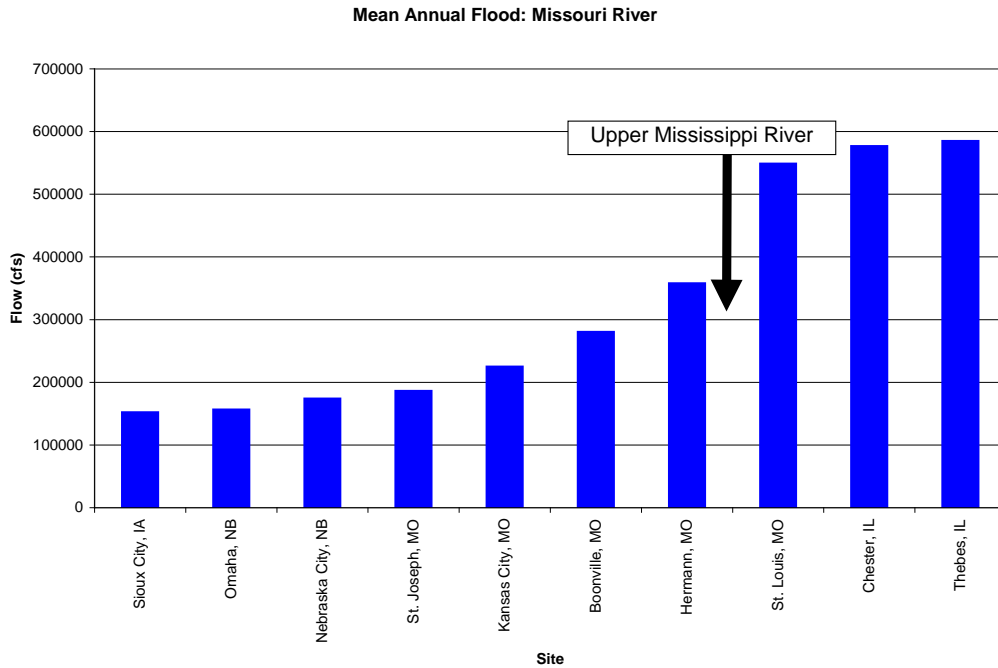


Figure 1.7: Average annual flood for each gage on the Missouri River and three gages on the Mississippi River (using unregulated flow data).

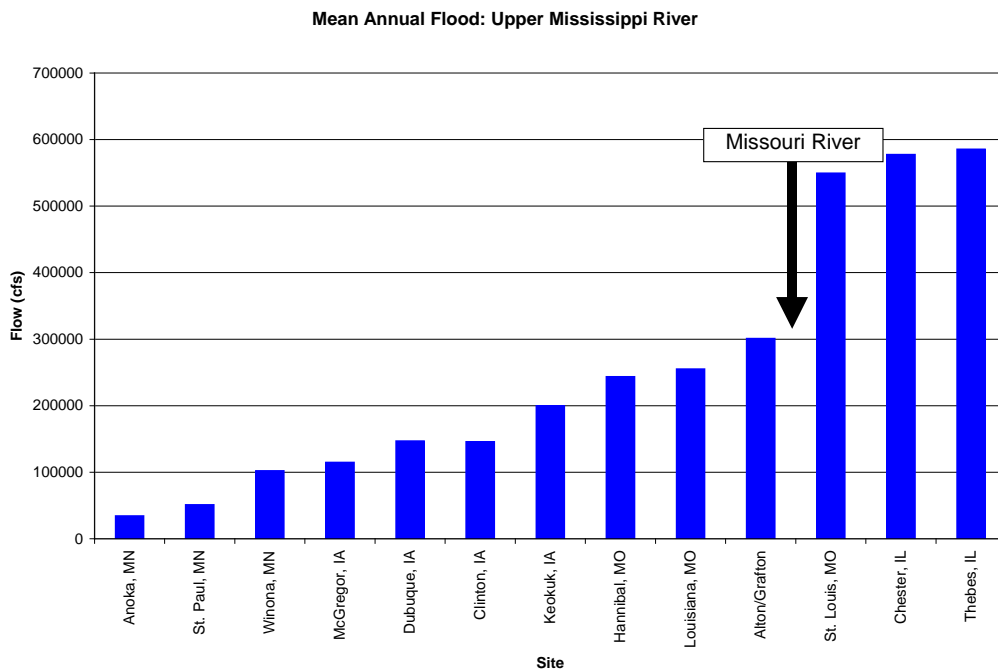


Figure 1.8: Average annual flood for each gage on the Mississippi River (using unregulated flow data).

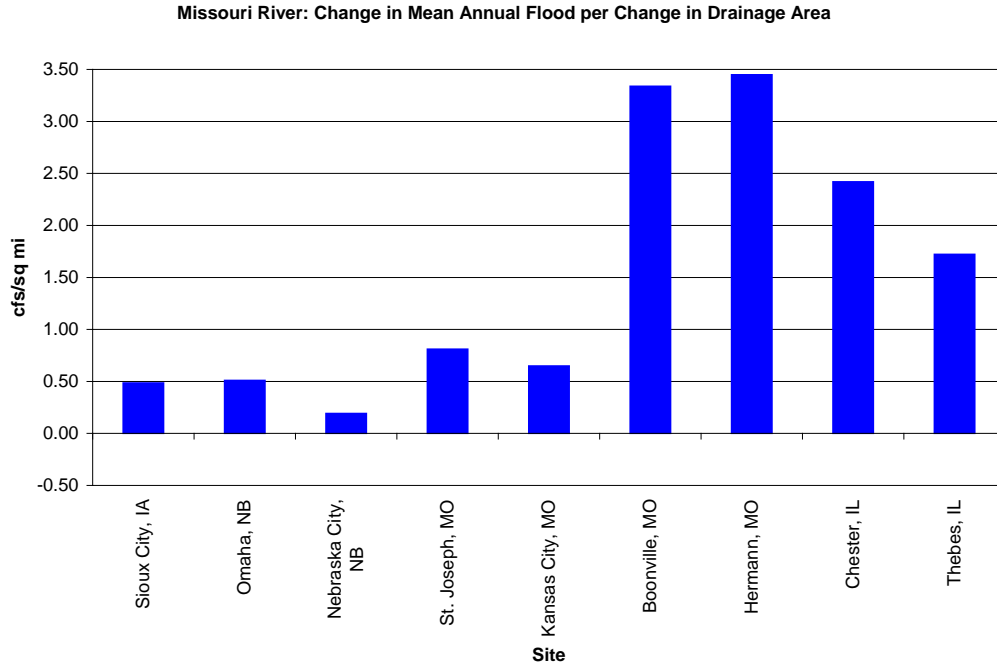


Figure 1.9: Change in average annual flood per change in drainage area for gages on the Missouri River and two gages on the Mississippi River (using unregulated flow data).

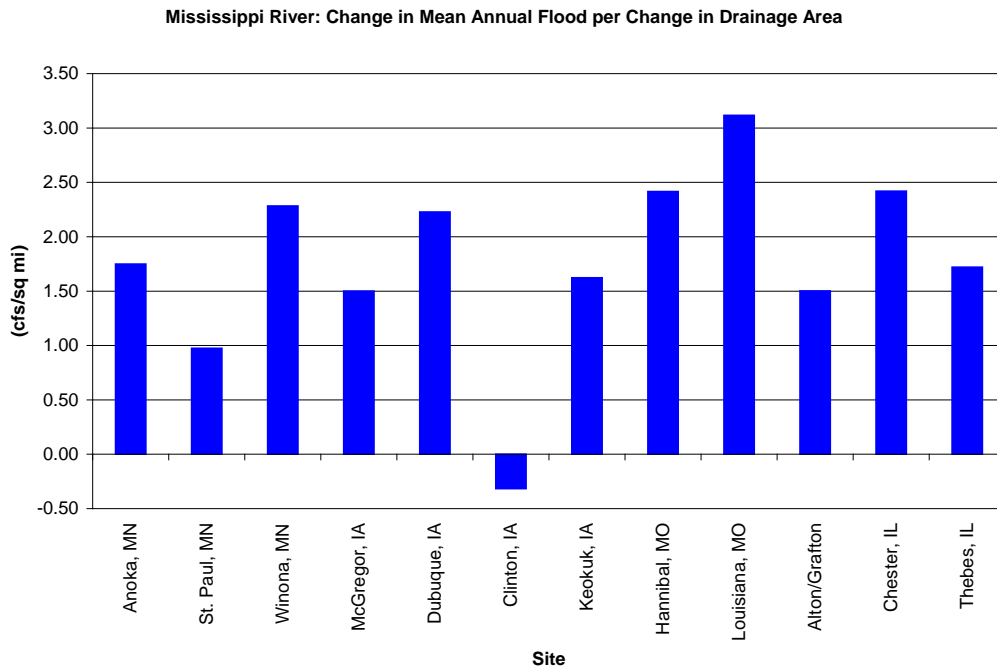


Figure 1.10: Change in average annual flood per change in drainage area for gages on the Mississippi River (using unregulated flow data).

2 Climatic Influences on Floods

2.1 *Precipitation Patterns*

Rodenhuis (1996) describes the central region of North America as a battle zone between the cold polar air mass to the north and the warm tropical air to the south. A west-east jet stream located about ten miles aloft determines the location of the storm track and the intensity of storms. The dominant source of moisture in this region is a low-level jet from the Gulf of Mexico located about 800 meters aloft and occurring primarily at night (Bonner, 1968). According to Helfand and Schubert (1995), the nocturnal low-level jet is related to the subtropical North Atlantic anticyclone associated with the Bermuda high. Rodenhuis notes two climate patterns in the Pacific Ocean that affect North America. A persistent low pressure is located near the Aleutian Islands and is a source of cyclonic storms that move over North America following the polar jet stream. El Niño refers to the warming of sea surface temperatures (SST) in the eastern tropical Pacific, especially in the ocean along the western coast of South America. During El Niño events, the ocean surface temperatures warm and significantly strengthen the subtropical jet stream. These meteorological influences are shown in Figure 2.1. The climate patterns will be discussed in more detail in the next chapter.

The Upper Midwest is characterized by a bimodal distribution of rainfall. The maximum rainfall usually occurs in June with a secondary maximum in September or August. Midsummer and winter are usually drier. The precipitation in the Great Plains also has a bimodal distribution, but the maximum usually occurs in May. The bimodal pattern has not been present in all decades. The 1950s and 1970s had a single mode in June and August respectively (Keables, 1989). The monthly precipitation is more

dependent on the frequency of precipitation events rather than a small number of high-intensity storms. According to Keables, monthly precipitation is more a result of synoptic-scale systems than thermal convection. For example, dry Junes are characterized by a northerly circulation over the Upper Midwest. One explanation for the bimodal precipitation pattern is based on the location and movement of the polar front. The heavier rainfall in June may result from the northern migration of the polar front and associated storm tracks, and the southern migration in September may again cause heavier rainfall (Keables, 1993).

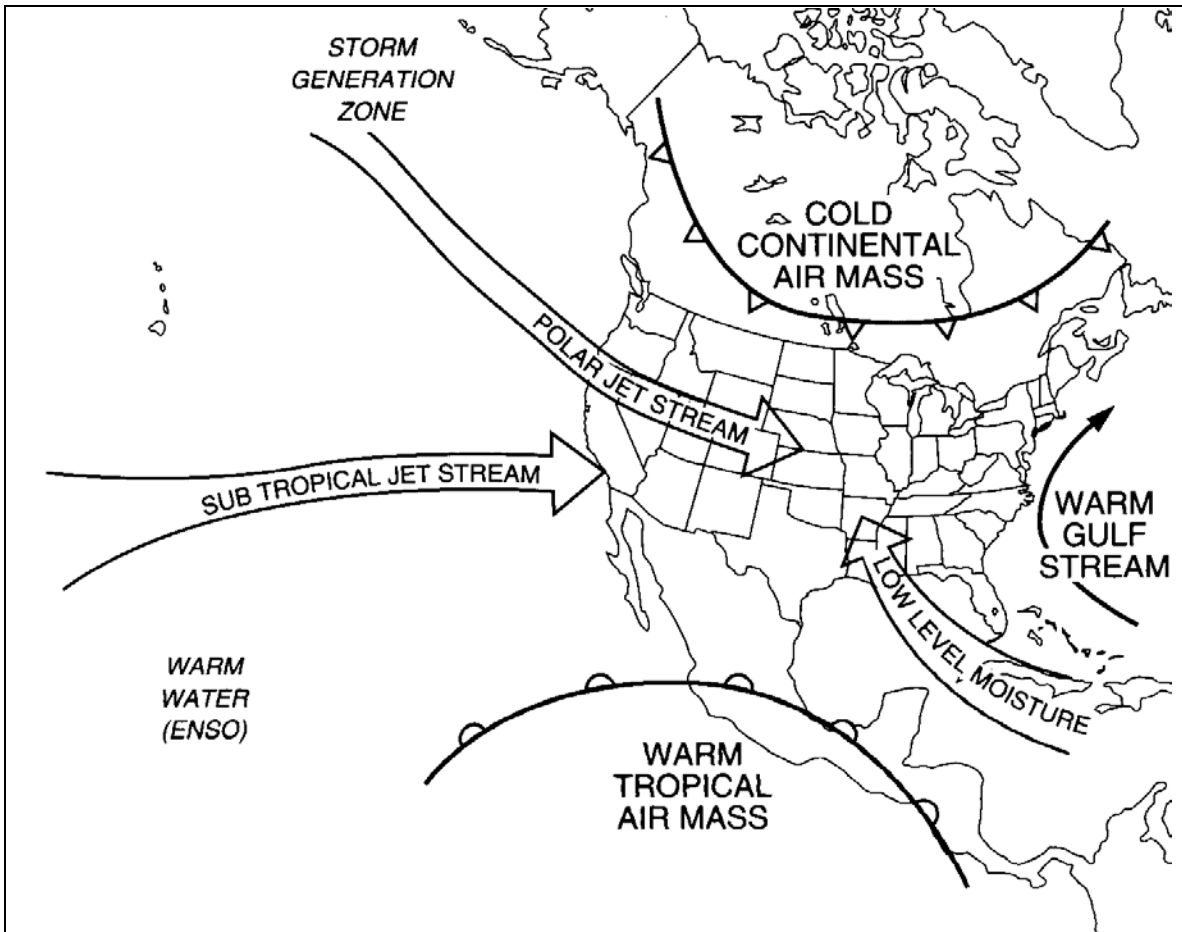


Figure 2.1: Major meteorological influences on the weather and climate of the Upper Mississippi and Lower Missouri basin (Rodenhuis, 1996).

Angel and Huff (1995) also looked at the seasonal distribution of rainfall. More storms occur in summer and the least occur in winter. In the more northerly states with shorter convective seasons, such as Minnesota, Wisconsin, and Iowa, the difference between the seasons is most prominent. In Minnesota, the soil moisture is low during the summer months when the rainfall is highest.

During the warm season, mesoscale convective systems (MCSs) are a major source of rainfall for the central United States. Larger MCSs are called mesoscale convective complexes (MCC). Kunkel *et al.* (1993) identified major large-scale events where the 7-day precipitation levels exceeded 100 mm. The pattern associated with MCCs are characterized by an upper trough to the west and an upper ridge to the east (Kunkel *et al.*, 1994). However, according to Kunkel *et al.* (1994), extreme flooding of the Mississippi and Missouri Rivers seldom occurs in the summer “because of the highly space- and time-variable nature of convective rainfall in the Midwest, coupled with the high rates of evapotranspiration.” The flood in the summer of 1993 was an anomaly.

Knox (1988) evaluated the association between various climatic factors and the magnitudes of floods for the tributary basins of the Upper Mississippi River. Magnitudes of annual floods correlate best with magnitudes of winter snow depth and early summer rainfall. Knox observed that most annual maximum floods in the smaller tributary basins do not have a long memory of antecedent conditions since the correlation with the preceding summer and fall precipitation is not significant.

2.2 *Streamflow Seasonality*

Floods can result from rainfall, snowmelt or a combination of both. Snowmelt or snowmelt and rainfall floods occur primarily from December to April, while floods from

excessive rainfall usually occur from April to November. According to Knox, most floods in the Upper Mississippi River occur during the months of March through July. Knox studied a partial duration series of 29 tributary river systems in the Mississippi basin from 1941 through 1969. March and June were the months with the highest frequency of floods. March floods result from the nearly annual spring snowmelt. June floods are more variable because they are caused by variable June rain.

Baldwin and Lall (1998) examined seasonal streamflow patterns using records for the Mississippi River at Clinton, Iowa. They identified three periods of higher streamflow. Larger flows typically occur in the spring due to snowmelt runoff. The magnitude of the runoff depends on the amount of snow on the ground. Spring rainfall or higher temperatures can accelerate the snowmelt. There are also peaks in June/July and October. These peaks correspond to the precipitation patterns discussed earlier (Keables *et al.* 1993), but there is a time delay between the rainfall and runoff.

2.2.1 Snowmelt Floods

According to Knox, the spring snowmelt dominates the annual maximum flood series in the northern part of the basin. Precipitation in the winter primarily occurs as snow and is stored until the spring snowmelt. Relatively few floods occur in the months of December through February. The month of March is the mode for the snowmelt floods in the Upper Mississippi River basin. The timing of the flood on the tributary basins occurs later in the spring with northward position and as the drainage basin size increases. On the mainstem of the Mississippi River, spring snowmelt floods typically occur in April due to the downstream travel time and the combining of floods from the northern tributaries (Knox, 1988).

2.2.2 Rainfall Floods

June floods result from excessive and intense rainfalls. Warm air masses from the Gulf of Mexico collide with cooler drier air from Canada and can cause large amounts of rainfall. Antecedent soil moisture increases the likelihood of flooding. Floods in July and August are less likely. Reduced precipitation during these months may be one reason for the lower streamflow. In addition, potential evapotranspiration is higher during these months. Lower precipitation and higher potential evapotranspiration lead to lower antecedent soil moisture which favors higher infiltration and reduced runoff. Land use and infiltration may also contribute to reduced runoff. In June, many agricultural fields still have exposed soil favoring reduced infiltration capacity. In July and August these fields are covered with vegetation and more rainfall is likely to infiltrate. As noted earlier, precipitation increases in September. September floods are rare because antecedent soil moisture levels are low and the land is covered with vegetation. Floods in October and November are also rare for similar reasons as September. Precipitation also decreases in these months (Knox, 1988).

2.3 Flood Records and Dates

A review of the annual peak floods at several gages along the Mississippi and Missouri Rivers shows this flood seasonality. United States Geological Survey (USGS) data for annual floods were used for this analysis. The data are observed flood peaks and do not include the effects of regulation. Figure 2.2 shows the monthly distribution of annual peak floods for five stations on the Mississippi River for the years 1900 to 1996. For all the locations, April is the month with the most floods. The majority of the floods occur in the spring from March to June. However, at St. Louis the peak annual flood has

occurred at least once in each month, but this is not the case at the other locations. St. Louis receives a large proportion of its flood flow from the Missouri River.

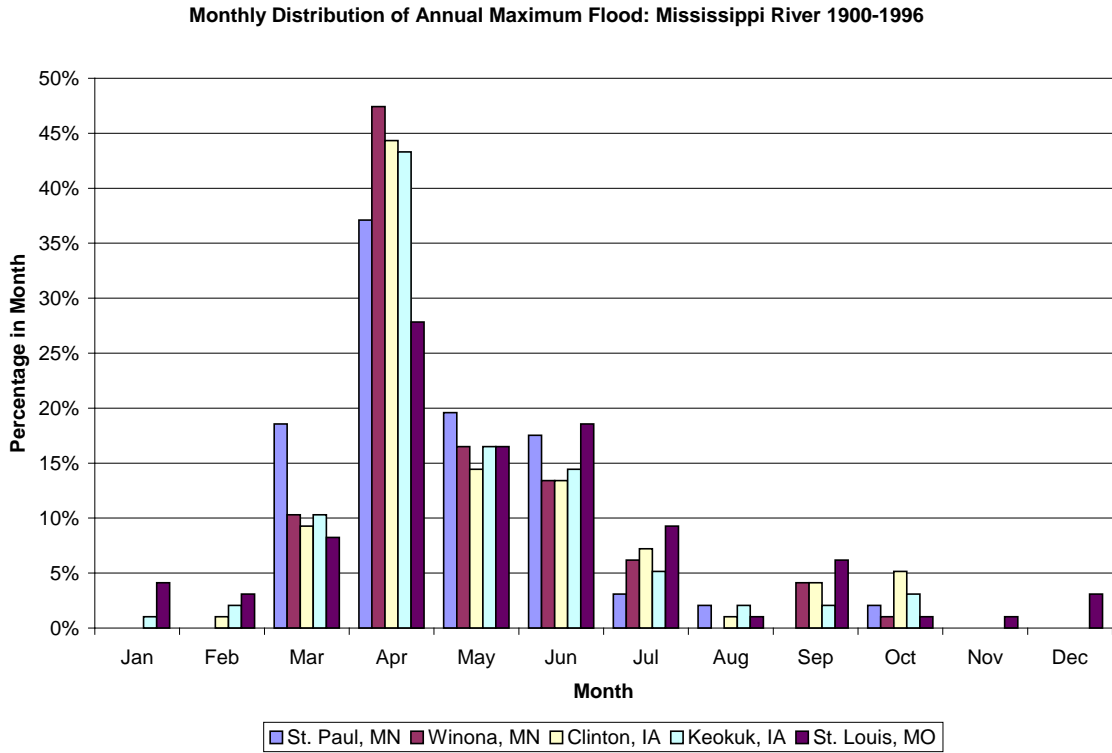


Figure 2.2: Monthly distribution of annual peak floods for five gage sites on the Mississippi River (1900 to 1996).

A review of the five largest floods at these locations shows that spring floods are predominant. Table 2.1 shows the monthly distribution of the five largest floods. For the three most northern locations, all the major floods occurred in April with the exception of the 1993 flood. The 1993 flood peaked in June in Minnesota, July in Iowa, and August in St. Louis.

Table 2.1: Monthly distribution of the five largest annual peak floods for five gage sites on the Mississippi River (1900 to 1996).

	St. Paul, MN	Winona, MN	Clinton, IA	Keokuk, IA	St. Louis, MO
April	4	4	4	2	1
May				1	1
June	1	1		1	1
July			1	1	
August					1
December					1

Figure 2.3 shows the monthly distribution of the annual peak floods from 1930 to 1996 for four locations on the Missouri River and for St. Louis. This table is based on observed peak flows; regulation of the Missouri above Gavins Point may have affected the timing of the floods. For the Missouri River, June is the month with the most floods. For the two most northern locations, there is a bimodal monthly distribution of peak floods with March and April and then June having large number of floods. Hermann, the last gage on the Missouri River before the confluence with the Mississippi River, has almost equal number of floods in April, May, and June. Hermann, like St. Louis, has had annual peak floods in every month of the year. The other locations on the Missouri have not had peak floods in the winter months of December and January.

Monthly Distribution of Annual Maximum Flood: Missouri River 1930-1996

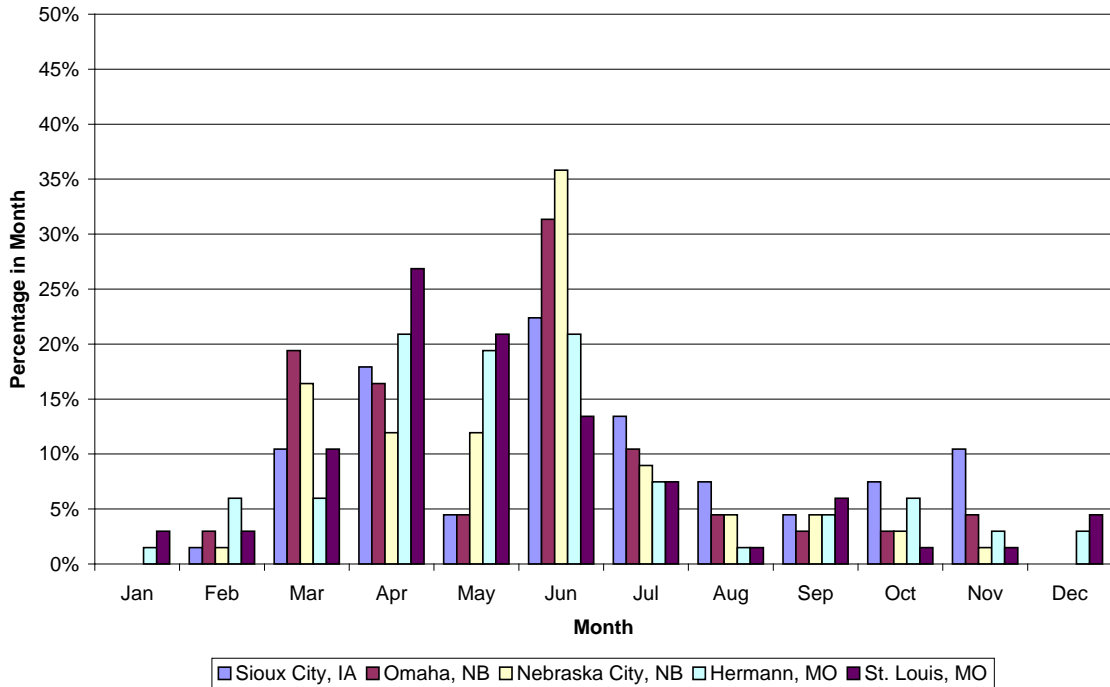


Figure 2.3: Monthly distribution of annual peak floods for four gage sites on the Missouri River and for St. Louis on the Mississippi River (1930 to 1996).

The monthly distribution of the five largest floods shows that the largest floods tend to occur in April for the three most northern stations on the Missouri River (Table 2.2). The largest floods at Hermann have occurred in April, May, and July.

Table 2.2: Monthly distribution of the five largest annual peak floods for four gage sites on the Missouri River and for St. Louis on the Mississippi River (1930 to 1996).

	Sioux City, IA	Omaha, NB	Nebraska City, NB	Hermann, MO	St. Louis, MO
April	5	5	3	1	1
May				2	1
June			1		1
July			1	2	
August					1
December					1

2.4 Hydrometeorological Causes of Extreme Floods

The flood of record varies depending on the location. Table 2.3 shows the two largest observed floods for ten gages along the Missouri and Mississippi River.

Regulation may affect the size and timing of the peak flood, especially on the Missouri River. The flood of record for the northern locations on the Missouri River was in April 1952. The largest flood on the Missouri at Kansas City occurred in July 1951. The 1993 flood is the record flood at Hermann, Missouri, Keokuk, Iowa, and St. Louis, Missouri. In the more northern reach of the Mississippi River, the flood of record was in April 1965. A large flood also occurred in April 1973 on the Mississippi. The meteorological conditions leading to these floods will be discussed here.

Table 2.3: The two largest floods of record for ten locations along the Missouri and Mississippi Rivers (observed peak flow).

Gage Location	Record Flood		Second Largest Flood	
	Date	Discharge (cfs)	Date	Discharge (cfs)
Missouri River				
Omaha, NB	4/18/52	396,000	4/12/43	200,000
Nebraska City, NB	4/19/52	414,000	6/14/44	214,000
St. Joseph, MO	4/23/52	397,000	7/26/93	335,000
Kansas City, MO	7/14/51	573,000	7/27/93	541,000
Hermann, MO	7/31/93	750,000	7/19/51	615,000
Mississippi River				
St. Paul, MN	4/16/65	171,000	4/15/69	156,000
Winona, MN	4/19/65	268,000	4/19/69	218,000
Clinton, IA	4/28/65	307,000	7/7/93	239,000
Keokuk, IA	7/10/93	446,000	4/24/73	344,000
St. Louis, MO	8/1/93	1,080,000	4/28/73	852,000

(UMRCBS, 1972; Parrett, et al., 1993; USACE, 1994; Koellner, 1996; USGS NWIS-W data)

2.4.1 1993 Flood

Precipitation amounts in the first seven months of 1993 were substantially above normal. In January through March the precipitation was near to slightly above normal. In

April and May, precipitation ranged from near normal to much greater than normal. In June, the weather pattern was characterized by a large high-pressure system over the Southeastern United States and a strong low-pressure system over the Western United States. The jet stream flowed northeasterly across the upper Midwest. A convergence zone between the warm, moist air from the Gulf of Mexico and cooler, drier Canadian air resulted in thunderstorms in the upper Midwest. This weather pattern persisted during June and July and brought extraordinary rains in both areal extent and accumulated amounts (Wahl *et al.*, 1993). This weather pattern is shown in Figure 2.4. Kunkel *et al.* (1994) concluded that the 1993 floods were a result of seven conditions:

- 1) The precipitation totals for 2- through 12- month intervals exceeded all previous events by a large margin.
- 2) There was a high incidence of moderate to heavy rain events for single and multiday periods.
- 3) Heavy rains in spring resulted in saturated or near-saturated conditions throughout the basin.
- 4) The semi-stationary frontal condition produced not only nearly continuous daily rain, but also heavy rains over an extensive area.
- 5) The orientation of the rain areas may have increased the magnitude of the flooding.
- 6) There was a large number of localized extreme rains capable of producing flash floods, in addition to the frequent incidence of large areas of heavy rainfall.
- 7) The seventh factor was below-normal evapotranspiration due to the frequent cloud cover over the area.

Mo *et al.* (1995) described the large-scale weather pattern leading to the 1993 flood. They noted that the weather pattern is not that infrequent, but its long persistence in 1993 was unusual. A Pacific jet originated in response to warm El Niño conditions during the winter of 1992/1993. This jet persisted until June when it started to weaken and move to its normal position. At that time the North American jet stream strengthened. Strong westerly winds were forced to rise over the Rockies and by

conservation of potential vorticity created a lee trough that remained over the Midwest through July. An associated low-level jet east of the Rockies brought in tropical moisture to the region.

Bell and Janowiak (1995) noted that the 1993 flood was associated with anomalous climatic patterns over the North Pacific. This circulation pattern was associated with an intensified storm track across the Pacific from February through May 1993. This pattern changed in late May establishing a strong zonal flow from the Pacific to the eastern United States. This flow provided a track for intense cyclones to move directly into the Midwest causing intensive convective complexes over the region in June. The July weather pattern was dominated by a ridge over the Gulf of Alaska and a trough over the western United States. A northeast-southwest-oriented quasi-stationary frontal boundary persisted over the region and sustained moisture transport and the major convective storms.

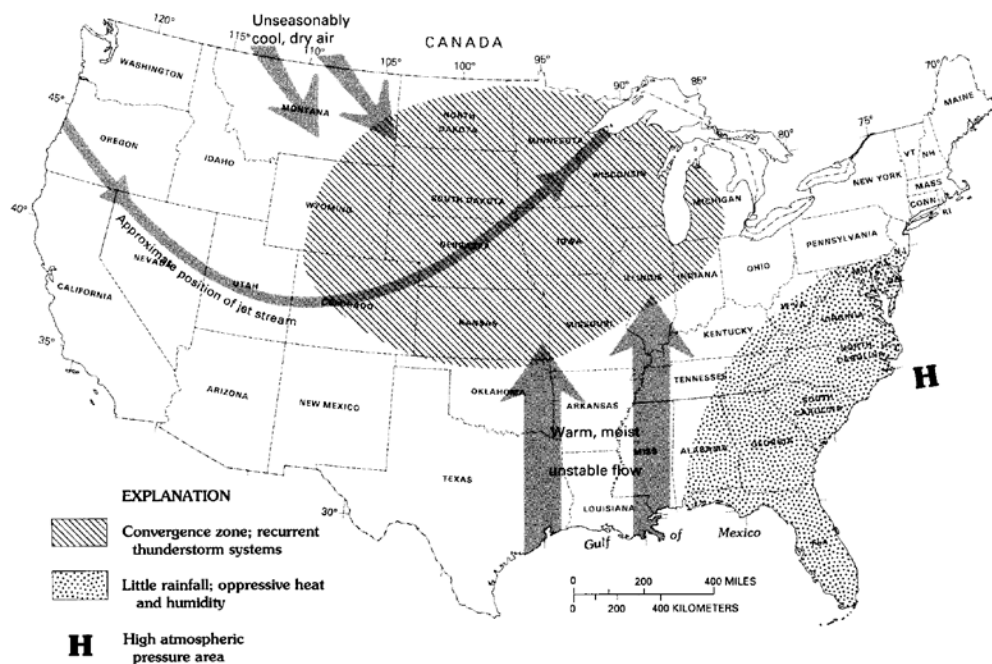


Figure 2.4: Weather patterns that led to the 1993 Mississippi floods (Wahl *et al.*, 1993).

2.4.2 1952 Flood

The flood of record on the northern Missouri River is the flood of April 1952. These conditions also produced the third largest flood at St. Paul, Minnesota, Winona, Minnesota, and Clinton, Iowa. Although the flood in lower parts of the Missouri and Mississippi Rivers was above average, it was not recordbreaking. This flood can be characterized as a snowmelt flood. Weather reports from the time noted that the precipitation was relatively light in the area, but the temperatures were more than 10° F above normal. The “flood conditions were brought about chiefly by heavy snow melt and rapid ice breakup in the northern states at the beginning of April” (Martin, 1952).

2.4.3 1965 Flood

The flood of record on the northern Mississippi River (St. Paul, Winona, and Clinton) is the flood of April 1965. Prior to the floods of 1973 and 1993, it was the flood of record for Keokuk. The Missouri River was not affected by major flooding during 1965. This flood was caused by both snowmelt and heavy rains. A large winter snowfall occurred in 1965 with an especially cold and snowy March. In the first week in April, daytime melting of snow caused high flood stages. In the second week of April, heavy rainfall and more warming caused rapid snowmelt and record flood stages. The precipitation in the Upper Midwest was more than twice normal April levels (O’Connor, 1965).

2.4.4 1973 Flood

The 1973 flood affected the Mississippi River from Winona to the Mississippi Delta. The flood set a record for consecutive number of days above flood stage for many gaging stations. The previous winter was relatively mild and wet. The snow cover in the

region “was both limited in extent and depth” (Chin *et al.*, 1975). When compared to the heavy precipitation, the contribution from snowmelt was relatively small.

March 1973 was an extremely wet month. A double trough was present over the Southwestern and Central United States with a ridge over the Eastern United States. The area east of a trough is typically associated with strong surface convergence and divergence aloft. This pattern provides the mechanism for frontal formation, storm development, uplift, and release of excess moisture. A strong southerly flow also helped bring in warm moist maritime air into the region (Hirschboeck, 1988; Chin, *et al.*, 1975). In mid-April, a Bermuda high was present over the Western Atlantic leading to a strong southerly flow over the Central Mississippi Valley. This flow brought moist tropical air from the Gulf of Mexico and caused continuous heavy rain in the region (Chin, *et al.*, 1975).

2.4.5 1951 Flood

Heavy rains caused a summer flood along the Lower Missouri in 1951. It was the flood of record for over thirty years at the gage at Hermann, Missouri. Above normal rainfall began in April and continued into July. Four days of heavy rains occurred on July 9-13 and because of the moist soil conditions resulted in heavy runoff. The circulation pattern consisted of high pressure over the Gulf of Alaska and a trough of low pressure extending from the northern Plains southwestward. Intense local showers resulted when warm moist Gulf air was lifted over the frontal surface of a cold air mass. These rainfalls occurred during the night as is typical of summer precipitation in the Middle Plains (Carr, 1951).

2.5 Analysis of Rainfall and Snowmelt Floods

The largest floods in the northern part of the basin (1965 and 1969) were floods caused by snowmelt. Figure 2.5 shows the peaks at sites along the Mississippi River corresponding to these flood events. The maximum flood discharges downstream do not increase significantly for this type of flood. The mean snowfall in Minnesota is about four times the amount in St. Louis, as shown in Figure 2.6 (UMRCBS, 1972). On the other hand, the rainfall floods increase significantly moving downstream. The state of Missouri receives about twice the annual rainfall as Minnesota in the northern part of the Mississippi basin (UMRCBS, 1972). (See Figure 2.7.) Large floods on the Mississippi River have broad peaks. Figures 2.8-2.11 show hydrographs for water years 1965 and 1993 for Keokuk and St. Louis. The floods can have durations of one month or longer.

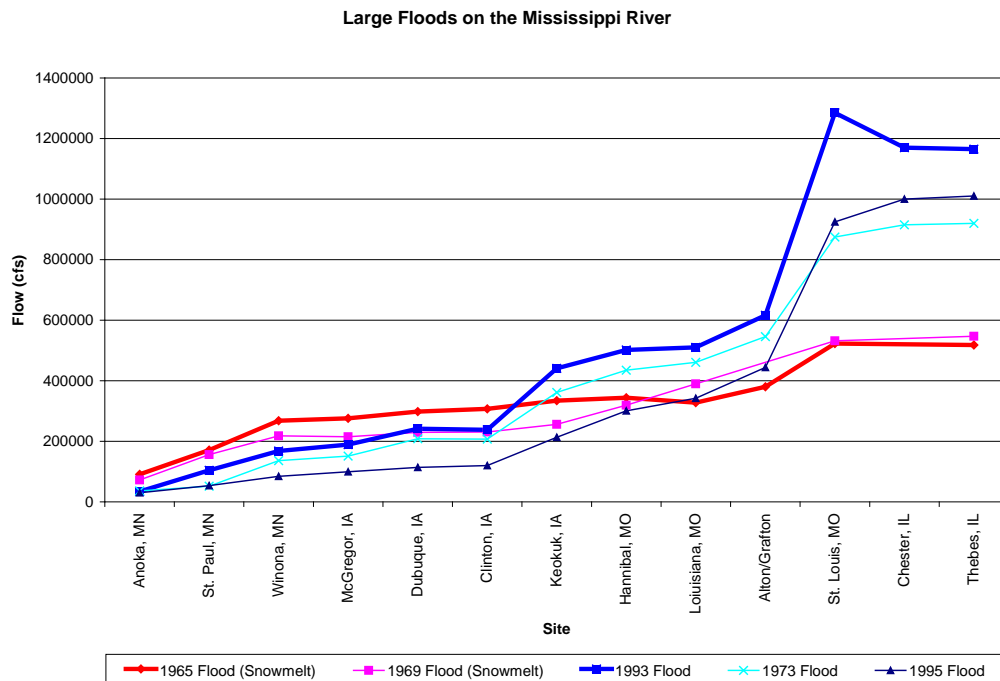


Figure 2.5: The peak flow at sites along the Mississippi River for five large flood events. The 1965 and 1969 are snowmelt floods while the other floods were caused by rainfall.



Figure 2.6: Mean annual snowfall in inches, Upper Mississippi River Basin, 1931-1952 (UMRCBS, 1972).

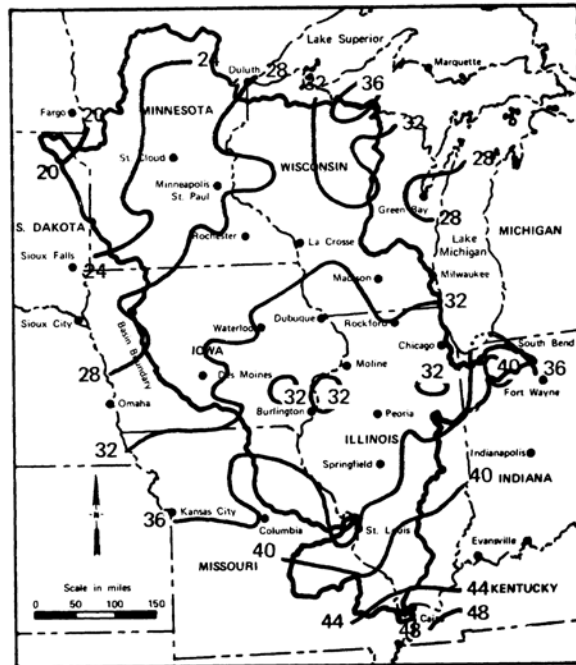


Figure 2.7: Normal annual precipitation, inches, Upper Mississippi River Basin, 1931-1960 (UMRCBS, 1972).

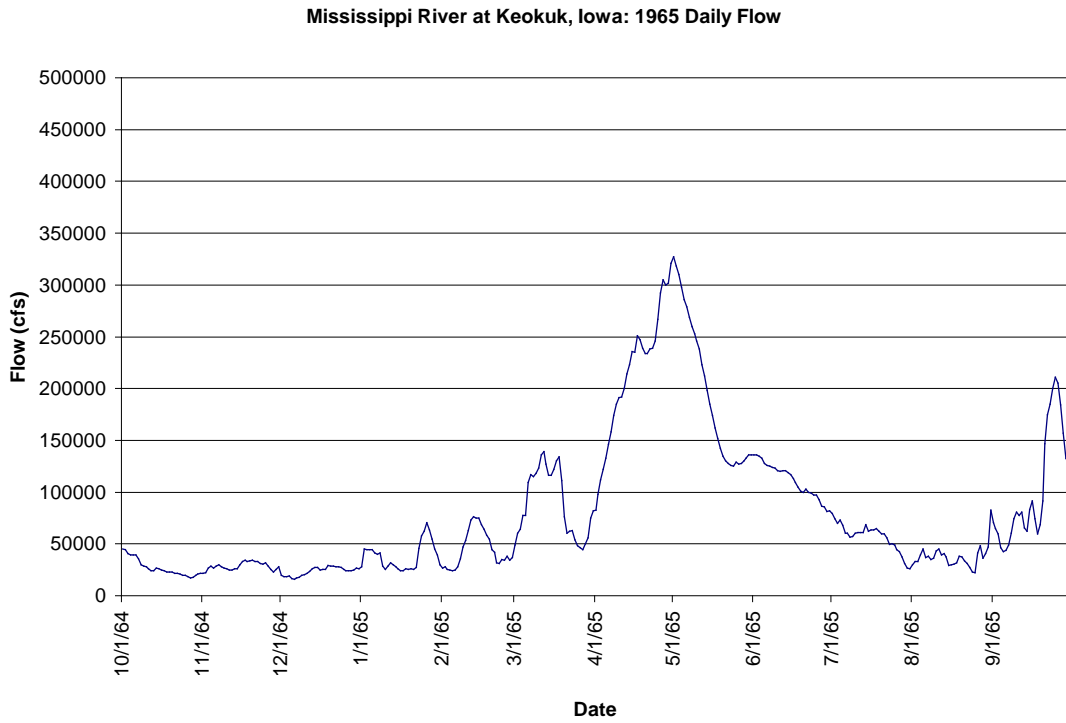


Figure 2.8: The hydrograph for the Mississippi River at Keokuk for water year 1965.

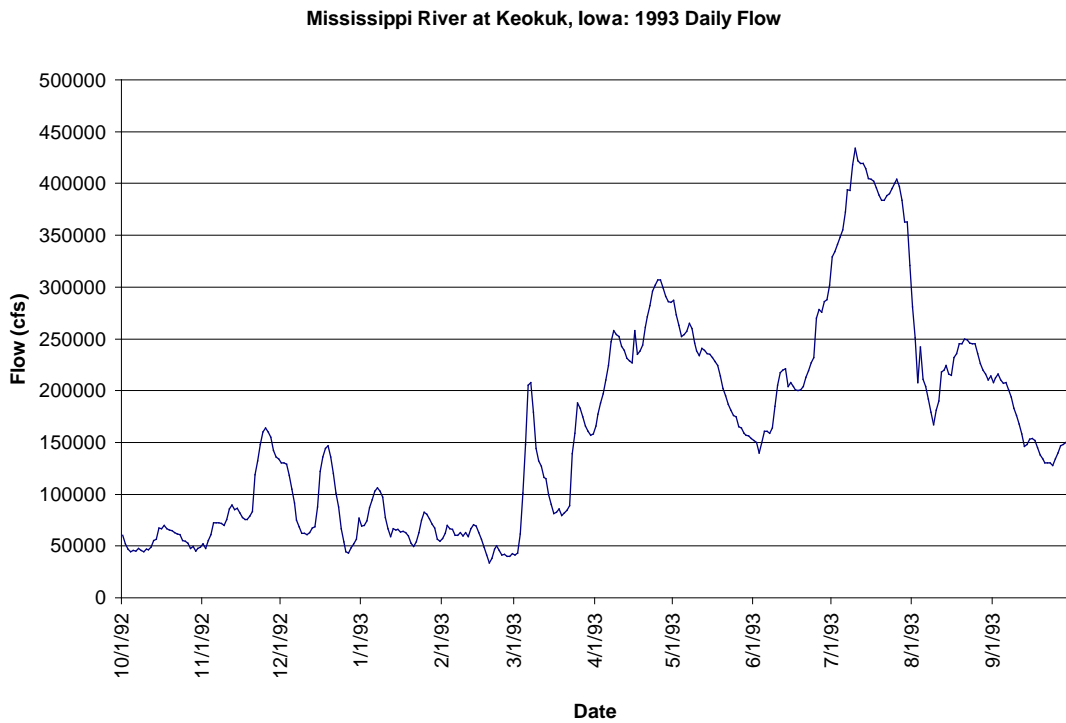


Figure 2.9: The hydrograph for the Mississippi River at Keokuk for water year 1993.

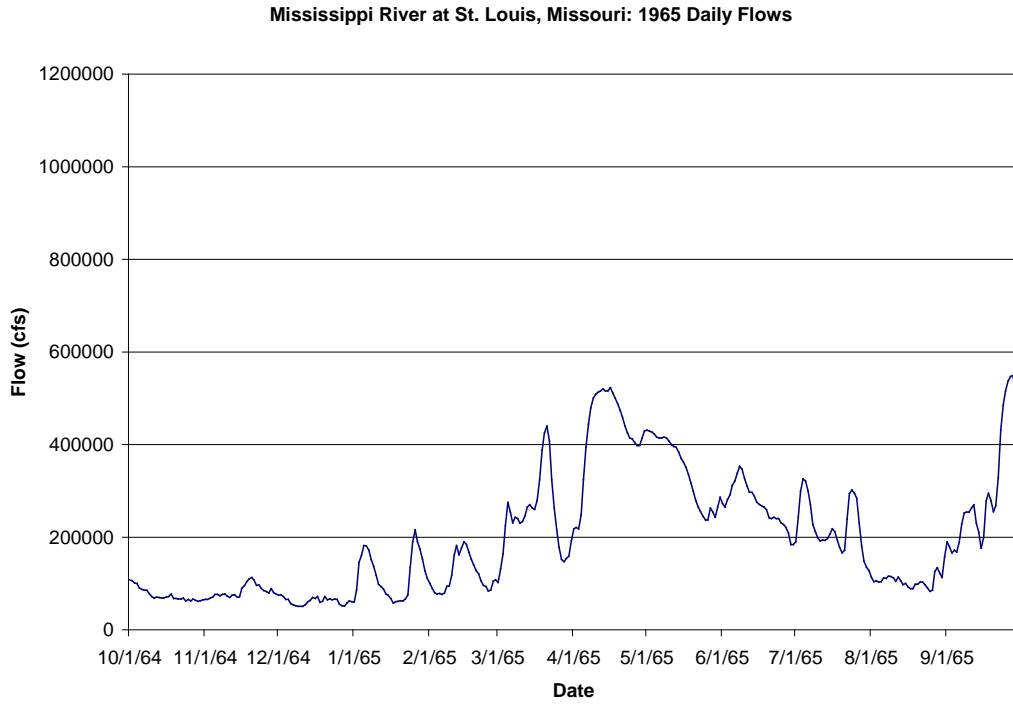


Figure 2.10: The hydrograph for the Mississippi River at St. Louis for water year 1965.

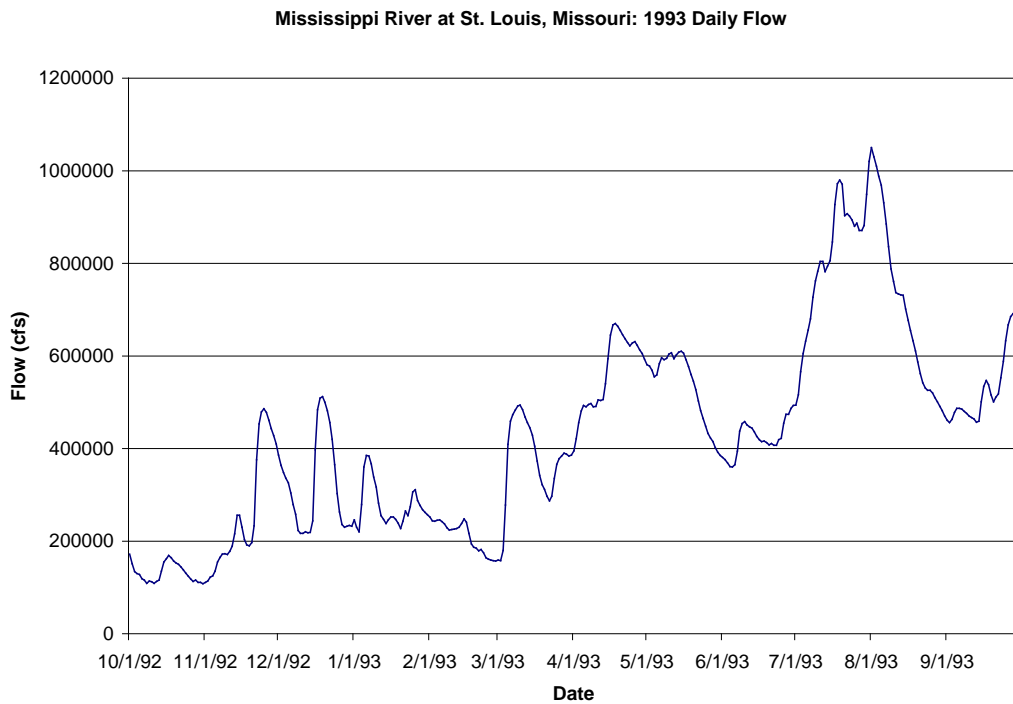


Figure 2.11: The hydrograph for the Mississippi River at St. Louis for water year 1993.

We analyzed the floods at Keokuk in more detail, since figure 2.5 appears to show that the annual floods here could be split into a mixed distribution of rainfall and snowmelt floods. The year was divided into three periods: October to February, March to April, and May to September. The largest flows in each water year from 1901 to 1997 were determined and plotted using the Weibull plotting position formula. The results are shown in Figure 2.12. The March-April period would in general correspond to snowmelt floods while the May-September period are rainfall floods. The distribution of these floods overlap. There is a large amount of correlation between the March-April and May-September floods (correlation coefficient of 0.6). Large rainfall floods often follow large snowfall floods due to increased soil moisture. Figure 2.13 illustrates this relationship. From this evidence, there is no need to use a split distribution to model the annual flood peaks at Keokuk.

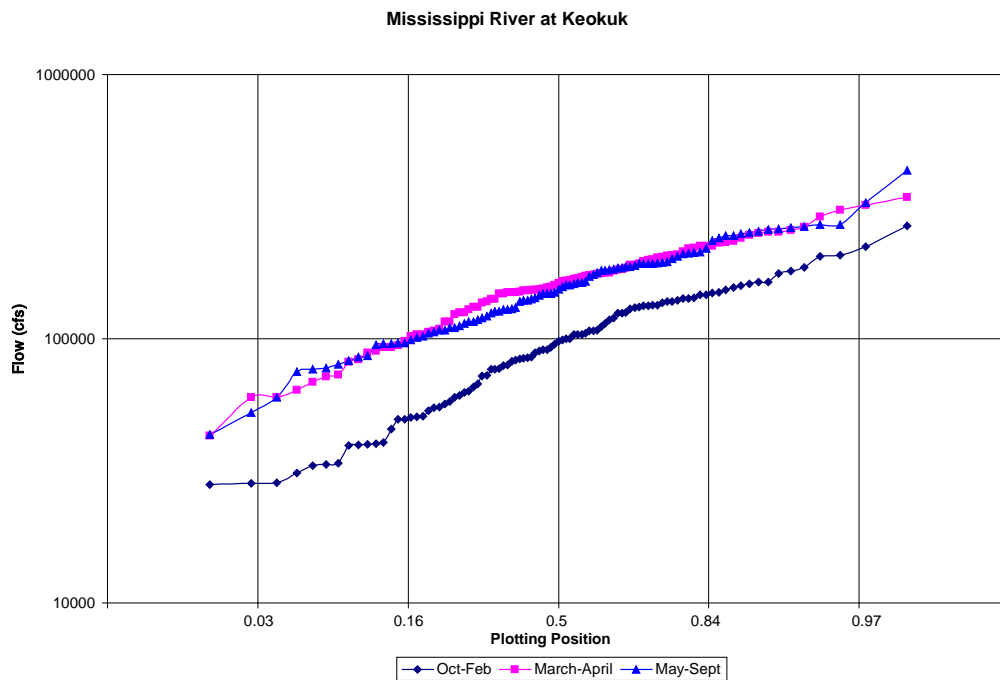


Figure 2.12: A plot of the largest flows for three different periods in a water year sorted by size.

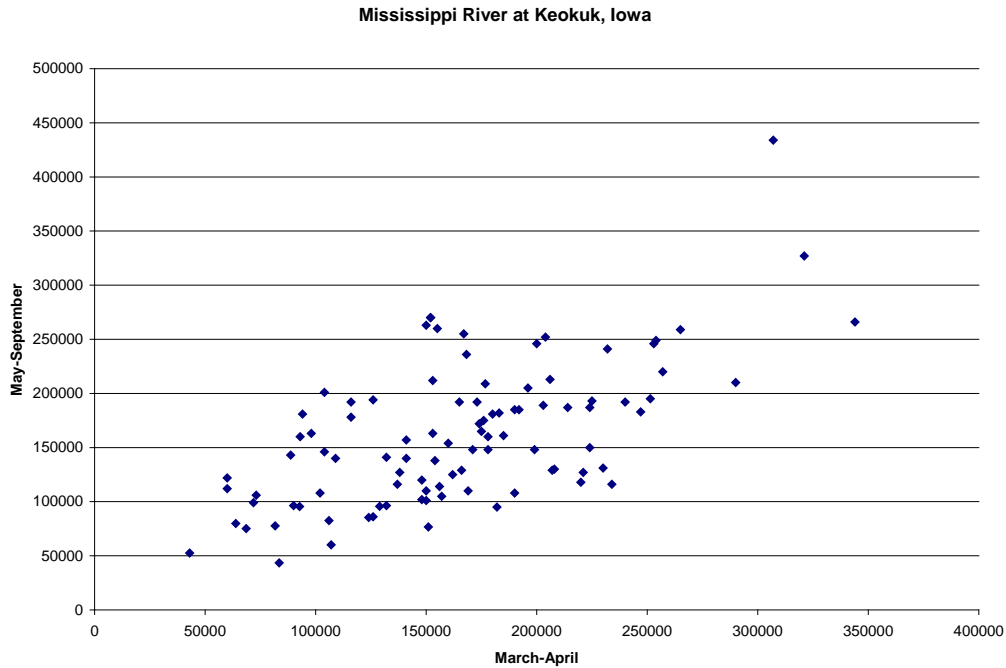


Figure 2.13: A plot of the March-April flood versus the May-September flood for each water year.

2.6 Summary

Weather in the Upper Mississippi and Lower Missouri basin is influenced by several factors including storm tracks originating in the Pacific Ocean and moisture brought in from the Gulf of Mexico by a low-level jet. In the northern part of the basin, the floods of record are snowmelt floods brought about by spring warming or rain on snow events. The maximum flood downstream does not increase significantly for snowmelt floods. Floods caused by rainfall are the largest floods at the more southerly sites on the Missouri and Mississippi Rivers. These floods occur when rain occurs for a long duration following wet antecedent conditions. These rainfall floods increase significantly moving downstream. Both rainfall and snowmelt floods can be major floods on the Mississippi River at Keokuk. However, it is not necessary to use a split

distribution to model the flood peaks. The distribution of rainfall and snowmelt floods overlapped and are highly correlated.

2.7 References

- Angel, James R., and Floyd A. Huff, 1995. "Seasonal Distribution of Heavy Rainfall in Midwest." *Journal of Water Resources Planning and Management*, Vol. 121: 110-115.
- Baldwin, Connely K., and Upmanu Lall, 1998. "Seasonality of Streamflow: the Upper Mississippi River." submitted to *Water Resources Research*.
- Bell, Gerald D., and John E. Janowiak, 1995. "Atmospheric Circulation Associated with the Midwest Floods of 1993," *Bulletin of the American Meteorological Society* Vol. 76, No. 5: 681-695.
- Bonner, William D., 1968. "Climatology of the Low Level Jet," *Monthly Weather Review*, Vol. 96, No. 12: 833-850.
- Carr, J.A., 1951. "Some Aspects of the Heavy Rains over Eastern Kansas, July 10-13, 1951," *Monthly Weather Review*, Vol. 79, No. 7: 147-152.
- Chin, Edwin H., John Skelton, and Harold P. Guy, 1975. *The 1973 Mississippi River Basin Flood: Compilation and Analyses of Meteorologic, Streamflow, and Sediment Data*. Geological Survey Professional Paper 937: U.S. Government Printing Office: Washington.
- Helfand, H. Mark, and Siegfried D. Schubert 1995. "Climatology of the Simulated Great Plains Low-Level Jet and Its Contribution to the Continental Moisture Budget of the United States," *Journal of Climate*, Vol. 8: 784-806.
- Hirschboeck, Katherine K., 1988. "Flood Hydroclimatology." in V.R. Baker *et al.*, ed., *Flood Geomorphology*. John Wiley: New York: 27-49.
- Keables, Michael J., 1989. "A Synoptic Climatology of the Bimodal Precipitation Distribution in the Upper Midwest." *Journal of Climate*, Vol. 2: 1289-1294.
- Knox James C., 1988. "Climatic Influence on Upper Mississippi Valley Floods." in V.R. Baker *et al.*, ed., *Flood Geomorphology*, John Wiley: New York: 279-300.
- Koellner, William H., 1996. "The Flood's Hydrology," in Stanley A. Changnon, ed, *The Great Flood of 1993 Causes, Impacts, and Responses*, Boulder, CO: Westview Press: 29-51.

- Kunkel, Kenneth E., 1994. "A Climatic Perspective on the 1993 Flooding Rains in the Upper Mississippi River Basin." *Water International*, Vol. 19: 186-189.
- Kunkel, Kenneth E., Stanley A. Changnon, and Robin T. Shealy, 1993. "Temporal and Spatial Characteristics of Heavy Precipitation Events in the Midwest," *Monthly Weather Review*, Vol. 121: 858-866.
- Kunkel, Kenneth E., Stanley A. Changnon, and James R. Angel, 1994. "Climatic Aspects of the 1993 Upper Mississippi River Basin Flood," *Bulletin of the American Meteorological Society*, Vol. 75, No. 5: 811-822.
- Martin, Major Donald E., 1952. "The Weather and Circulation of April 1952," *Monthly Weather Review*, Vol. 80, No. 4: 70-72.
- Mo, Kingtse C., Julia Nogues-Paegle and Jan Paegle, 1995. "Physical Mechanisms of the 1993 Summer Floods." *Journal of the Atmospheric Sciences*, Vol. 52, No. 7: 879-895.
- O'Connor, James F., 1965. "The Weather and Circulation of April 1965 Disastrous Floods and Tornadoes in the Midwest," *Monthly Weather Review*, Vol. 93, No. 7: 465-473.
- Parrett, Charles, Nick B. Melcher, and Robert W. James, Jr., 1993. *Flood Discharges in the Upper Mississippi River Basin, 1993*. U.S. Geological Survey Circular 1120-A, U.S. Government Printing Office.
- Rodenhuis, David R., 1996. "The Weather that Led to the Flood," in Stanley A. Changnon, ed, *The Great Flood of 1993 Causes, Impacts, and Responses*, Boulder, CO: Westview Press: 29-51.
- Upper Mississippi River Comprehensive Basin Study Coordinating Committee (UMRCBS), 1972. *Upper Mississippi River Comprehensive Basin Study* .
- U.S. Army Corps of Engineers, 1994. *The Great Flood of 1993 Post-Flood Report Upper Mississippi River and Lower Missouri River Basins*.
- Wahl, Kenneth L., Kevin C. Vining, and Gregg J. Wiche, 1993. *Precipitation in the Upper Mississippi River Basin, January 1 Through July 31, 1993*. U.S. Geological Survey Circular 1120-B, U.S. Government Printing Office.

3 Climate Variability and Mississippi and Missouri Floods

3.1 Introduction

Large floods are often associated with anomalous climate patterns. Flood frequency analysis generally assumes that the annual floods are independent and that there is not a trend or persistence in the annual flood data. On the other hand, some global climate patterns may persist over several years or show oscillations on an interannual to interdecadal time scale. Because of the large heat capacity of the oceans, one of the most important factors in climatic variability on time scales of several years to decades is how heat is absorbed, stored and released by the oceans (Burroughs, 1992). Anomalies related to changes in ocean temperatures and the associated changes in atmospheric circulation are a key to understanding climate patterns. Some of these patterns show long-term (interdecadal) oscillations, such as North Pacific sea surface temperatures. Other patterns, such as tropical Pacific sea surface temperatures, fluctuate on an interannual frequency and this frequency varies over the historical record. This section will examine some global climate patterns and review evidence that these patterns affect the likelihood of extreme wet weather in the Mississippi and Missouri basin.

3.2 *El Niño/Southern Oscillation (ENSO)*

The El Niño/Southern Oscillation (ENSO) is the best known of these patterns. El Niño refers to the warming of sea surface temperatures (SST) in the eastern tropical Pacific especially in the ocean along the western coast of South America. Fluctuations in atmospheric mass are associated with these changes in sea surface temperature. The Southern Oscillation refers to the sea-level pressure ‘seesaw’ between the southeastern tropical Pacific and the Australian-Indonesian region that is caused by differences in sea

surface temperature. One measure of the Southern Oscillation is the Southern Oscillation Index (SOI), which is determined by the difference between standardized sea-level pressure between Tahiti and Darwin, Australia (Diaz and Kiladis, 1992). The SST and SOI are highly correlated indices. Lower pressure in Tahiti implies a negative SOI and is correlated with warmer SSTs in the eastern tropical Pacific. Anomalous colder sea surface temperatures in the eastern equatorial Pacific are referred to as La Niña and are associated with a positive SOI. Figure 3.1 shows a graph of the 12-month moving average for the Southern Oscillation Index and an index of sea surface temperatures from 1933 to 1997.

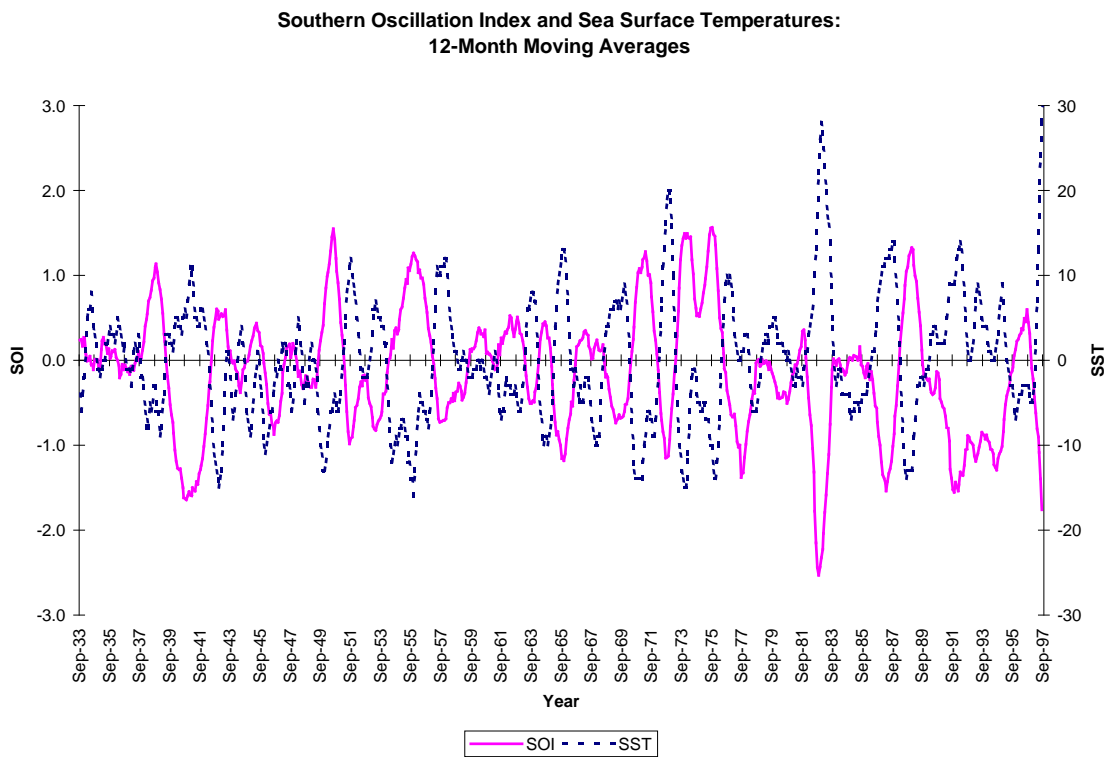


Figure 3.1: 12-month moving averages of the Southern Oscillation Index (SOI) and an index of tropical Pacific sea surface temperature anomalies from the Japan Meteorological Agency. Large negative SOI and positive SST indices indicate El Niño events.

The warm ocean surface causes increased evaporation and conditions favorable for convection and precipitation. During an El Niño episode rainfall increases over the warmer eastern tropical Pacific. Rainfall patterns change throughout the tropics. The increased convection affects atmospheric circulation patterns. Warm surface air is heated and rises. The rising moist air leads to convection and precipitation which releases the latent heat of vaporization and further heats the atmosphere. Changes in ocean temperature can bring about changes in the atmospheric circulation pattern. The tropical ENSO signal is propagated to the extratropics by large-scale atmospheric processes (Tribbia, 1991). Anomalous wave patterns can occur and affect the path of jet streams across the northern hemisphere. The storm track across North America may therefore be altered due to changes in the tropics. These linkages of weather anomalies are called “teleconnections.”

3.3 Studies of ENSO and Midwestern Hydroclimatology

Several studies have looked at how ENSO may affect precipitation and streamflow in the United States. Since El Niño events vary by length and intensity, different analysts have defined different years for El Niño. Either sea surface temperature (SST) or the Southern Oscillation Index (SOI) can be used to classify El Niño years. These two indicators are highly correlated, but some differences may result. Some examples of different interpretations of El Niño years are shown in Table 3.1. The correlation with Mississippi River basin precipitation and streamflow will vary depending on the years used. Differences in the definition of El Niño years add uncertainty to the analysis of ENSO impacts.

Table 3.1: Definitions of El Niño years used by various researchers.

Investigator	Comments	El Niño Years	Reference
U.S. Streamflow and El Niño, Kahya and Dracup	Positive SST phase begins in the December of the preceding year	1951, 1953, 1957, 1965, 1969, 1972, 1976, 1982, 1986	Kahya and Dracup (1993)
Climate Diagnostics Center (CDC), NOAA		1941-42, 1957-58, 1965-66, 1972-73, 1982-83, 1986-87, 1991-92	http://www.cdc.noaa.gov/ENSO/
Center for Ocean-Atmospheric Predictions Studies, Florida State University	El Niño phase runs from October of year to September of the next year	1951, 1957, 1963, 1965, 1969, 1972, 1976, 1982, 1986, 1987, 1991	http://www.coaps.fsu.edu/~legler/jma_index1.shtml
Climate Prediction Center (CPC), NOAA	El Niño years are classified by seasons:		http://nic.fb4.noaa.gov:80/products/analysis_monitoring/ensostuff/
	Sep-Nov	1905, 1914, 1918, 1941, 1965, 1987, 1991, 1994	
	Nov-Jan	1915, 1919, 1941, 1942, 1958, 1964, 1966, 1973, 1983, 1987, 1988, 1992, 1995	
	Jan-Mar	1915, 1919, 1941, 1958, 1966, 1969, 1973, 1983, 1987, 1992	
	Mar-May	1915, 1941, 1958, 1992	

3.3.1 Precipitation

Ropelewski and Halpert (1986) investigated the relationship between ENSO and North American precipitation and temperature patterns using spectral analysis. They analyzed two-year periods corresponding to ENSO events, designating the July preceding the ENSO event as July(-). Positive sea surface anomalies appear in December(-) with the maximum anomalies in year (0). The first harmonic of the monthly precipitation data is determined and plotted as a two-year harmonic dial vector. An example of a harmonic dial is shown in Figure 3.2. The vector points to the month with the peak positive magnitude. Regions of coherent response were determined by plotting these vectors on a map of North America (Figure 3.3). Ropelewski and Halpert noted three regions of both

a coherent response and a clearly defined wet or dry period within the two-year ENSO cycle: High Plains, the Great Basin, and the Gulf of Mexico. The High Plains (HP) region includes the watersheds of the Platte and Kansas Rivers which discharge into the Lower Missouri River. The direction of the vector indicates that the precipitation response in the High Plains to El Niño would occur in the spring to fall of the El Niño year. Note that the Upper Midwest region appears to also include coherent harmonic vectors (Kahya and Dracup, 1993) but was not noted by Ropelewski and Halpert. Time series of the precipitation for the regions were analyzed to determine the percentage of the time that the identified response actually occurred with the ENSO events. Above median precipitation occurred in 8 of 11 ENSO events between 1931 and 1983. However, using a longer time series, above normal precipitation occurred in only 16 of 24 ENSO events. This result is not significant at the 90% level. Ropelewski and Halpert concluded, “it does not appear that ENSO is a reliable discriminator of precipitation anomalies for the HP region” (Ropelewski and Halpert, 1986).

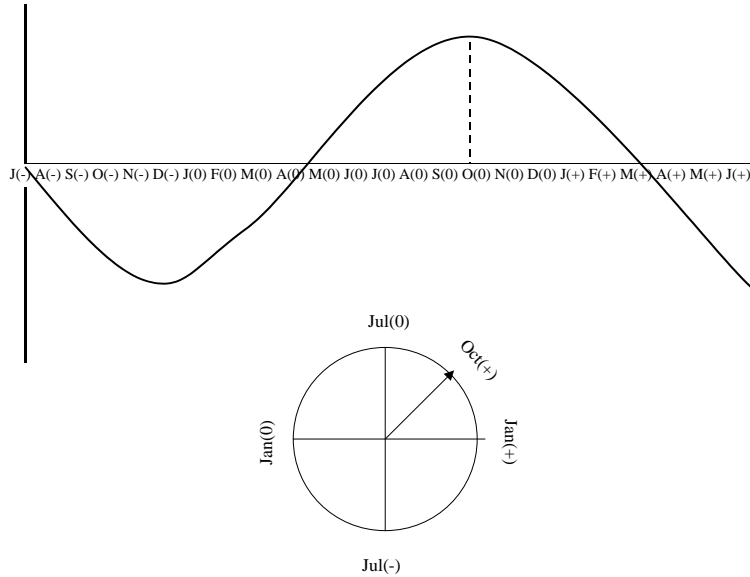


Figure 3.2: An example of a plot of a first harmonic and a harmonic dial. The vector points to the month with the peak positive magnitude, which in this example is in October of the ENSO year (year (0)).

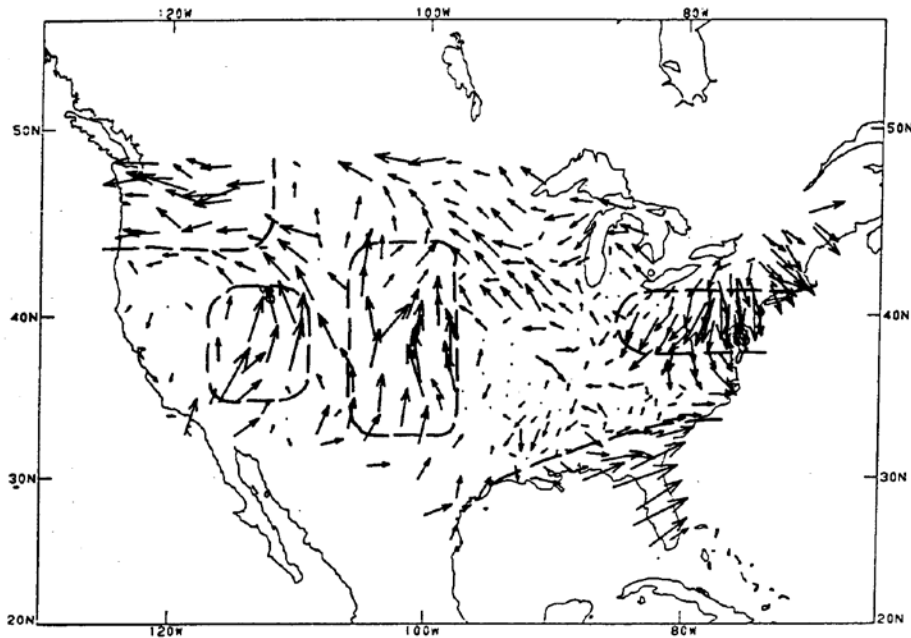


Figure 3.3: The phase and magnitude of precipitation vectors of the 24-month aggregate composite of ENSO events are plotted as a harmonic dial with the direction indicating the phase and the length the magnitude. The response for the North Central region was not identified as a coherent region by Ropelewski and Halpert while the High Plains vectors generally point toward the north, indicating the maximum positive response occurring in the April to October period of the ENSO year (Ropelewski and Halpert, 1986).

The National Oceanic and Atmospheric Administration also has examined the relationship between El Niño and precipitation in the contiguous United States. The Climate Prediction Center (CPC) ranked the mean precipitation for particular periods from wettest to driest and then looked at the average for strong ENSO events. (See Figure D-3.1 in Appendix D.) For the Upper Mississippi and Lower Missouri basins, the autumn months were wetter during ENSO events. Some regions also were wetter during the November to March period. However, some areas were drier than normal during the spring months of March to May. The CPC also determined the number of times that the mean precipitation for strong ENSO events ranked among the wettest or driest third of the record using four different time periods. (See Figure D-3.2 in Appendix D.) Several regions in the Upper Midwest were in the wettest third for the September to November period. Some areas were also wet in the January to March period.

The Midwestern Climate Center (MCC) compared snowfall levels during eight strong El Niño events with levels during other winters. They concluded that there is a significant reduction during the El Niño winters. For much of the Upper Mississippi basin, the reductions were in the range of 10 to 20 inches (MCC, 1997) (Figures D-3.3, D-3.4 in Appendix D). The MCC also examined temperature and precipitation patterns for the Midwest for El Niño periods and found that a wide variety of climate conditions occurred. They concluded that “there are other factors influencing our climate, perhaps the most important is the natural variability of the climate system” (MCC, 1997).

3.3.2 *Streamflow*

Kahya and Dracup (1993) used a methodology similar to that of Ropelewski and Halpert to analyze the relationship between ENSO and streamflow in the contiguous

United States. Their goal was to identify regions which “have strong and consistent ENSO-related streamflow signals.” Streamflow includes the effects of not only precipitation changes, but also changes in soil moisture storage and evapotranspiration. They used a similar criteria as Ropelewski and Halpert, designating the year with the maximum positive sea surface anomalies as year (0). The data were from 1948 to 1988 and included nine ENSO events. The first harmonic of the 24-month composite time series corresponding to ENSO events was assumed to be an ENSO-related signal appearing in the streamflow record. Four regions were identified by the similarity in the direction of the vector: the Northeast, the Gulf of Mexico, the North Central, and the Pacific Northwest (Figure 3.4). The North Central region includes parts of both the Upper Mississippi and Missouri Basins. The North Central region experiences dry conditions in the year preceding the ENSO event (year (-)), wet conditions during the ENSO year (year (0)), and normal conditions during the following year (year (+)).

The streamflow for each gage was fitted to a lognormal probability distribution. The 81 stations in the North Central region were combined to form an aggregate streamflow composite. Figure 3.5a shows the streamflow composites for the El Niño cycle indicating the dry and wet periods. Kahya and Dracup (1993) considered the April(0) to January(+) wet period as the period of the ENSO signal. This period includes the spring, summer, and autumn following the maximum sea surface temperature anomaly.

An index time series was created by averaging the lognormal streamflow percentiles for the ENSO signal season. This yearly time series is shown in Figure 3.5b. Only 15 of the 41 index values were wetter than the median. Six of these wet years

occurred in the 9 El Niño years. The four wettest years occurred during an ENSO event. In Figure 3.5b, the dotted lines are the upper (90%) and lower (10%) quantiles for the distribution of the index time series values based on plotting position. It does not show statistical significance.

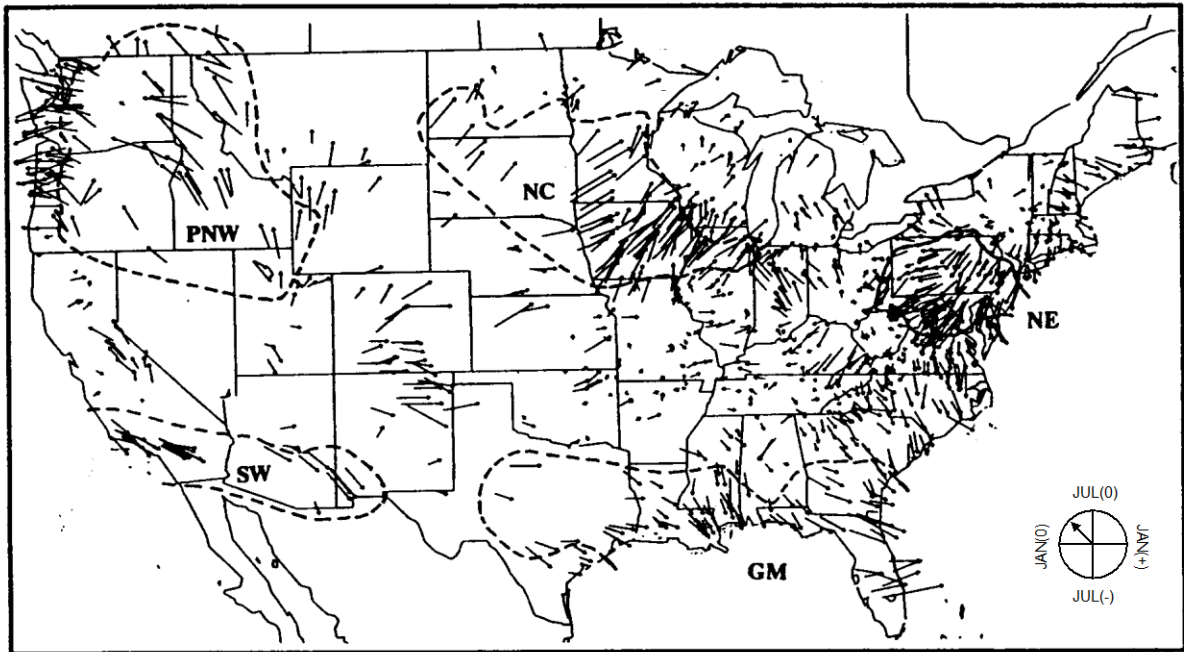


Figure 3.4: The phase and magnitude of the 24-month aggregate composite of ENSO events are plotted as a harmonic dial with the direction indicating the phase and the length the magnitude.

The streamflow vectors for 1009 gages are shown here. The vectors for the North Central region generally point toward the northeast, indicating the maximum positive response occurring in the autumn of the ENSO year (Kahya and Dracup, 1993).

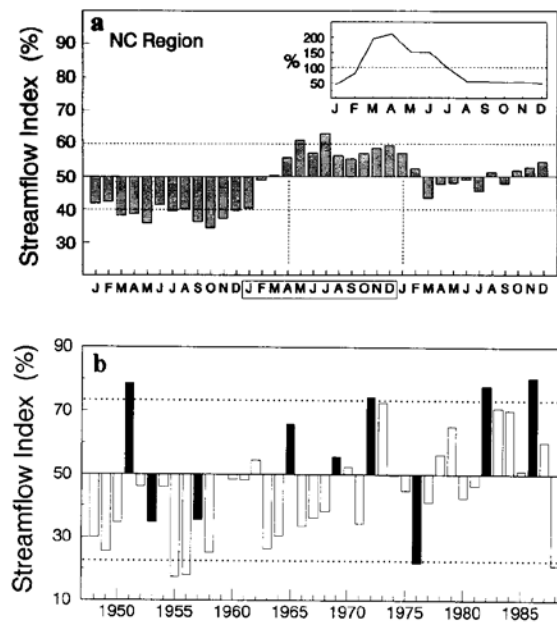


Figure 3.5: (a) An ENSO aggregate composite for the North Central region of the United States.

The season with an ENSO response is April(0) to January(+). The months in the box refer to the El Niño (or 0) year. The inset diagram shows the regional pattern of streamflow with the y-axis values corresponding to monthly normals as a percentage of the annual mean. (b) An index time series for the North Central region for the April to January season. ENSO years are solid bars. The dotted lines are the upper (90%) and lower (10%) quantiles for the distribution of the index time series values (Kahya and Dracup, 1993).

Dracup and Kahya (1994) also looked at the relationship between La Niña and streamflow for nine La Niña events between 1948 and 1988. They assumed that below average anomalies during the period July(0) to January(+) was the response of streamflow in the North Central region to La Niña. Figure 3.6a shows a composite of monthly flows associated with La Niña with drier conditions being evident. In addition, lower than normal streamflow occurred in the July(0) to January(+) period in seven of the nine La Niña events (Figure 3.6b). Dracup and Kahya also tested the statistical significance of the relationship between streamflow and the two extreme phases of the Southern Oscillation.

The relationship for the North Central region was significant at the 95% level for El Niño events and significant at the 99.9% level for La Niña events.

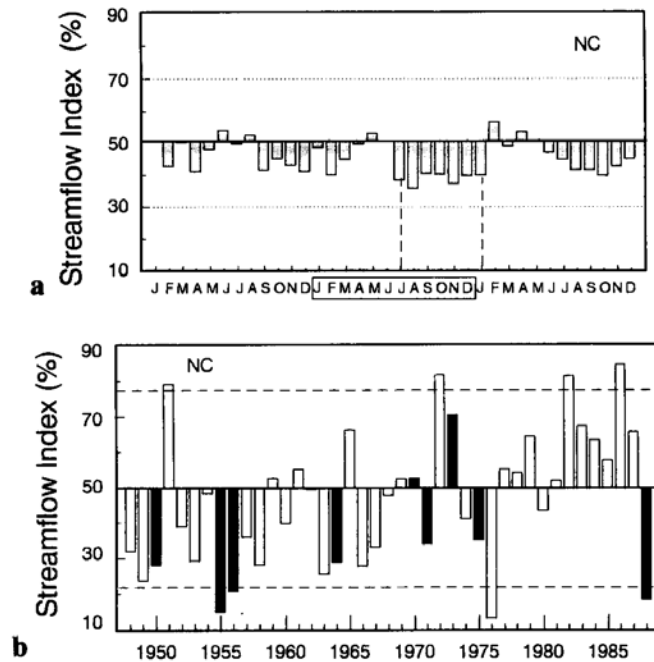


Figure 3.6: (a) A La Niña aggregate composite for the North Central region of the United States.

The season with a La Niña response is July(0) to January(+). The months in the box refer to the La Niña (or 0) year. (b) An index time series for the North Central region for the July to January season. ENSO years are solid bars. The dotted lines are the upper (90%) and lower (10%) quantiles for the distribution of the index time series values (Dracup and Kahya, 1994).

Guetter and Georgakakos (1995) also looked at the relationship of the Southern Oscillation and streamflow in the Upper Midwest, in particular the Iowa River in Iowa. They found that high streamflows were generally associated with El Niño and low flows with La Niña. The high flows tended to lag an El Niño winter by three to five seasons. The probability of above-normal spring flow five seasons following a warm ENSO winter was 70%. Guetter and Georgakakos hypothesized the lag time was due to (1) time to develop circulation patterns that bring excess rainfall to the Midwest and (2) time for soil water levels to increase which in turn leads to higher streamflow.

3.3.3 Floods

The influence of El Niño on Mississippi River floods was assessed by graphing annual floods at several stations on the Mississippi and Missouri Rivers against the average Pacific sea surface temperature during the months of March through June. For the more recent period (1950-1996), El Niño events appear to be associated with larger floods and La Niña events with smaller peak annual floods. Figure 3.7 shows a graph for St. Louis. However, there does not appear to be as much correlation in a longer record period (1868-1996) (Figure 3.8). There are several possible explanations of this difference; climate patterns may be different in the more recent period, the data before 1949 may not be as accurate, and the more recent period is a small sample out of the population of El Niño years.

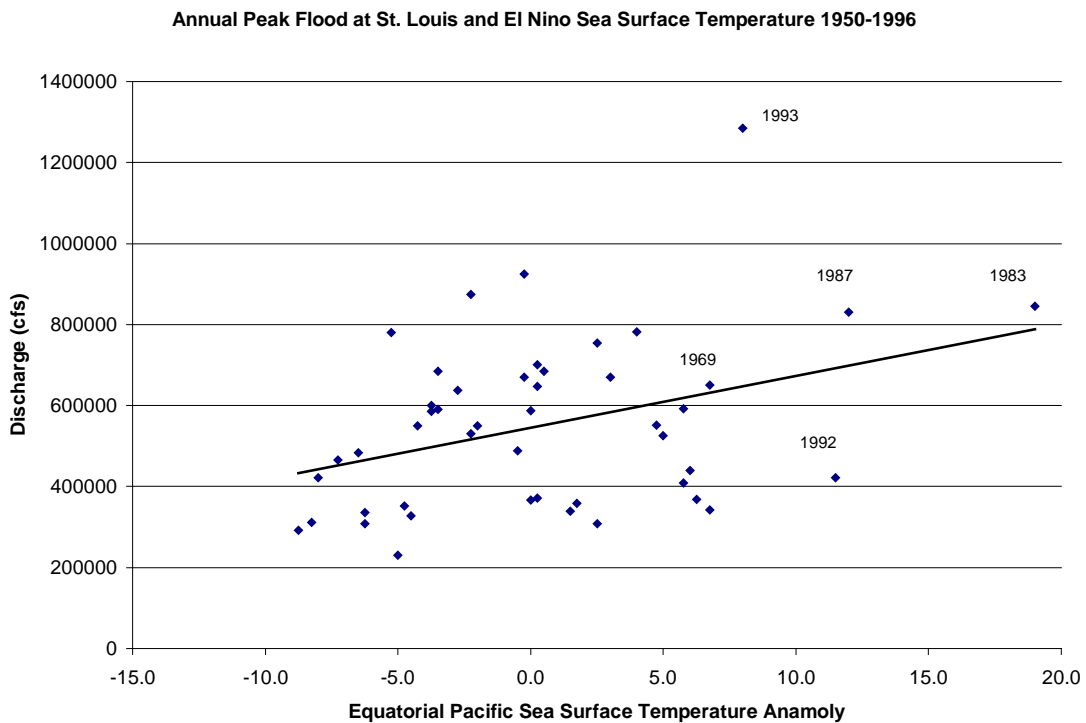


Figure 3.7: Annual floods (1950-1996) for the Mississippi River at St. Louis and tropical Pacific sea surface temperature anomalies.

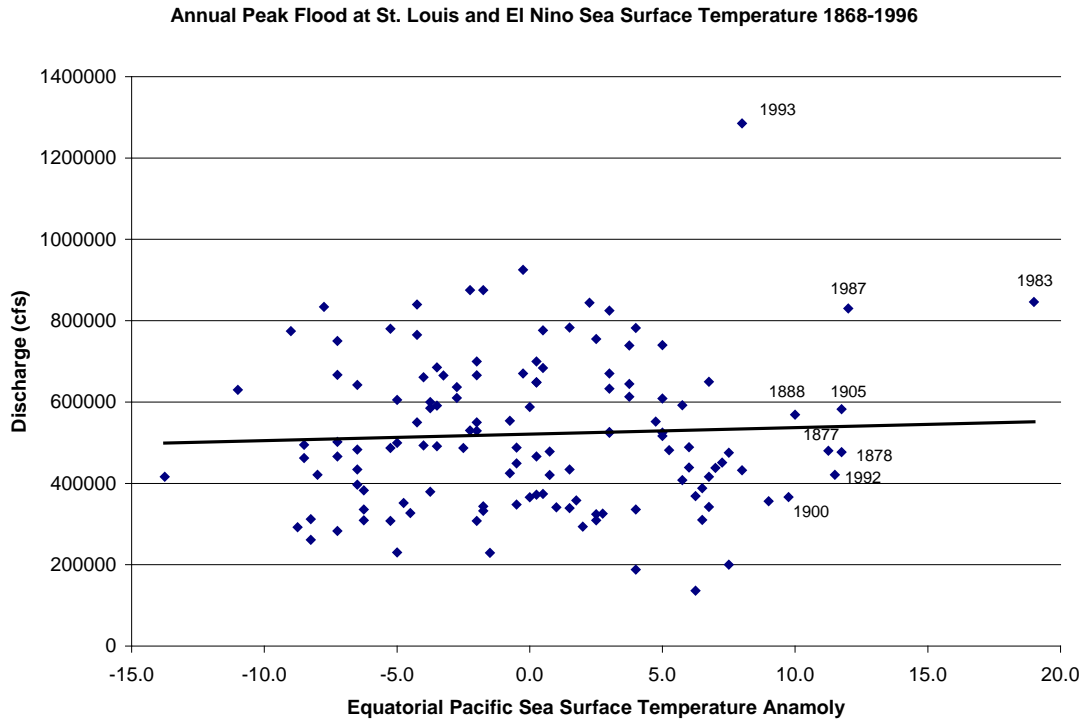


Figure 3.8: Annual floods (1868-1996) for the Mississippi River at St. Louis and tropical Pacific sea surface temperature anomalies.

Figure 3.9 shows a log Pearson III probability distribution fitted to the Mississippi River at Hannibal annual peak flood data using the data for 1879 to 1996. "El Niño" year floods and other floods are plotted using the Weibull plotting position based upon the entire record of 129 years. The El Niño years were defined as the fifteen years with the highest positive sea surface temperature anomalies during the months of March to June. The El Niño floods and the other floods in general fit the distribution. The 1993 flood is the largest flood of record at Hannibal and is classified as an El Niño flood. As long as the frequency and intensity of El Niño events are not changing, flood frequency analysis can account for climate variability associated with El Niño events.

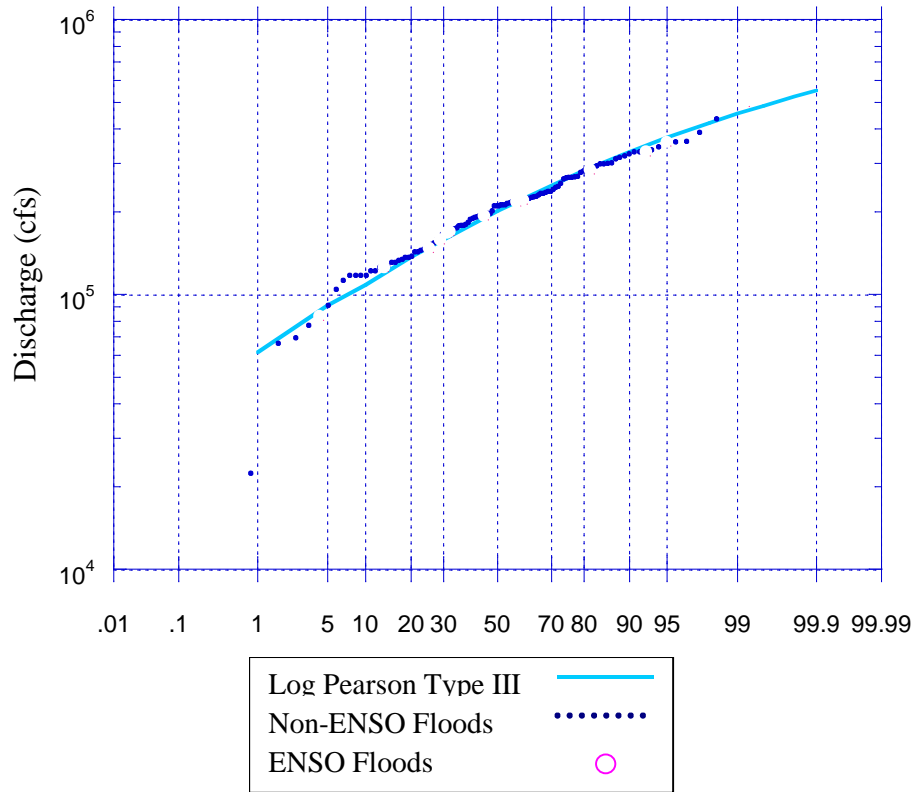


Figure 3.9: El Niño floods and other floods plotted with the Log-Pearson III distribution fitted to the peak annual floods for the Mississippi River at Hannibal, Missouri.

3.4 Pacific Ocean Climate Patterns

3.4.1 North Pacific Patterns

Climate variations over the north Pacific also influence the climate over North America. The northern Pacific Ocean sea surface temperature exhibits low frequency variability. Low frequency fluctuations in sea surface temperature are positively correlated with changes in sea level pressure in the area (Latif and Barnett, 1996). An index based on sea level pressure was defined by Trenberth and Hurrell (1994) as the area weighted mean sea level pressure over the region 30 to 65°N and 160°E to 140°W and was designated as the NP index. Another sea level pressure index, the central North

Pacific (CNP) index, measures a slightly different area (35 to 55°N and 170°E to 150°W (Cayan and Peterson, 1989).

Another index of climate variability in the north Pacific is the Pacific/North American pattern (PNA) (Figure D-3.5; Appendix D). The PNA index is based on 500-mb monthly mean geopotential height at four centers of the pattern (Trenberth and Hurrell, 1994). During the winter, the center over the Aleutian Islands covers most of the North Pacific. A center of opposite sign is located near the Canadian-United States border between the Rocky Mountains and the Pacific Ocean. A center with the same sign like the Aleutian center is near the southeastern United States. Another center of opposite sign occurs near Hawaii. This pattern appears in all months except June and July. During the spring, the Aleutian center contracts while the Hawaii center expands. According to Lins *et al.* (1990), the pattern is “almost certainly the primary determinant of winter weather for most of the North American continent.” The PNA index is negatively correlated with the NP index (about -0.9) (Trenberth and Hurrell, 1994).

Other indices use sea level pressure (NPPI) or for sea surface temperature (PDO or Pacific Decadal Oscillation). Variability on both an interdecadal and interannual timescale can be seen in these north Pacific indices. The interdecadal variability is shown in Figure 3.10. The sea level pressure index NPPI is moderately correlated with sea surface temperature (PDO) (correlation about 0.5). The NPPI and the SOI are slightly negatively correlated so the Aleutian Low tends to be more intense during winters with weakened easterly winds near the equator in the Pacific.

The positive phase of the PNA pattern is associated with a dry ridge over the western United States and a wet trough over the eastern United States. The negative

phase has an opposite pattern. There is a strong wintertime relation between low frequency anomalies of atmospheric pressure south of the Aleutian Islands and air temperature over North America. Higher than normal pressure in the Aleutians correspond with lower than normal temperatures over the northern United States, including the Upper Mississippi and Missouri region. There is also a significant correlation between pressure south of the Aleutians and precipitation over North America. In the Upper Mississippi and Lower Missouri region, the correlation is about 0.4 (Latif and Barnett, 1996). The PDO is negatively correlated with precipitation over much of the interior of North America (Mantua *et al.*, 1998).

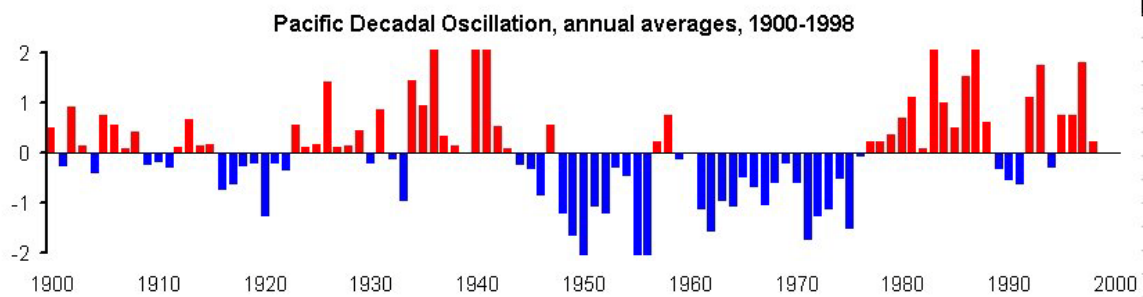


Figure 3.10: The annual average Pacific Decadal Oscillation from 1900 to 1998 (International Pacific Halibut Commission, University of Washington).

3.4.2 Other Pacific Ocean Patterns

Another pattern that appears in the winter is the Tropical/Northern Hemisphere Pattern (TNH) (Figure D-3.6; Appendix D) (Lins, *et al.*, 1990). The TNH is similar to the PNA, but the TNH centers are displaced eastward and are out of phase with the PNA (Barnston and Livezey, 1987). One center is positioned off the Pacific Northwest in the Gulf of Alaska. An oppositely signed center is located north of the Great Lakes. A third center with a similar sign as the Pacific center is located in the vicinity of Cuba (Lins *et*

al., 1990). The TNH is associated with changes in the location of the Pacific jet stream. Negative phases of the TNH are often observed during El Niños in the tropical Pacific.

The West Pacific oscillation (WP) (Figure D-3.7; Appendix D) occurs over the North Pacific in all months. It has the most influence on North American weather in the winter and spring (November to April). In the winter and spring, there is one center over the Kamchatka peninsula and an oppositely signed anomaly over southeast Asia and the low latitudes of the western north Pacific. There is also a moderately strong center over the southern and central United States with a sign similar to the Kamchatka center (Barnston and Livezey, 1987). According to Lins *et al.* (1990), the Western Pacific pattern produces a pattern of either dry or wet conditions over much of the coterminous United States and Mexico.

The East Pacific pattern (EP) (Figure D-3.8; Appendix D) occurs in all months except August and September. It is marked by a northern center near Alaska and an opposite southern center east of Hawaii. A persistent negative phase of this pattern occurred from early 1992 to July 1993 along with mature El Niño in the tropical Pacific. The subtropical jet stream was stronger than normal and displaced toward the southwestern United States. This pattern brought above normal precipitation to the United States and contributed to above normal soil moisture conditions before the 1993 Mississippi River flood.

3.4.3 *Spring Climate Patterns*

Two patterns appear in the spring. Another pattern called the North Pacific pattern (NP) (Figure D-3.9; Appendix D) appears in March through July. The primary center is in the middle latitudes of the western and central North Pacific. There is a

weaker center of opposite sign located in Alaska and stretching from eastern Siberia to the western mountains of North America. Positive phases of the NP pattern are associated with a southward shift and intensification of the Pacific jet stream. The positive phase is often associated with El Niño conditions during the North American spring. One of the most pronounced and persistent positive NP phases occurred during the spring of 1993 and was an indirect cause of the 1993 Mississippi flood (Bell and Janowiak, 1995).

A second spring pattern which appears between May and August is the Pacific Transition pattern (PT) (Figure D-3.10). Two centers of similar sign are located over the intermountain region of the United States and the Labrador Sea east of Newfoundland. Two weaker centers of opposite sign are located over the Gulf of Alaska and the eastern United States. Pronounced negative phases of the PT pattern occurred during July 1993 with an anomalous trough over the Rocky Mountains and the upper Midwestern region downstream of the trough. An intensification and southward shift of the storm track resulted.

3.5 *North Atlantic Oscillation*

The North Atlantic Oscillation (NAO) (Figure D-3.11; Appendix D) consists of one center in the vicinity of Greenland and an oppositely signed center between 35°N and 40°N in the North Atlantic. The NAO index is the difference between sea level pressures between Iceland and the Azores (sometimes Iceland and Lisbon, Portugal are used). The positive phase of the NAO has below average pressures in the northern center and above average pressures over the central Atlantic and eastern United States, while the negative phase has an opposite pattern. The NAO pattern is present throughout the year but is

most pronounced in the winter. The sea surface temperatures and sea level pressure in the North Atlantic also exhibit variation on an interdecadal timescale (Kushner, 1994). Figure 3.11 illustrates this interdecadal variation. The NAO is associated with changes in the storm track across the North Atlantic. “The circulation of the anticyclone in the North Atlantic directly influences the atmospheric circulation and precipitation development in the central plains region of the United States” (Hu *et al.*, 1998). The low-level jet brings in a substantial amount of the moisture to the Missouri and Mississippi basin. The low-level jet is related to the anticyclone centered in the subtropical North Atlantic.

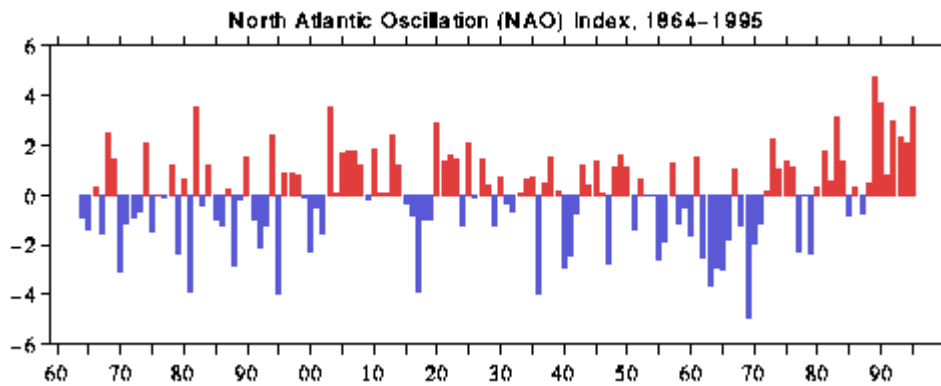


Figure 3.11: The average annual winter North Atlantic Oscillation Index from 1864 to 1995 (Climate Research Unit, University of East Anglia).

3.6 Relationship between Climate Patterns and Mississippi River Flow

When the average annual flow for the Mississippi River at Clinton is smoothed, a U-shaped Pattern can be seen with a low flow period occurring in the dry 1930s (Figure 3.12). Climate variability may explain this trend. Baldwin and Lall (1998) have attempted to relate climate indices with Mississippi River streamflow at Clinton, Iowa. They considered El Niño/Southern Oscillation, the North Atlantic Oscillation and the Central Pacific index. They found some lagged cross correlations significant at the 95% level. Fall and winter flows are correlated with ENSO, but not spring flows. There is

some correlation if the interaction between ENSO and the northern hemisphere indices are used. Summer flow is also correlated with the square of all the indices indicating that climate impacts may increase with the magnitude of the anomaly.

Baldwin and Lall (1998) also used spectral analysis to identify frequency bands common among Mississippi River streamflow and the climate indices. They found common bands at 3.1-3.6 years and 8.3-12.5 years. Baldwin and Lall speculated that the shorter interannual period was related to ENSO while the longer interdecadal period was related to the interaction of tropical and extratropical climate patterns. The frequencies corresponding to these two periods (0.1 cycles per year (cpy) and 0.28 cpy) are superimposed for streamflow in Figure 3.13. These two bands capture 73% of the interannual variance of streamflow including the 1988 low flow and the 1993 flood. The index showing the interaction of ENSO and the North Atlantic Oscillation show a similar oscillation pattern (Figure 3.14). Mississippi River streamflow may be related to these climate patterns.

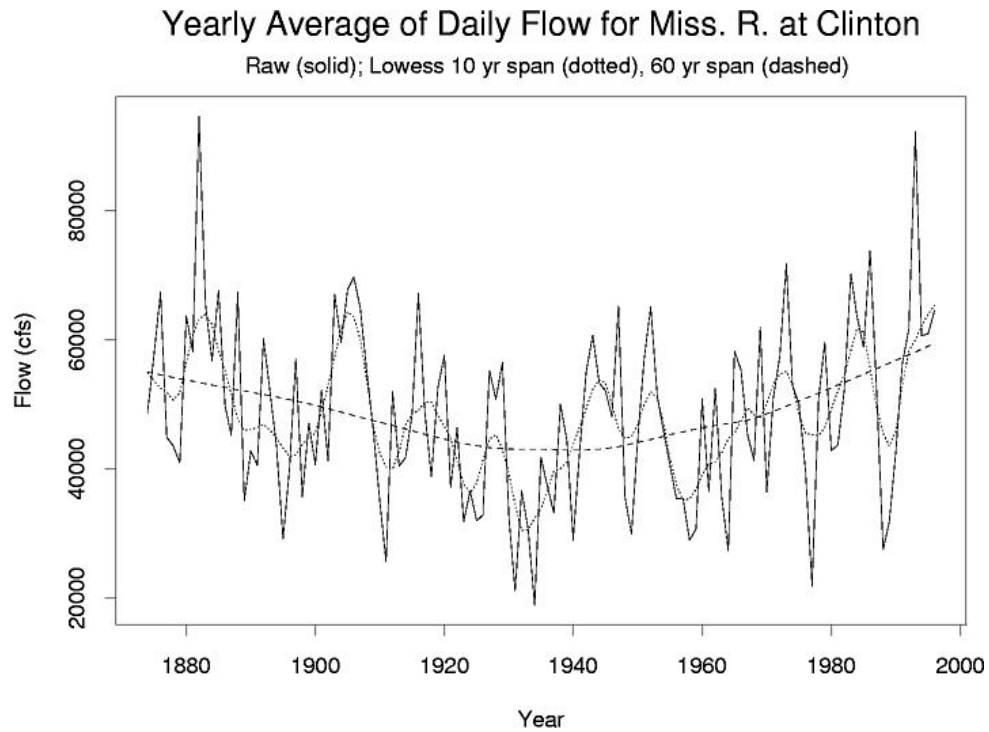


Figure 3.12: Annual average flow for each water year from 1874 to 1996 of the Mississippi River at Clinton, Iowa. LOESS is a technique to smooth the data (Baldwin and Lall, 1998).

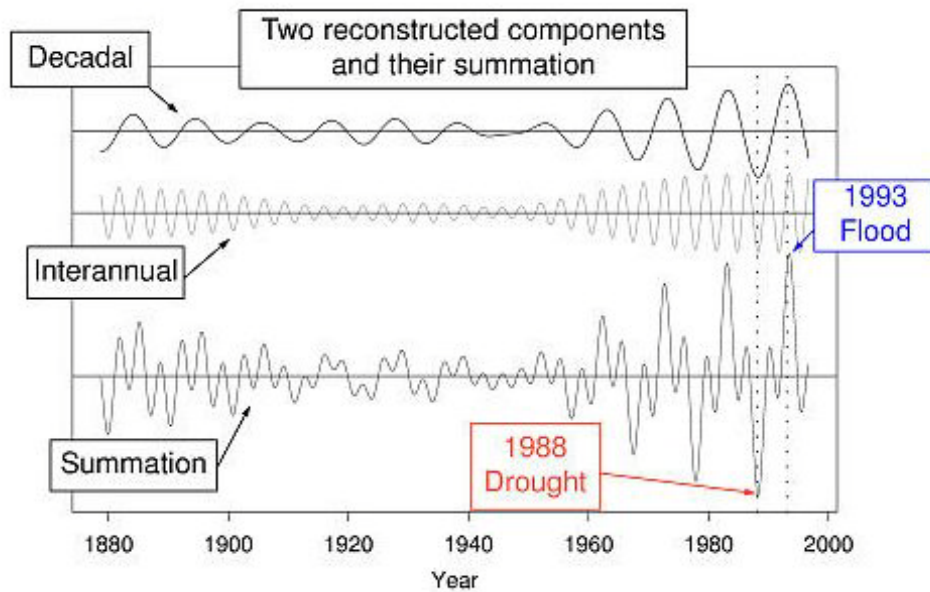


Figure 3.13: The superposition of the interannual (3.1-3.6 year) period and the interdecadal (8.3-12.5 year) period for Mississippi River flow at Clinton, Iowa (Baldwin and Lall, 1998).

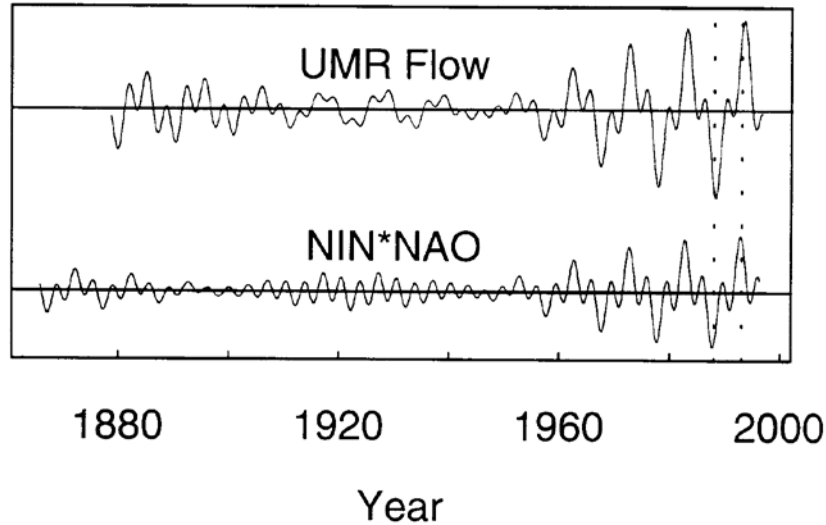


Figure 3.14: Superposition of the decadal (0.1 cycle per year) and interannual (0.28 cpy) frequencies for the Mississippi River at Clinton, Iowa and an index of ENSO (NIN) times North Atlantic Oscillation. The dotted lines highlight the 1988 low flow and the 1993 flood (Baldwin and Lall, 1998).

3.7 *Climate Patterns and Mississippi and Missouri Floods*

Low frequency interdecadal climate variation is a potential cause of apparent non-stationarity in the flood process. Global climate patterns such as the Pacific Decadal Oscillation (PDO) (Figure 3.10) and the North Atlantic Oscillation (NAO) (Figure 3.11) show this low frequency variability with recent excursions above and below the median lasting a decade or more. Another feature that required further analysis was the relationship between Mississippi and Missouri River floods with these large-scale climate patterns. A regression of the annual flood for three gages was performed on three climate indices and their interaction terms using 97 years of data. The gages were the Mississippi River at Hannibal, the Missouri River at Hermann, and the Mississippi River at St. Louis. The three climate indices were tropical Pacific sea surface temperature anomaly (SST), Pacific Decadal Oscillation (PDO), and the North Atlantic Oscillation. In addition, the squares of the indices were included (SST*SST, PDO*PDO, NAO*NAO) and the

interaction terms SST*NAO, SST*PDO, PDO*NAO. The analysis used data from two time periods 1900 to 1996 and 1950 to 1996. As shown in Table 3.2, using the entire 1900-1996 period, there is little relationship between the best explanatory variable and the observed floods. The R^2 for each site is less than 0.10. The p-values for the statistically significant variables included in the models using step backward regression are shown in Table 3.2. The interaction term for SST and NAO (SST*NAO) and SST are significant at the 10% level in the Hannibal model. PDO is significant at the 10% level for Hermann. PDO and the PDO*NAO are significant at the 5% level for St. Louis.

Also considered was the more recent and smaller data set for 1950-1996. The data after 1949 may be more accurate. Sea surface temperature data were directly observed after 1949, while the data prior to 1949 is reconstructed. The R^2 values increase for Hermann and St. Louis. Only SST is significant for Hannibal. PDO, PDO*SST, SST and SST*SST are significant at the 5% level for Hermann. Only PDO is significant for St. Louis.

Table 3.2: Terms with the most significance in multiple regression using 97-year (1900-1996) record.

Gage	Terms	P Value	R^2
Mississippi River at Hannibal	SST*NAO	0.03	0.06
	SST	0.09	
Missouri River at Hermann	PDO	0.06	0.04
Mississippi River at St. Louis	PDO	0.04	0.07
	PDO*NAO	0.04	

Table 3.3: Terms with the most significance in multiple regression using 47-year (1950-1996) record.

Gage	Terms	P Value	R ²
Mississippi River at Hannibal	SST	0.065	0.07
Missouri River at Hermann	PDO	0.024	0.31
	PDO*SST	0.028	
	SST	0.040	
	SST*SST	0.044	
Mississippi River at St. Louis (Model 1)	PDO	0.001	0.21
Mississippi River at St. Louis (Model 2)	SST	0.013	0.13

3.8 Summary

There is some evidence that global-scale climate patterns may affect Mississippi River flow. Some research indicates that El Niño/Southern Oscillation is related to higher flows in autumn and winter. However, these seasons have lower flows than other seasons and extreme floods usually do not occur in these periods. Climate in the north Pacific may affect the storm track across North America. Conditions in the north Atlantic may influence the low-level jet bringing moisture to the Midwest. Interdecadal oscillations are evident in the climate indices for the both the North Pacific and North Atlantic during the later half of the century. Simple regression analyses involving sea surface temperature (SST), the Pacific Decadal Oscillation (PDO), and the North Atlantic Oscillation (NAO) found little signal over the entire 97 year record. However, a significant signal could be observed over the last 47 years, so that PDO, SST and NAO values could partially explain the occurrence of large floods. However, even during this

more recent period, the regression analyses explained only a small percentage of the variability in the annual maximum floods.

3.9 References

- Baldwin, Connely K., and Upmanu Lall, 1998. "Interannual-to-Century Scale Variation and Climatic Teleconnections: The Upper Mississippi River," Utah Water Research Laboratory working paper, Utah State University.
- Barnston, Anthony G., and Robert E. Livezey, 1987. "Classification, Seasonality and Persistence of Low-Frequency Atmospheric Circulation Patterns," *Monthly Weather Review*, Vol 115: 1083-1126.
- Bell, Gerald D., and John E. Janowiak, 1995. "Atmospheric Circulation Associated with the Midwest Floods of 1993," *Bulletin of the American Meteorological Society*, Vol. 76, No. 5: 681-695.
- Burroughs, William James, 1992. *Weather Cycles Real or Imaginary?* Cambridge: Cambridge University Press.
- Cayan, Daniel R., and David H. Peterson, 1989. "The Influence of North Pacific Atmospheric Circulation on Streamflow in the West," Geophysical Monograph 55, American Geophysical Union: 375-397.
- Diaz, Henry F., and George N. Kiladis, 1992. "Atmospheric Teleconnections Associated with the Extreme Phases of the Southern Oscillation," *El Niño Historical and Paleoclimatic Aspects of the Southern Oscillation*, edited by Henry F. Diaz and Vera Markgraf, Cambridge: Cambridge University Press.
- Dracup, John A., and Ercan Kahya, 1994. "The Relationships between U.S. Streamflow and La Niña Events," *Water Resources Research*, 30 (7), 2133-2141.
- Guetter, Alexandre K., and Konstantine P. Georgakakos, 1995. "Are the El Niño and La Niña Predictors of the Iowa River Seasonal Flow," *Journal of Applied Meteorology*, 35, 690-705.
- Hu, Qi, C.M. Woodruff, and Stephen E. Mudrick, 1998. "Interdecadal Variations of Annual Precipitation in the Central United States," *Bulletin of the American Meteorological Society*, Vol. 79, No. 2: 221-229.
- Kahya, Ercan, and John A. Dracup, 1993. "U.S. Streamflow Patterns in Relation to the El Niño/Southern Oscillation," *Water Resources Research*, 29 (8), 2491-2503.

- Kushner, Yochanan, 1994. "Interdecadal Variations in North Atlantic Sea surface Temperature and Associated Atmospheric Conditions," *Journal of Climate*, Vol. 7: 141-157.
- Lins, Harry F., F. Kenneth Hare, and Krishnan P. Singh, 1990. "Influence of the Atmosphere," *Surface Water Hydrology*, edited by M. G. Wolman and H. C. Riggs, *The Geology of North America*, Vol O-1, Boulder, CO: The Geological Society of America, Inc.
- Latif, M., and T.P. Barnett, 1996. "Decadal Climate Variability over the North Pacific and North America: Dynamics and Predictability," *Journal of Climate*, Vol. 9: 2407-2423.
- Mantua, Nathan J., Steven R. Hare, Yuan Zhang, John M. Wallace, and Robert C. Francis, 1997. "A Pacific Interdecadal Climate Oscillation with Impacts on Salmon Production," *Bulletin of the American Meteorological Society*, Vol. 78, No. 6: 1069-1079.
- Midwestern Climate Center (MCC) 1997. "El Niño and the Midwest," <http://mcc.sws.uiuc.edu/elnino.html> , Champaign IL.
- Ropelewski, C.F., and M.S. Halpert 1986. "North American Precipitation and Temperature Patterns Associated with the El Niño/Southern Oscillation (ENSO)," *Monthly Weather Review*, 114, 2352-2362.
- Trenberth, Kevin E., and James W. Hurrell 1994. "Decadal Atmosphere-Ocean Variations in the Pacific," *Climate Dynamics*, Vol. 9: 303-319.
- Tribbia, Joseph J., 1991. "The Rudimentary Theory of Atmospheric Teleconnections Associated with ENSO," *Teleconnections Linking Worldwide Climate Anomalies*, edited by M.H. Glantz, R.W. Katz, and N. Nichols, Cambridge: Cambridge University Press.

4 Climate Change and Upper Mississippi and Missouri Basin Flooding

4.1 Mechanisms of Anthropogenic Climate Change

The atmospheric concentrations of carbon dioxide (CO₂), methane (CH₄), and nitrous oxide (N₂O) have grown significantly since pre-industrial times mainly due to human activities such as fossil fuel use and land use changes. The CO₂ concentration has increased by about 25% since 1850. Carbon dioxide in the atmosphere allows short-wave solar radiation to pass through, but absorbs the long-wave infrared radiation given off by the earth. Higher CO₂ concentrations therefore cause positive radiative forcing which can lead to higher temperature. Carbon dioxide remains in the atmosphere for decades to centuries, so the effect on radiative forcing is on a long-time scale. On the other hand, fossil fuel use and biomass burning can also increase levels of aerosols in the troposphere. Aerosols are microscopic particles suspended in the air, such as smoke and dust. These aerosols generally have had a cooling effect on particular regions. The aerosols are short-lived in the atmosphere.

The changes in atmospheric concentration of greenhouse gases are projected to lead to changes in climate. Global mean temperature is projected to increase 1 to 4.5°C by 2100 (Houghton *et al.*, 1996). Regional temperature changes could differ from the global mean. Higher temperatures may cause an intensification of the hydrological cycle. An increase in air temperature would increase evaporation. The capacity of air for water vapor increases 5 to 6% per degree Celsius (Rosenberg *et al.*, 1990). Evapotranspiration rates also depend on cloud cover, humidity, windiness, and vegetation characteristics

which all may change due to climate change. Actual evapotranspiration may increase or decrease depending on soil moisture.

There is more confidence in the projected increase in temperature than in predictions of future precipitation. Several models project an increase in precipitation due to the intensification of the hydrologic cycle. In addition, there is less confidence in regional projections than in the hemispheric to continental scale projections (IPCC, 1996). Most climate change models indicate increases in precipitation for North America. Stream runoff will be affected by changes in both potential evaporation and precipitation and could therefore increase or decrease depending on the region.

The timing of future runoff may also change. In general for the mid-latitude regions of North America, higher winter and spring temperatures may increase flows in winter and early spring and decrease flows in summer. Higher temperatures in winter might shorten the snow-cover season. One climate change scenario indicates a 70% decrease in the duration of snow cover in the Great Plains (IPCC, 1996). The warmer winter temperatures may cause less precipitation as snow and more as rainfall. On the other hand, increased precipitation could increase snowfall. Warmer temperatures could also lead to earlier snowmelt and ice break-up and more rain on snow events. Ice thickness may be reduced due to warmer temperatures reducing the potential for ice-jam flooding. One report projects a reduction in the duration and thickness of river ice cover and in the severity of ice jamming. However, sudden winter thaws and premature breakups may occur (Arnell *et al.*, 1996; IPCC, 1996).

4.2 *Climate Modeling and Prediction*

Climate models are mathematical descriptions of the atmosphere and ocean. The equations used in the models include equations of motion, the first law of thermodynamics, the equation of state and the balance equation for water vapor. Equations are used to model the input of solar radiation and the emission and absorption of terrestrial radiation. The climate equations are nonlinear and cannot be solved analytically. The equations are solved using numerical methods with a three dimensional grid over the globe. A grid cell in an atmospheric General Circulation Model (GCM) is about 250 km in the horizontal direction and 1 km in the vertical direction.

There are, however, many important processes which occur on a scale smaller than this size. For example, clouds both reflect solar radiation and block the escape of infrared radiation from the earth (Schneider, *et al.*, 1990). Cloudiness can affect both temperature and evapotranspiration but cannot be modeled explicitly in a GCM. These subgrid phenomena are represented by statistical relationships with larger scale variables resolved by the grid model, a technique called parameterization. The average cloudiness in a grid box is related to the average temperature and humidity in that box. The large-scale GCMs may also miss other localized forcing. These local effects could include inland water, topography, and vegetation (Giorgi and Mearns, 1991). There is additional uncertainty in some GCM output such as precipitation and evaporation because these smaller-scale processes cannot be adequately represented in the model.

4.3 *General Circulation Models and Regional Hydrologic Models*

Most hydrologic processes occur on a scale smaller than the resolution of the GCMs. The GCM output must be “downscaled” to model changes in a basin. Several

methods have been used to downscale GCM output. The IPCC has described four methods used in hydrologic modeling:

1. Direct use of GCM changes in temperature, precipitation, and evaporation applied to observed catchment data.
2. Stochastic generation of weather with parameters adjusted according to GCM output.
3. Estimation of catchment-scale weather from large-scale circulation patterns.
4. Use of nested regional models embedded within a GCM to simulate regional climate at a higher resolution.

The approach taken in the Corps of Engineers' study of the Missouri and Upper Mississippi River uses the first method (Lettenmaier *et al.*, 1996; 1998).

4.4 GCMs Used in Climate Simulations

Lettenmaier *et al.* (1996; 1998) investigated the potential effects of climate change on the Missouri River. The objective of this study, supported by the Institute for Water Resources, was to evaluate the performance of water management systems from transient climate changes. The approach in this study was to perturb historical precipitation and temperature records. The study used three transient GCM models and one scenario with doubled carbon dioxide ($2 \times \text{CO}_2$). The three transient GCM simulations were produced by (i) the Geophysical Fluid Dynamics Laboratory (GFDL) (Manabe *et al.*, 1991, 1992), (ii) the United Kingdom Meteorological Office (UKMO) (Murphy, 1995; Murphy and Mitchell, 1995), and (iii) the Max Planck Institute (MPI) (Cubasch *et al.* 1992). Each of these models is a coupled ocean-atmosphere model and simulated the time-dependent response of climate to increases in atmospheric CO_2 . A summary of these models is given in Table 4.1. In addition, a steady-state GCM using doubled atmospheric CO_2 was performed for comparison.

Table 4.1: Summary of the coupled ocean-atmosphere GCMs used in IPCC transient climate change experiments (Lettenmaier, *et al.*, 1998)

	<i>Geophysical Fluid Dynamics Laboratory (GFDL)</i>	<i>Max Planck Institute (MPI)</i>	<i>United Kingdom Meteorological Office (UKMO)</i>
Resolution (deg. Lat. by long.)	7.50 x 4.50 Ocean model: 3.75 x 4.5	5.62 x 5.62	3.75 x 2.50
Integration length (years)	100	100	75
Atmospheric Levels	9	19	11
Control ¹	300 ppmv	330 ppmv	323 ppmv
Climate change emission scenario	1%/yr	IPCC90 Scenario A	1%/yr
ΔT in year of double CO ₂	2.3	1.3	1.7
Year of double CO ₂	70	60	70

¹ equivalent global average trace gas concentration as CO₂, ppm by volume

There are several problems with the IPCC transient simulations. Different CO₂ concentration scenarios may be used by different GCMs for both the climate change runs and the control runs. Second, there is a “cold start” problem because the models assume an initial quasi-equilibrium state and neglect the thermal lag effect associated with ocean-atmosphere coupling due to greenhouse gases already in the atmosphere. Third, coupled atmosphere-ocean GCMs tend to drift away from a realistic climate as the simulation length increases. A lower boundary condition of the atmospheric model is the sea surface temperature while upper boundary conditions for the ocean model include the surface fluxes of heat, momentum, and fresh water. Inconsistencies between these surface fluxes cause the drift in the coupled models.

The IPCC transient climate scenarios use a “simple linked method” to deal with these problems. This method couples the interpretation of the three-dimensional GCM simulations to predictions from a simple one-dimensional climate model (Wigley and Raper, 1992) that starts with a pre-industrial climate and predicts the rate of change of

climate beginning in 1990. Greco *et al.* (1994) used the one-dimensional model to estimate the global average temperature changes for years 2020 and 2050 and then identified the corresponding decades with the same global average temperature change for each of the GCMs (designated as Decades 2 and 3).

4.5 Missouri River Basin

The Missouri River simulation was done by imposing mean monthly precipitation, temperature and solar radiation changes on historic records of precipitation and temperature. The analysis was actually five steady state analyses for each GCM scenario rather than an actual transient analysis. The temperature, precipitation and solar radiation changes had to be downscaled from the GCM results for forcing sequences for hydrologic models. Historical observations of daily temperature maxima and minima were adjusted by adding a fixed amount to the observed values. Historical observations of daily precipitation and solar radiation were multiplied by a fixed amount. The adjustment factors were the monthly average changes from base climate to the altered climate for the five quasi steady states from the transient GCMs. These changes were interpolated from gridded GCM output fields to specified locations used for the hydrologic model inputs. The basin-wide average temperature and precipitation adjustments for the Missouri River basin are shown in Figures 4.1 and 4.2.

A hydrologic model was used to produce hypothetical time series of streamflow. The National Weather Service River Forecast System snow model was used to estimate rain plus snow melt. This model output was used as input for a two-layer variable infiltration capacity model (VIC-2L). The hydrologic models were calibrated by comparing observed and simulated streamflow and adjusting model parameters to match

daily peak streamflow, baseflow recession, monthly flow volumes and long term average flow volumes as closely as possible. The basin-wide percent changes in potential evapotranspiration (PET) and streamflow for each GCM scenario are shown in Figures 4.3 and 4.4. Graphs of observed and simulated streamflow for two points on the Missouri River are shown in Figure 4.5.

Temperatures would increase under each scenario in each decade (Figure 4.1). Most of the increase occurs by decade 2 in contrast to the more even trend predicted for the global average temperature. The average temperature increases for the Missouri basin are projected to be higher than for the global average (0.53 C by decade 2 and 1.16 C by decade 5). Precipitation changes are less consistent among the different GCM simulations than temperature (Figure 4.2). The GFTR simulation produced a precipitation increase for the Missouri basin, while the other two transient GCMs showed decreases in precipitation. PET changes (Figure 4.3) were driven by temperature changes and increased for each scenario.

The streamflow changes (Figure 4.4) show disagreement between the GFTR model and the other two transient GCMs. The basin average streamflow changes reflect two hydrological effects: increased potential evapotranspiration and precipitation changes. The HCTR and MPTR show decreases in average annual streamflow of about 25 and 35 percent since they both project precipitation decreases. The GFTR model, on the other hand, projects a slight decrease in streamflow and the 2 x CO₂ GFDL model projects a slight increase. These are average annual changes in stream flow throughout the basin.

The average monthly flows for specific locations on the Missouri River generally show decreases. Average monthly flows for one IPCC decade for the four GCMs are given in Figures 4.6 and 4.7 for the Missouri River at Omaha, Nebraska and Hermann, Missouri. The simulated streamflows from the transient GCMs are generally reduced throughout the year. The GFDL 2 x CO₂ scenario shows increased streamflow in the winter and late spring and reduced flow in early spring and summer.

4.6 Changes in Climate Patterns

Global warming may also change global climate patterns such as El Niño. Since the late 1970s, El Niño events have become more frequent and La Niña events less frequent. A warm event in the tropical Pacific from 1990 to 1995 was the longest on record. Trenberth and Hoar (1996; 1997) calculated that the probability of this prolonged event is about one in 2,000 based on their statistical model of the time series. They therefore conclude that the ENSO changes may be linked to greenhouse warming. Rajagopalan *et al.* (1997), however, noted that this probability calculation is very sensitive to the choice of statistical model. They conclude that recent changes in ENSO behavior may be due to natural climate variability and not necessarily an effect of global warming. Knutson and Manabe (1998) used a global ocean-atmosphere model to examine decadal variability and trends in Pacific Ocean sea surface temperatures. They conclude that the recent trend in ENSO is not likely to be attributable only to natural variability but is a result of thermal forcing such as an increase in greenhouse gases in the atmosphere.

Simulations of future climate using both transient CO₂ and doubled CO₂ conclude that ENSO will continue to occur. Meehl *et al.* (1993) noted that ENSO anomalies

continued to occur in a General Circulation Model simulating a doubling of CO₂. They noted that increased CO₂ caused alternations in the extratropical teleconnections. A more recent Australian study found that the amplitude of ENSO events is slightly reduced but the frequency of events increases (Wilson and Hunt, 1997). Changes in the frequency, intensity, and duration of ENSO events may affect the calculation of flood frequencies if the ENSO events are associated with larger floods. However, there is not yet a clear understanding of if and how ENSO patterns will change as a result of global warming. In addition, the evidence for the link between ENSO and Mississippi and Missouri floods is also ambiguous.

4.7 Summary

There is a lot of uncertainty regarding the effects of future climate change on runoff. The General Circulation Models (GCM) considered here all agree that it is likely that temperatures will increase in the Upper Mississippi and Lower Missouri basin. The models disagree on whether precipitation will increase or decrease. Higher temperatures will tend to increase potential evapotranspiration, which in turn reduces soil moisture and lowers runoff. Forecasts of future runoff for the Missouri River therefore are uncertain and depend on which GCM is used. Simulations using GCM scenarios for the Lower Missouri River generally project lower average monthly flows. Simulations of Upper Mississippi streamflow using GCM scenarios will be conducted in the next phase of the study.

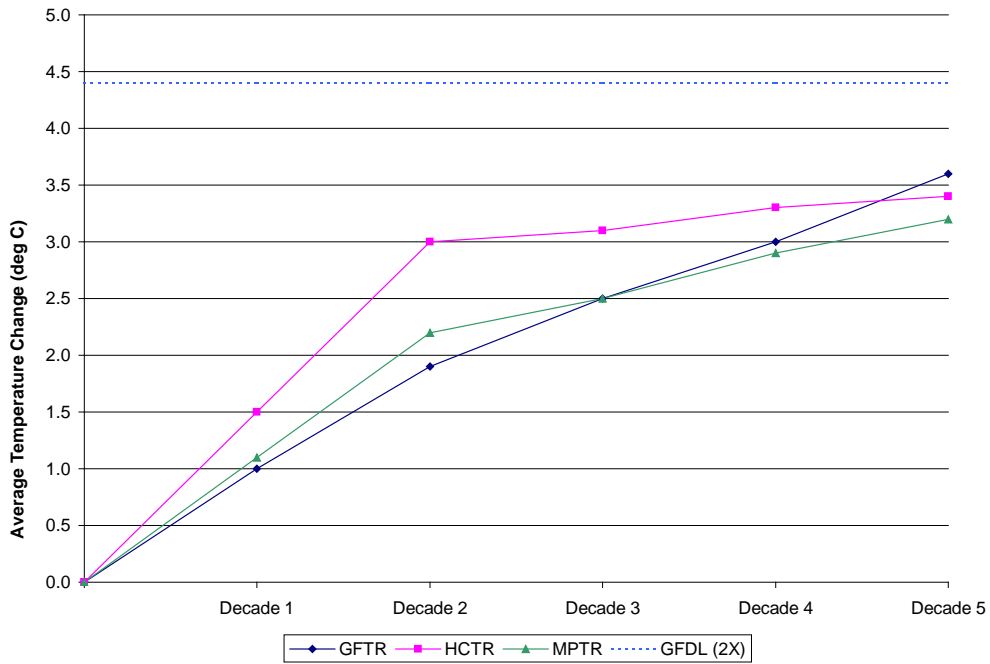


Figure 4.1: Average temperature changes in degrees Celsius for the Missouri Basin for four GCMs.

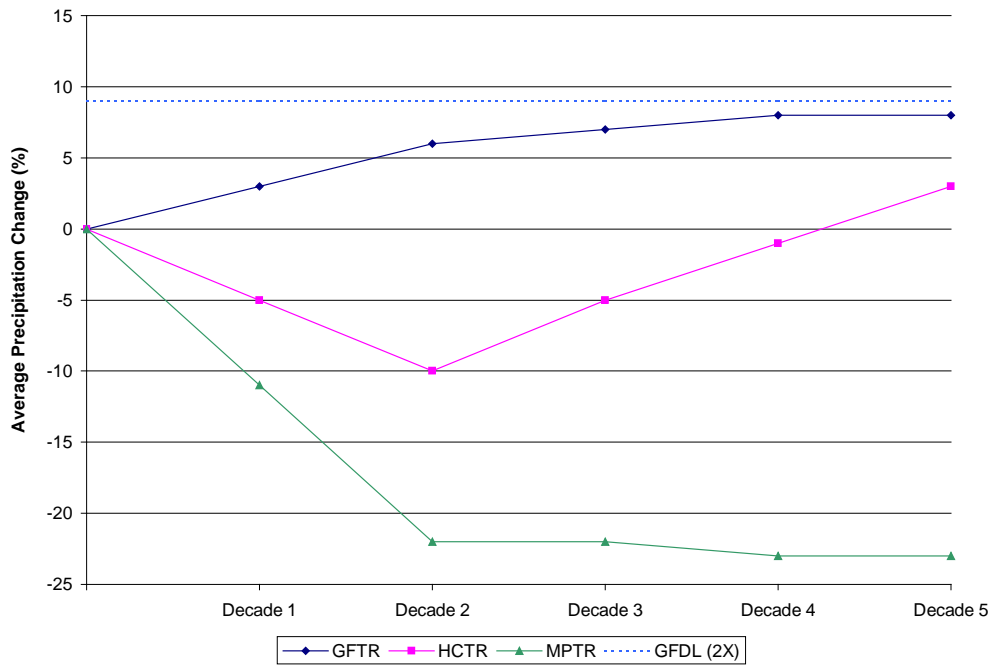


Figure 4.2: Average percentage change in precipitation for the Missouri Basin for four GCMs.

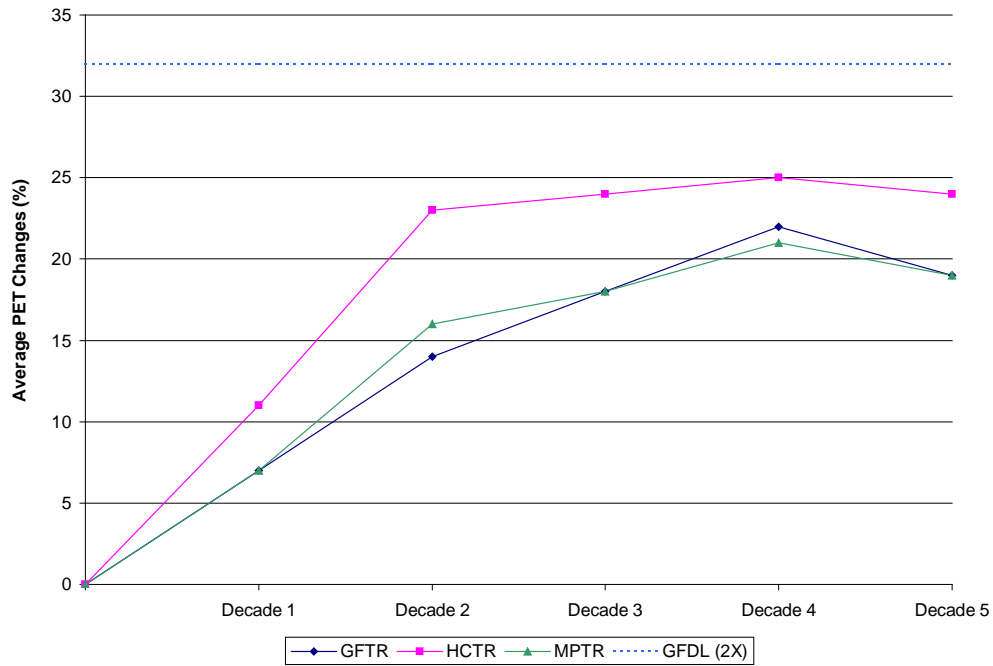


Figure 4.3: Average percentage change in potential evapotranspiration for the Missouri Basin for four GCMs.

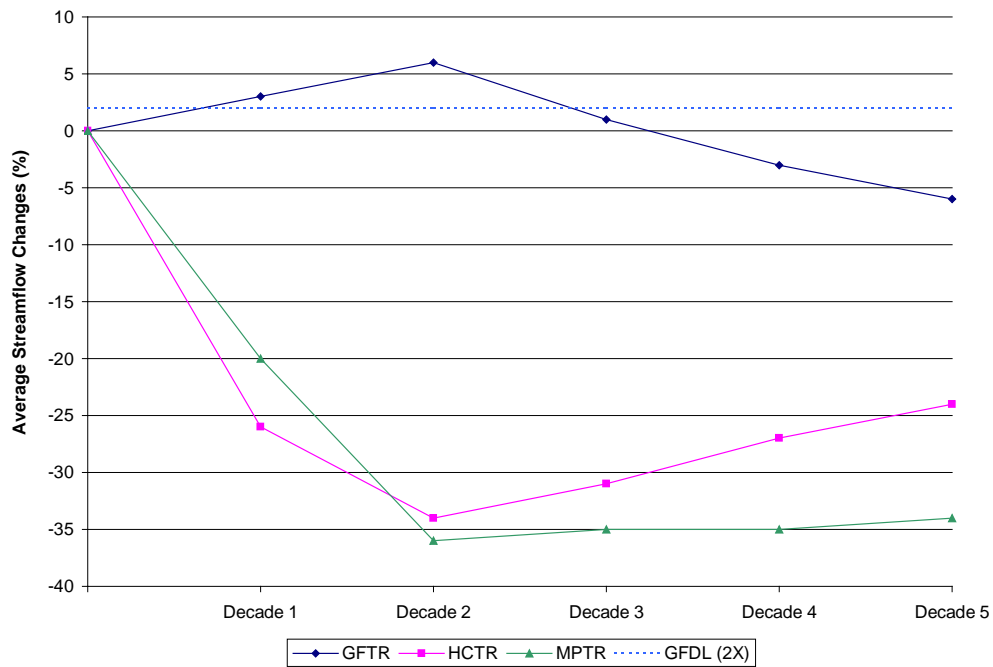


Figure 4.4: Average percentage change in streamflow for the Missouri Basin for four GCMs.

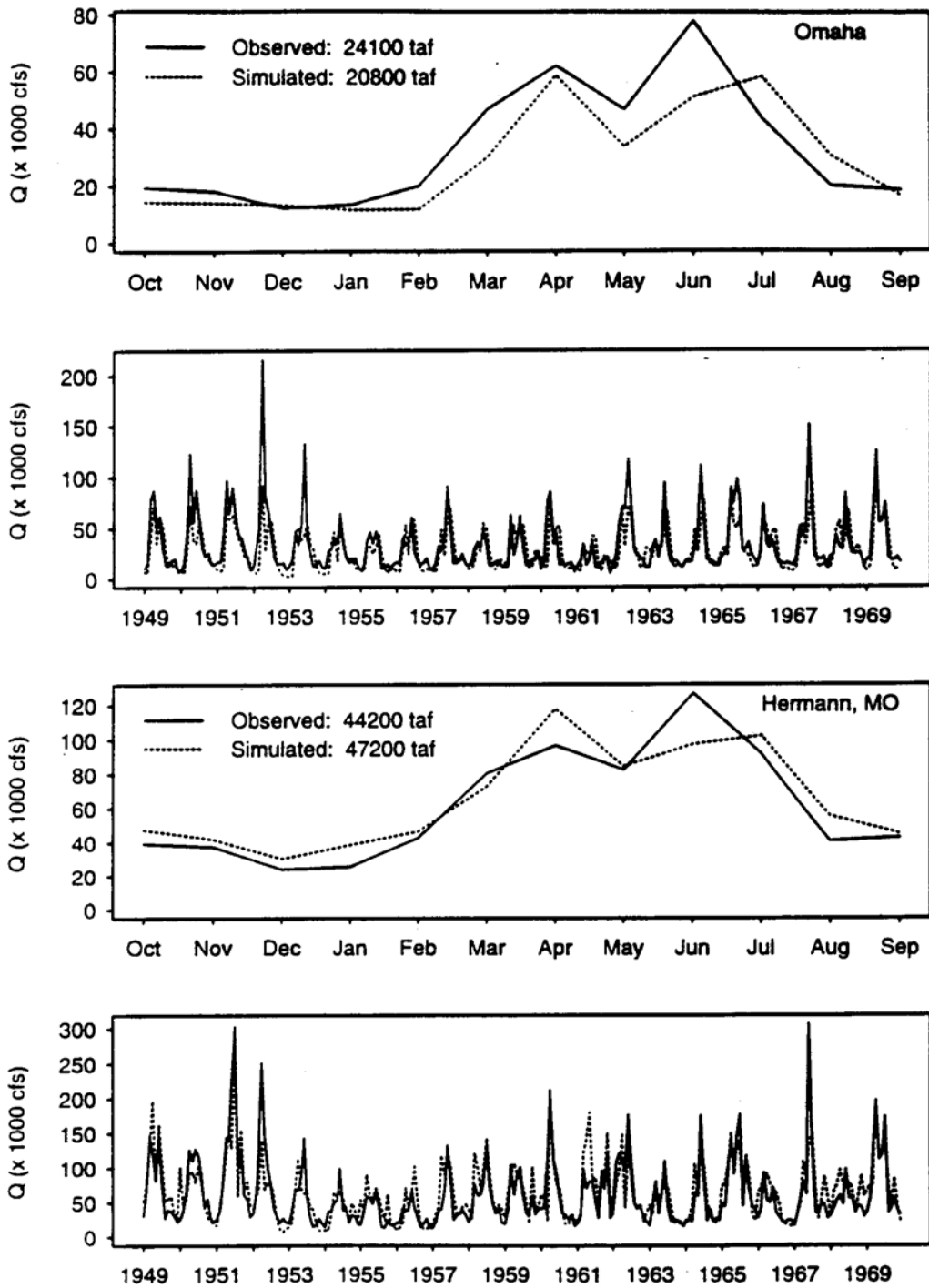


Figure 4.5: Observed versus simulated flows for the Missouri River at Omaha, Nebraska, and Hermann, Missouri (Lettenmaier *et al.*, 1996).

Missouri River at Omaha, NE

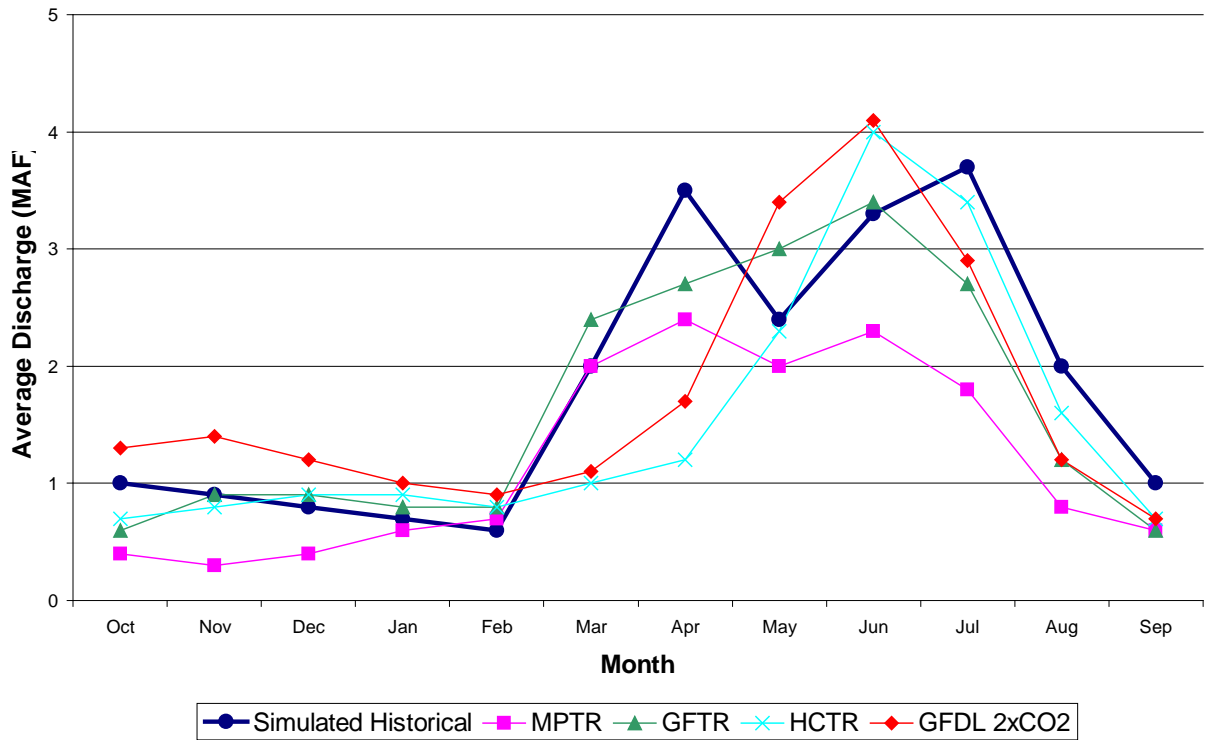


Figure 4.6: Change in average monthly streamflow for the Missouri River at Omaha as projected by four GCMs (Decade 3 for transient GCMs)

Missouri River at Hermann, MO

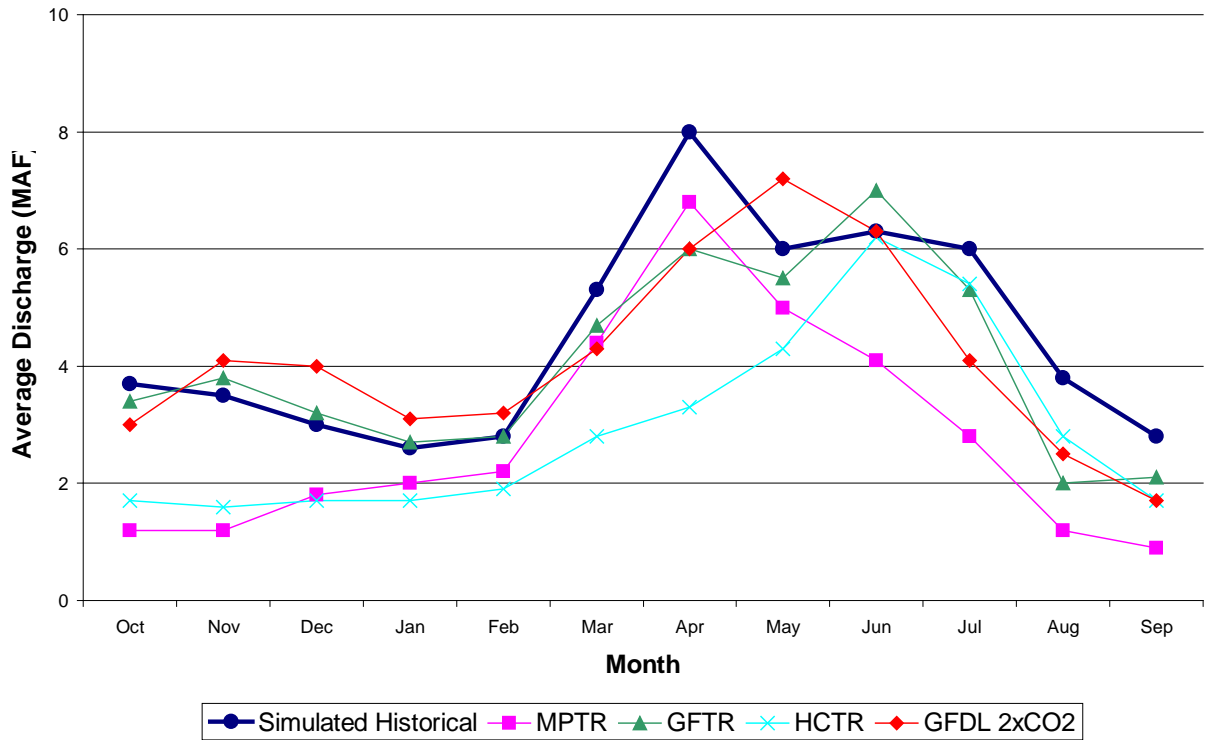


Figure 4.7: Change in average monthly streamflow for the Missouri River at Herman as projected by four GCMs (Decade 3 for transient GCMs)

4.8 References

- Arnell, Nigel, Bryson Bates, Herbert Lang, John J. Magnuson, Patrick Mulholland, S. Fisher, C. Liu, D. McKnight, O. Starosolszky and M. Taylor, 1996. "Hydrology and Freshwater Ecology" in Robert T. Watson, Marufu C. Zinyowera, and Richard H. Moss, editors *Climate Change 1995 Impacts, Adaptations and Mitigation of Climate Change: Scientific-Technical Analyses*, Cambridge University Press.
- Cubasch, U., K. Hasselmann, H. Hock, E. Maier-Reimer, U. Mikolajewicz, 1992. "Time-dependent Greenhouse Warming Computations with a Coupled Ocean-Atmosphere Model," *Climate Dynamics*, **8**, 55-69.
- Frederick, Kenneth D., and David C. Major, 1997. "Climate Change and Water Resources," *Climatic Change*, **37**: 7-23.
- Giorgi, Filippo, and Linda O. Mearns, 1991. "Approaches to the Simulation of Regional Climate Change: A Review," *Reviews of Geophysics*, **29**: 191-216.
- Greco, S., R.H. Moss, D. Viner, and R. Jenne, 1994. *Climate Scenarios and Socioeconomic Projections for IPCC WG II Assessment*. Working document for WG II lead authors, printed by Consortium of International Earth Science Information Network.
- Houghton, J.T., L.G. Meira Filho, B.A. Callander, N. Harris, A. Kattenberg, and K. Maskell, 1996. *Climate Change 1995 The Science of Climate Change*, Cambridge University Press.
- Intergovernmental Panel on Climate Change (IPCC), 1996. *The Regional Impacts of Climate Change*, Cambridge University Press.
- Kaczmarek, Zdzislaw, Arnell, N.W. and E.Z. Stakhiv, 1996. "Water Resources Management" in Robert T. Watson, Marufu C. Zinyowera, and Richard H. Moss, editors *Climate Change 1995 Impacts, Adaptations and Mitigation of Climate Change: Scientific-Technical Analyses*, Cambridge University Press.
- Knutson, Thomas R., and Syukuro Manabe, 1998. "Model Assessment of Decadal Variability and Trends in the Tropical Pacific Ocean," *Journal of Climate*, **11**: 2273-2294.
- Lettenmaier, Dennis P., David Ford, James P. Hughes, and Bart Nijssen, 1996. *Water Management Implications of Global Warming: 5. The Missouri River Basin*, Report to Interstate Commission on the Potomac River Basin and Institute for Water Resources, U.S. Army Corps of Engineers, Seattle, WA: DPL and Associates.

- Lettenmaier, Dennis P., Andrew W. Wood, Richard N. Palmer, Eric F. Wood, Eugene Z. Stakhiv, 1999. "Water Resources Implications of Global Warming: A U.S. Regional Perspective," *Climatic Change*, (to appear).
- Lettenmaier, Dennis P., Gregory McCabe, and Eugene Z. Stakhiv, 1996. "Global Climate Change: Effect on Hydrologic Cycle," in Larry W. Mays, ed. *Water Resources Handbook*, McGraw-Hill: 29.3-29.33.
- Manabe, S., R. J. Stouffer, M. J. Spelman, and K. Bryan, 1991. "Transient Responses of a Coupled Ocean-Atmosphere Model to Gradual Changes of Atmospheric CO₂ Part I: Annual Mean Response," *Journal of Climate*, **4**: 785-818.
- Manabe, S., M. J. Spelman, and R. J. Stouffer, 1992. "Transient Responses of a Coupled Ocean-Atmosphere Model to Gradual Changes of Atmospheric CO₂ Part II: Seasonal Response," *Journal of Climate*, **5**: 105-126.
- Meehl, Gerald A., Grant W. Branstator, and Warren M. Washington, 1993. "Tropical Pacific Interannual Variability and CO₂ Climate Change," *Journal of Climate*, **6**: 42-63.
- Murphy, J. M., 1995. "Transient Response of the Hadley Centre Coupled Ocean-Atmosphere Model to Increasing Carbon Dioxide: Part I: Control Climate and Flux Correction," *Journal of Climate*, **8**(1): 36-56.
- Murphy, J. M., and J. F. B. Mitchell, 1995. "Transient Response of the Hadley Centre Coupled Ocean-Atmosphere Model to Increasing Carbon Dioxide: Part II: Spatial and Temporal Structure of the Response," *Journal of Climate*, **8**(1): 57-80.
- Rajagopalan, Balaji, Upmanu Lall, and Mark A. Cane, 1997. "Anomalous ENSO Occurrences: An Alternate View," *Journal of Climate*, **10**: 2351-2357.
- Rosenberg, Norman J., Bruce A. Kimball, Phillippe Martin, and Charles F. Cooper, 1990. "From Climate and CO₂ Enrichment to Evapotranspiration," in *Climate Change and Water Resources*, Paul Waggoner, ed. John Wiley & Sons: New York, 151-175.
- Trenberth, Kevin E. and Timothy J. Hoar, 1996. "The 1990-1995 El Niño-Southern Oscillation Event: Longest on Record," *Geophysical Research Letters* **23** (1): 57-60.
- Trenberth, Kevin E. and Timothy J. Hoar, 1997. "El Niño and Climate Change," *Geophysical Research Letters* **24** (23): 3057-3060.

Waggoner, Paul E., 1990. *Climate Change and U.S. Water Resources*, John Wiley & Sons: New York.

Wigley, T.M.L., and S.C.B. Raper, 1992. "Implications for Climate and Sea-Level of Revised IPCC Emission Scenarios," *Nature* **357**: 293-300.

Wilson, S.G., and B.G. Hunt, 1997. *Impact of Greenhouse Warming on El Niño/Southern Oscillation Behavior in a High Resolution Coupled Global Climatic Model*, CSIRO Division of Atmospheric Research.

5 Climate Trends

5.1 Temperature

According to the 1995 IPCC (Nicholls *et al.*, 1996) report, average global temperatures have increased by approximately 0.3 to 0.6°C since the late 19th century and about 0.2 to 0.3°C in the past 40 years. Not all regions have increased in temperature; some regions have cooled. The Upper Midwest has on average increased about 0.25°C from the period 1955-1974 to the period 1975-1994, although autumn temperatures have declined about 0.25°C (IPCC, 1996b). Lettenmaier *et al.* (1994) applied a seasonal Kendall test to monthly temperature, precipitation, and streamflow records from 1948 to 1988. They found that the southeastern part of the United States generally had temperature decreases, while the western part had generally increasing temperatures with the line of demarcation running from Lake Michigan to New Mexico. The Upper Midwest showed an increase in temperatures in March and some stations showed a decrease in October. Karl *et al.* (1996) found a similar pattern of temperature trends (Figure 5.1).

5.2 Precipitation

The annual precipitation in the contiguous United States has increased especially after 1950. Much of the precipitation increase has occurred during the autumn. In North America, the autumn increase in precipitation is reflected also in an increase in streamflow. Lettenmaier *et al.* (1994) found that annual precipitation generally showed an uptrend west of a line from Lake Erie to the Texas panhandle. Karl *et al.* (1996) found a similar trend in precipitation with most of the Midwest showing an increase of 10% to

20% (Figure 5.2). In addition, the proportion of the U.S. with above normal number of wet days has significantly increased (Karl *et al.* 1996).

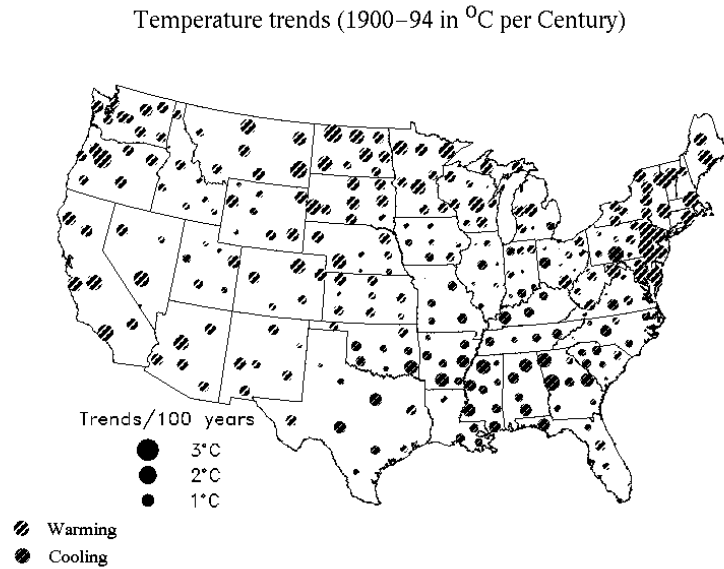


Figure 5.1: Trend in temperature from 1900 to 1994 in degrees C per century (Karl *et al.*, 1996).

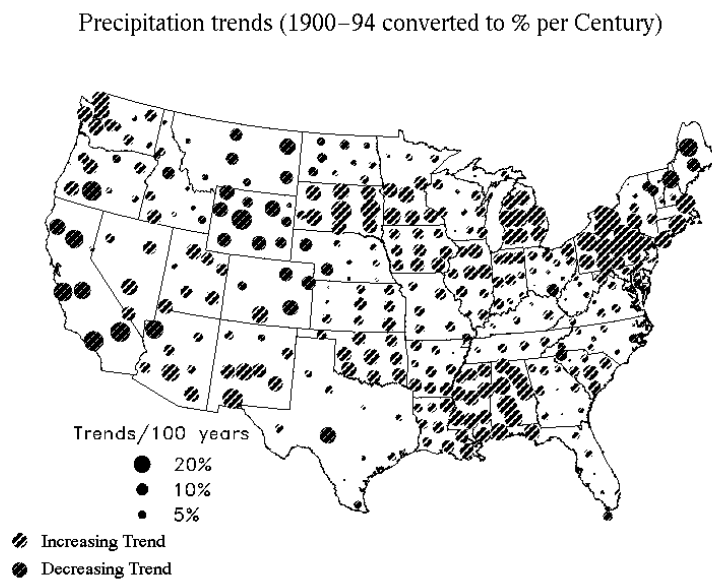


Figure 5.2: Trend in precipitation from 1900 to 1994 in % change per century (Karl *et al.*, 1996).

5.3 *Snow Cover and Depth*

Long-term trends in snow cover and depth are difficult to assess because of the lack of long-term data. Warmer temperatures would tend to accelerate the retreat of snow cover. Annual North American snow cover is negatively correlated with surface air temperature ($r = -0.73$) (Karl *et al.*, 1993). Land surface snow cover has decreased in North America in recent years based on satellite data for the last 21 years. The Upper Mississippi and Missouri basin was identified by Karl *et al.* as a temperature-sensitive snow cover region during the winter months because the mean maximum temperature is not much different from 0° C. In the northern United States, the ratio of liquid to solid precipitation is higher due to the temperature increase (IPCC, 1996a; Nicholls *et al.*, 1996).

5.4 *Precipitation Extremes*

Karl *et al.* (1995) found a trend of increasing percentages of total annual precipitation falling as heavy one-day or three-day rainfall events in the United States. They grouped daily precipitation into five categories from very light to “extreme” (2 inches or greater). A more appropriate term for this level of rainfall is “heavy” precipitation. A 24-hour precipitation of 2 inches (50 mm) happens every year in almost every location east of the Mississippi and across much of the west and south (Hershfield, 1961). The use of the term “extreme” connotes that this amount of precipitation happens less frequently.

From 1910 to 1990, the proportion of precipitation derived from the “heavy” precipitation events increased. The proportion of the country affected by these “heavy” precipitation events has also increased. This increase occurred in all seasons, but it is

predominant during convective seasons (summer and spring). This increase in heavy daily precipitation events translates into one additional heavy precipitation event every two years. There was no change in precipitation intensity using the total precipitation divided by the number of days of precipitation as the definition.

Heavy precipitation would result in more runoff if the rain falls on saturated soil. P.Ya. Groisman calculated the trend in the mean number of days per year with precipitation greater than 2 inches following two other days of rain. Nationwide the number of these events has increased about 32% from 1901 to 1996. However, the mean annual number of these events is very small: just 0.21 days for the Upper Midwest and 0.08 days for the Great Plains (P.Ya. Groisman, personal communication, 1999).

Angel and Huff (1997) also analyzed annual maximum rainfall for the upper midwestern states. They found an approximately 20% increase from 1901 to 1994 in the number of daily precipitation events of 2 inches or more. The historical record was divided into two periods: 1901-1947 and 1948-94. The authors used a nonparametric test to determine if daily 2-, 3-, 5- and 10-day annual maximum rainfall showed a statistically significant increase or not. The results are shown in Table 5.1. The number of stations with a statistically significant increase outnumbered stations with significant decreases by a ratio of 5 to 1.

Table 5.1: Changes in annual maximum precipitation for various durations at 304 Midwestern stations (significance level = 95%) (Angel and Huff, 1997).

Duration of Precipitation	Number of Stations with Significant Increases	Number of Stations with Significant Decreases
Daily	45	5
2-day	52	5
3-day	44	9
5-day	53	7
10-day	64	12

In another analysis Karl and Knight (1998) noted that precipitation has increased over much of the United States from 1910 to 1995 especially in the spring and autumn. Here they defined heavy precipitation events as the upper 10 percentile of precipitation amounts. They stated that on an annual basis over half of the precipitation increase is due to the increase in the upper 10 percentile of daily precipitation amounts. In the Upper Mississippi region, the highest percentile showed an annual increase and increases in the spring, summer, and autumn, but a decrease in the winter. In the Missouri River region, there was a smaller annual increase and increases in the spring and summer and decreases in the autumn and winter. There were small increases in the number of precipitation events for most quantiles in both regions. Karl and Knight conclude that for the United States the probability of precipitation on a given day has increased and the intensity of the precipitation has increased for heavy precipitation days only.

5.5 Streamflow

Lettenmaier *et al.* (1994) found that precipitation in the Upper Midwest generally has increased in the months of September, October, and November. March also showed an increase in precipitation. Average streamflow has also tended to increase in the Upper Midwest, particularly in the months of December to April. The lag in the streamflow uptrend can be accounted for by the effect of soil moisture. Soil moisture is depleted in the summer by evaporation. The increased autumn precipitation recharges soil moisture before increasing runoff. The magnitudes of the precipitation and streamflow trends were sometimes large. The number of stations with strong trends is more than would be expected by chance. Lettenmaier *et al.* conclude that "there is a low-frequency signal in

the climate record, although this may not necessarily be indicative of anthropogenic climate change" (1994).

Lins and Michael (1994) found statistically significant increases in regional monthly streamflow using a combination of principal components analysis and the Mann-Kendall test. They found an increasing trend in the Upper Mississippi basin from September to December. The authors say these increases are consistent with IPCC scenarios that show increased winter precipitation in the central United States.

5.6 *Streamflow Extremes*

Lins and Slack (1998) evaluated trends for seven different quantiles of streamflow at 395 selected stream gages in the United States representing relatively undisturbed watersheds. The assessment of trends is sensitive to the time period under consideration, so different time periods all ending in 1993 were considered. They found that the contiguous United States was becoming wetter but less extreme. For the annual minimum daily mean discharge, there were more statistically significant uptrends than downtrends nationally. The lower to middle quantiles of streamflows show a similar pattern. At higher levels of streamflows, the percentage of stations showing an increasing trend drops as the discharge increases. For the annual maximum flow, only 11 percent of the stations have a significant trend and the number of uptrends and downtrends is approximately equal (Figure 5.3). The Upper Mississippi and Missouri River basin follows this pattern. The area has a number of gages with significant uptrends in the annual minimum and median flows. However, only a few stations show a significant trend in the annual maximum flow, and the number of uptrends and downtrends are roughly equal (Figure 5.4).

These results are not necessarily inconsistent with the results of Karl *et al.* (1995). The extreme precipitation category used by Karl *et al.* is daily rainfall greater than 2 inches. This amount of rainfall may not be sufficient to cause increased flooding, since it occurs almost every year. It is more in the middle of the daily distribution of flows, where Slack and Lins did observe many more up-trends than down-trends. In addition, higher temperatures raise potential evapotranspiration which may lower antecedent soil moisture conditions. The timing of the increased extreme precipitation is also important. Extreme rainfall in the late summer or autumn has less likelihood of causing flooding due to lower antecedent soil moisture.

5.7 Summary

There is some evidence for increasing temperatures and precipitation in the Upper Midwest. Snow cover in the region may have decreased in the past twenty years. Less snow cover may reduce the severity of snowmelt floods. Heavy rainfalls (defined as more than 2 inches per day) may also be increasing. The Upper Mississippi and Missouri River basin has a number of gages with significant uptrends in the annual minimum and median flows, but only a few gages show a significant trend in the annual maximum flow, and the number of uptrends and downtrends are roughly equal.

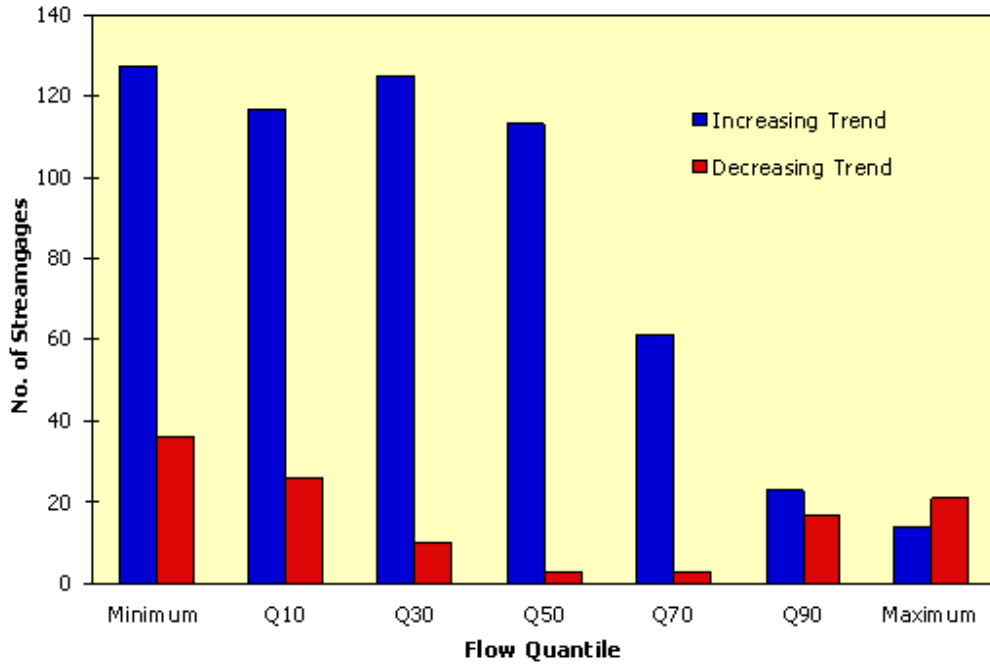


Figure 5.3: Number of stream gages, out of a total of 395, with statistically significant ($p < 0.05$) trends for the 50-year period 1944-1993 (Lins and Slack, 1999).

Trends in annual maximum daily flow in relation to water-resources regions of the U.S.

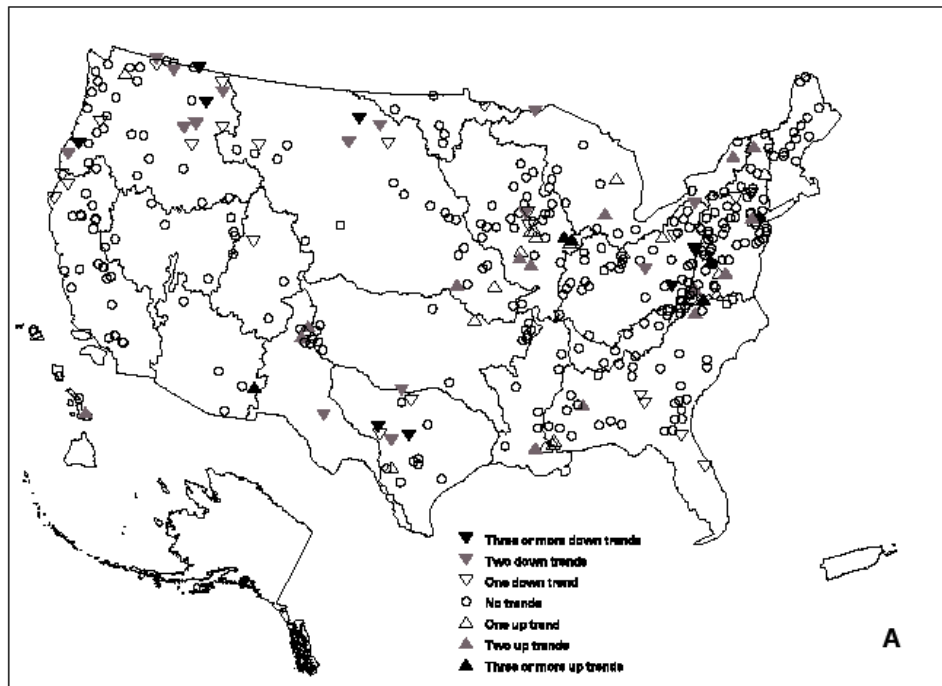


Figure 5.4: Trends in the annual maximum flow for various regions of the United States (Lins and Slack, 1999).

5.8 References

- Angel, James R., and Floyd A. Huff, 1997. "Changes in Heavy Rainfall in Midwestern United States," *Journal of Water Resources Planning and Management*, Vol. 123: 246-249.
- Hershfield, D.M., 1961. Rainfall frequency Atlas of the United States for Durations from 30 minutes to 24 hours and Return Periods from 1 to 100 Years, Tech. Paper 40, U.S. Weather Bureau, Washington, DC.
- Intergovernmental Panel on Climate Change (IPCC), 1996a. *Climate Change 1995 The Science of Climate Change*, Cambridge University Press.
- Intergovernmental Panel on Climate Change (IPCC), 1996b. *The Regional Impacts of Climate Change*, Cambridge University Press.
- Karl, Thomas R., Pavel Ya. Groisman, Richard W. Knight, and Richard R. Helm, Jr., 1993. "Recent Variations of Snow Cover and Snowfall in North America and Their Relation to Precipitation and Temperature Variations," *Journal of Climate*, Vol. 6: 1327-1344.
- Karl, Thomas R., Richard W. Knight, and Neil Plummer, 1995. "Trends in high frequency climate variability in the twentieth century," *Nature*, Vol. 377: 217-220.
- Karl, Thomas R., Richard W. Knight, David R. Easterling, and Robert G. Quayle, 1996. "Indices of Climate Change for the United States," *Bulletin of the American Meteorological Society*, Vol 77, No. 2: 279-292.
- Karl, Thomas R., and Richard W. Knight, 1998. "Secular Trends of Precipitation Amount, Frequency, and Intensity in the United States," *Bulletin of the American Meteorological Society*, Vol 79, No. 2: 231-241.
- Lins, Harry F., and James R. Slack, 1998. "Streamflow Trends in the United States," *Geophysical Research Letters*, Vol. 26: 227-230.
- Lins, Harry F., and Patrick J. Michaels, 1994. "Increasing U.S. Streamflow Linked to Greenhouse Forcing," *EOS* Vol. 75, No. 25: 281-285.
- Lettenmaier, Dennis P., Eric F. Wood, and James R. Wallis 1994. "Hydro-Climatological Trends in the Continental United States, 1948-88," *Journal of Climate*, Vol. 7: 586-607.
- Nicholls, N., G.V. Gruza, J. Jouzel, T.R. Karl, L.A. Ogallo, and D.E. Parker, 1996. "Observed Climate Variability and Change," in Intergovernmental Panel on

Climate Change (IPCC), *Climate Change 1995 The Science of Climate Change* ,
Cambridge University Press, 133-192.

6 Trends in Mississippi and Missouri River Floods

6.1 Trend Analysis of Mississippi and Missouri River Floods

The analysis of some climate variables suggest that positive trends may be present in hydrologic series in the Upper Mississippi River Basin. The possibility of such trends in Mississippi and Missouri Rivers unimpaired flow records to be used in the USACE flood-flow frequency study of the Upper Mississippi River basin was investigated. Table 6.1 summarizes the results of linear regression analyses of flow (annual flood) on time (year) that are described more fully in Tables 6.2 through 6.6. Linear regression fits the linear model

$$Y = a + b t + \varepsilon$$

where Y is the annual flood, t is the year, ε is a random error term, a is the intercept and b is the slope coefficient. R^2 is the coefficient of determination, or the fraction of the variance explained by regression. The correlation is a measure of the linear association between the annual flood and time. The null hypothesis is that the slope coefficient $b \leq 0$. The p-value is the probability of obtaining the test statistic, or one less likely, when the null hypothesis is true. The smaller the p-value, the less likely is the observed test statistic when the null hypothesis is true. The α -value, or significance level, is the probability of incorrectly rejecting the null hypothesis when it is in fact true. The null hypothesis is rejected when the p-value is less than the α -value determined by the decision maker. P-values less than $\alpha = 5\%$ are designated in bold italics in Tables 6.1 to 6.6 (Helsel and Hirsch, 1992).

High in the basin, the St. Croix River, the Minnesota River, and the Mississippi River at St. Paul all show significant trends at the 5% level using a one-sided test. The trend at Anoka, Minnesota, which is a gage much higher in the basin and with half the drainage area of St. Paul, is not significant. The record at Anoka is 64 years in length, whereas St. Paul has a 129-year record. (See Table 6.2.) Table 6.2 shows that the trend is also statistically significant at Winona, McGregor and Dubuque. For the most part, this is the region dominated by snowmelt floods. Tables 6.1 and 6.2 and Figure 6.1 show that a trend at Clinton is not significant. A trend is significant at the 6% level at Keokuk farther downstream. Table 6.2 categorizes this as the transition region between the area dominated by snowmelt floods to the north, and the region dominated by rainfall events to the south.

Tables 6.1 and 6.3 report regression results for the Missouri River. For sites reflecting flood flows from the West, corresponding to Sioux City, Omaha, Nebraska City (Figure 6.2), and Kansas City, there is no significant trend. A trend was significant at St. Joseph, but was lost after the Kansas River enters the Missouri before Kansas City. The trend starts to show up again at Boonville, and is significant at the 2% level at Hermann. (See Figure 6.3.) Thus on the Missouri, the local inflow above St. Joseph, and then those that result in floods at Hermann at the bottom of the system seem to exhibit a statistically significant and potentially important change in flood risk over the 100-year period. The Nishnabotna and Thompson Rivers included in Table 6.5 show significant trends. The Nishnabotna River joins the Missouri above St. Joseph. The Thompson River is a tributary of the Grand River, which joins the Missouri River above Boonville. A positive trend for the Gasconade River was evident, but not statistically significant. These

tributaries were chosen because they have good gaged records and have relatively little regulation (Slack et al., 1993).

The Hannibal and Alton/Grafton gages above the confluence of the Missouri River have highly significant trends with $p < 0.1\%$. The trend in the Hannibal record shown in Figure 6.4 is extraordinary. The 300,000 cfs flow threshold was never crossed until the 1940s, and was exceeded almost every-other-year in the 1970-1997 period. (See nonparametric analysis in Appendix D.) The Hannibal gage is not a USGS recording station. The Hannibal gage is stage only, with a rating relationship to estimate flows. Some have expressed concern that the rating curve has shifted and has not been updated. The St. Louis District has long noted significant peak discharge differences between the Hannibal gage and the Louisiana gage downstream. The latter gives consistently larger values of peak discharge as compared to Hannibal, more than can be explained by the limited increase in drainage area between the two gages (Gary Dyhouse, personal communication, 1999). The regression of floods on time was also highly significant at the Alton/Grafton gage 100 miles downstream from Hannibal. Table 6.6 reports results for Meredosia on the Illinois River (Figure 6.5) and the Meremac River which enters the Mississippi below St. Louis. These two rivers also show highly significant trends.

Table 6.4 shows the three gages downstream of the confluence of the Missouri and Mississippi: St. Louis, Chester, and Thebes. These gages also have significant trends, but are highly correlated ($\rho > 0.975$) and thus represent essentially the same hydrologic experience over the recent period of record for which the Chester and Thebes gages have been active. The longest record is at St. Louis (Figure 6.6).

Correlations among the annual floods at Hermann, Hannibal, and St. Louis are 0.65 (Hermann-Hannibal), 0.90 (Hermann-St. Louis), and 0.77 (Hannibal-St. Louis). This reflects the observation that the Missouri contributes more to the flood peaks at St. Louis than does the Upper Mississippi River. The three records do not constitute independent experiences. However the data provide very strong evidence that flood risk has increased in recent decades in the lower part of the Missouri basin, on the Mississippi near Hannibal, on the Illinois River, and at St. Louis below the junction of the two rivers. Analysis of flows on tributaries of the Missouri and Meremac River add to the evidence of a significant change in flood risk with time over the last century.

Table 6.1: Linear Trend Analyses for Upper Mississippi Basin Gages

Station	Location	Record Length	R ²	Correlation	Significance Level
Anoka	Upper Upper Mississippi	64	0.01	0.11	0.18
St. Croix Falls, WI	St. Croix River	86	0.09	0.30	0.003
Jordan, MN	Minnesota River	63	0.06	0.24	0.03
St. Paul, MN	Upper Upper Mississippi	129	0.03	0.16	0.03
Clinton	Upper Upper Mississippi	122	0.00	0.01	0.47
Keokuk	Middle Upper Mississippi	117	0.02	0.15	0.06
Hannibal	Middle Upper Mississippi	118	0.20	0.45	<1x10⁻⁶
Alton/ Grafton	Middle Upper Mississippi	67	0.17	0.42	<0.001
Nebraska City	Missouri	100	0.01	-0.08	0.22
Boonville	Missouri	100	0.01	0.10	0.16
Hermann	Lower Missouri	100	0.05	0.22	0.02
Meredosia, IL	Illinois River	63	0.10	0.31	0.01
Meremac River near Eureka, MO*	Between St. Louis and Chester	73	0.06	0.27	0.02
St. Louis	Below Junction Miss. & Missouri	136	0.04	0.19	0.01

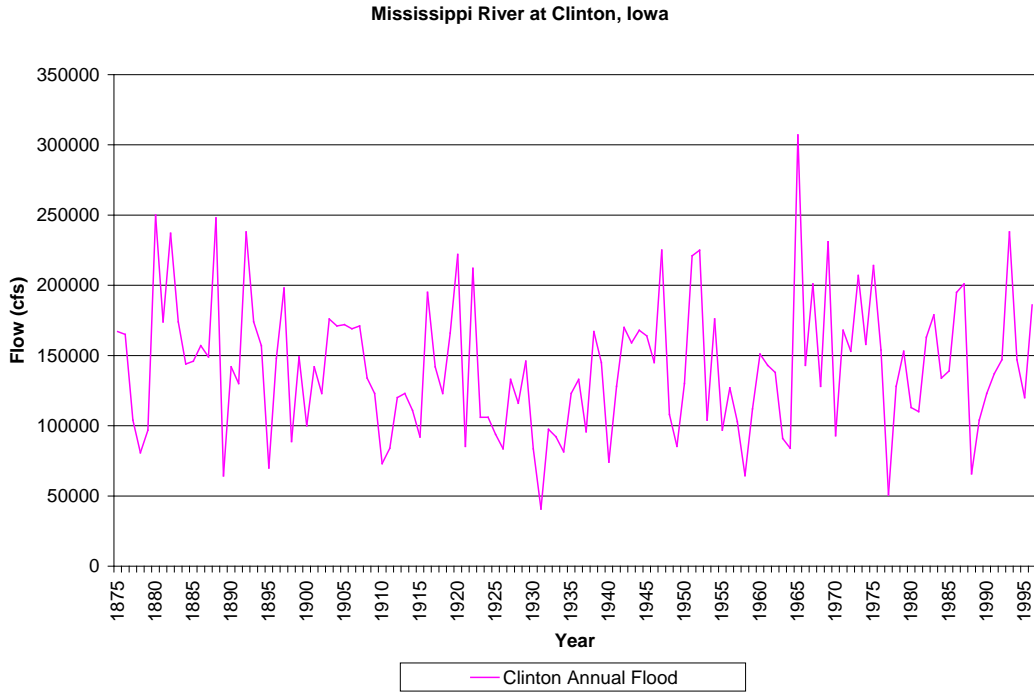


Figure 6.1: Annual floods for the Mississippi River at Clinton.

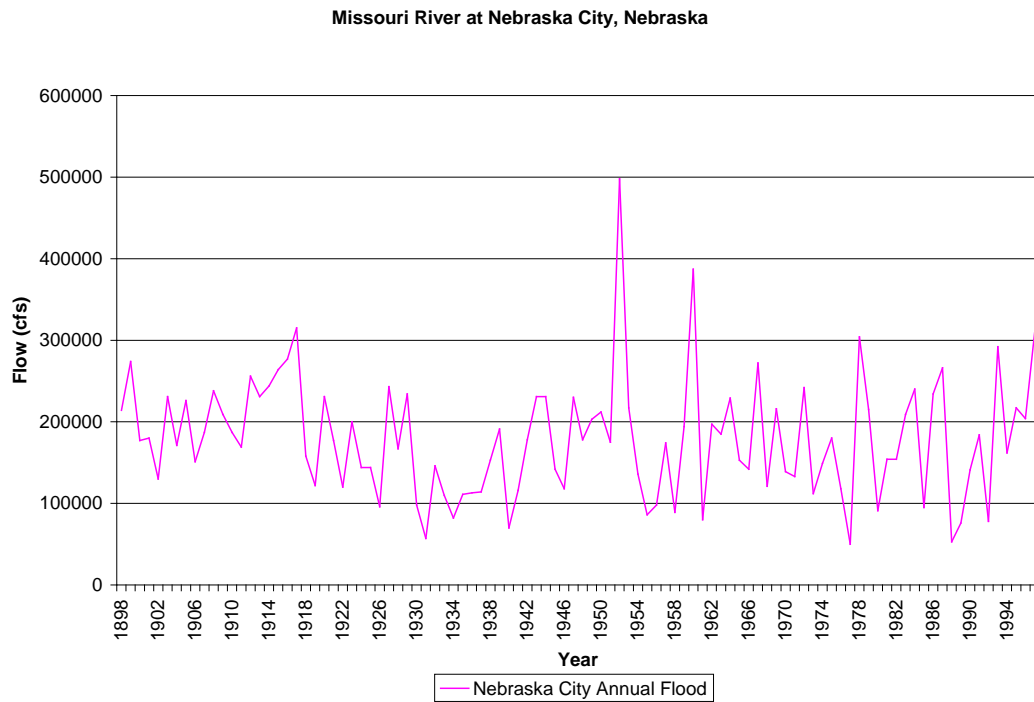


Figure 6.2: Annual floods for the Missouri River at Nebraska City.

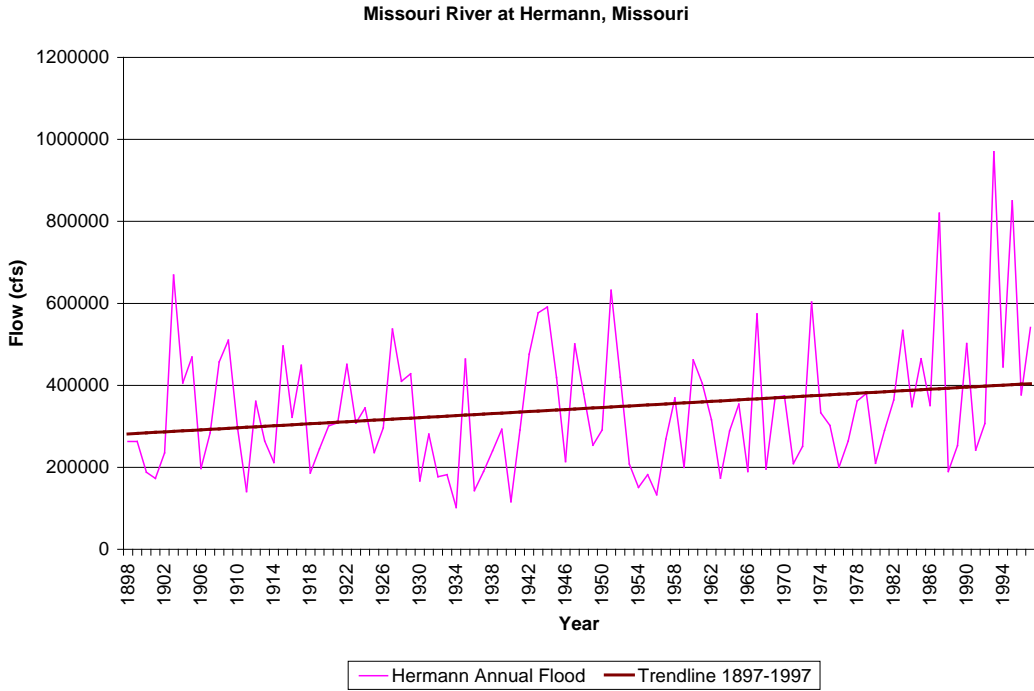


Figure 6.3: Annual floods for the Missouri River at Hermann and trendline

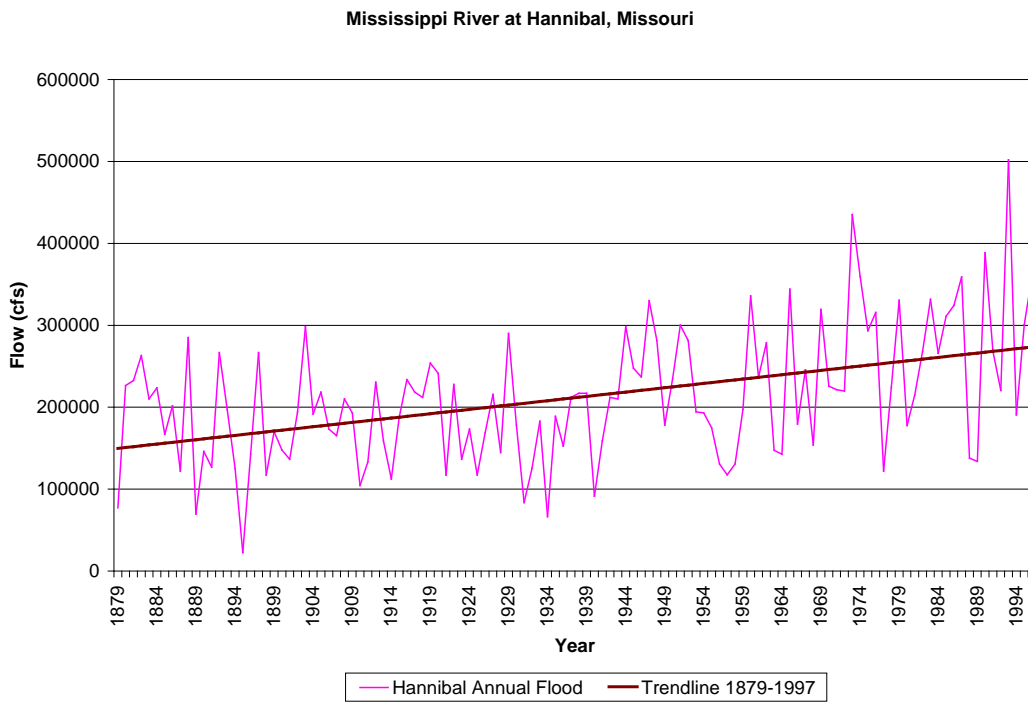


Figure 6.4: Annual floods for the Mississippi River at Hannibal and trendline.

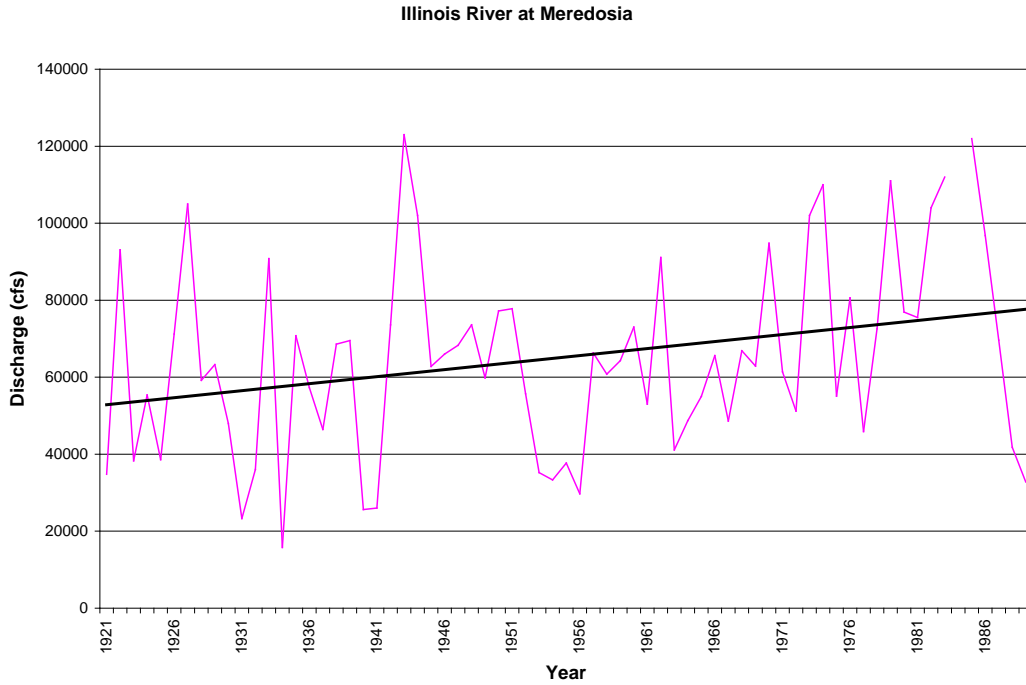


Figure 6.5: Annual floods for the Illinois River at Meredosia.

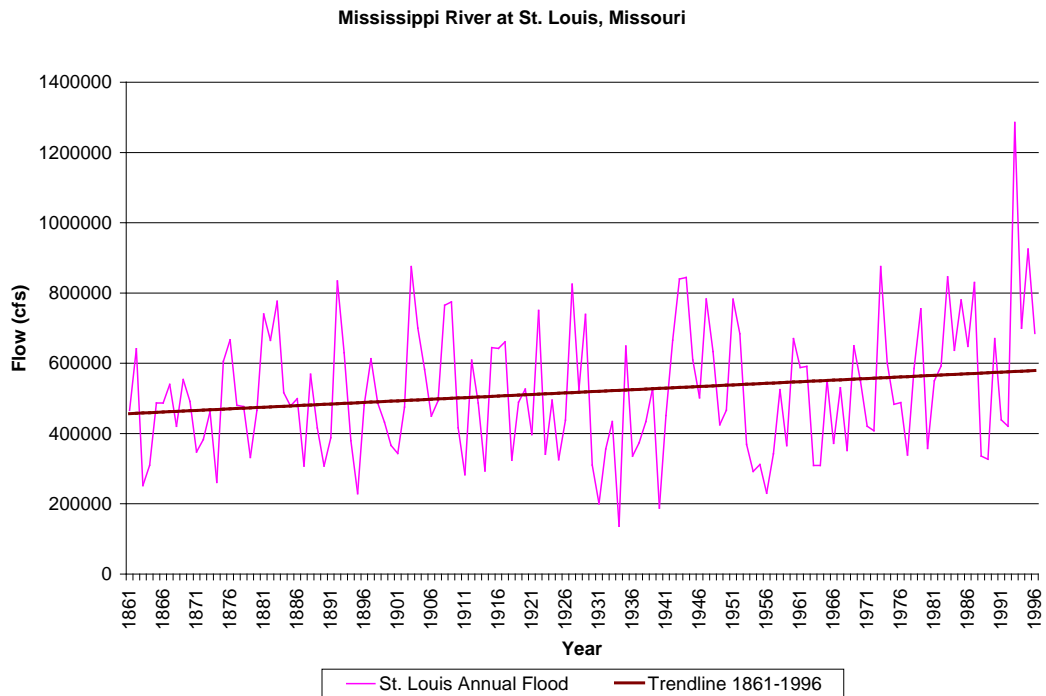


Figure 6.6: Annual floods for the Mississippi River at St. Louis and trendline.

Table 6.2: Mississippi River (USACE Records)

Station	Location	Drainage Area	Record Length	R²	Correlation	Significance Level
<i>Northern Upper Mississippi River (Snow Melt Floods Dominate)</i>						
Anoka	Upper Mississippi (Minnesota)	19,600	64	0.01	0.11	0.18
St. Paul	Upper Mississippi (Minnesota)	36,800	129	0.03	0.16	0.03
Winona	Upper Mississippi (Minnesota)	59,200	109	0.02	0.16	0.06
McGregor	Upper Mississippi (Iowa)	67,500	60	0.05	0.21	0.05
Dubuque	Upper Mississippi (Iowa)	82,000	117	0.10	0.31	0.001
<i>Transition Region Snowmelt and Rainfall Floods</i>						
Clinton	Upper Mississippi (Iowa)	85,600	121	<0.001	0.01	0.47
Keokuk	Upper Mississippi (Iowa)	119,000	117	0.02	0.15	0.06
<i>Upper Mississippi River above Confluence with Missouri (Rainfall Floods Dominate)</i>						
Hannibal	Upper Mississippi (Missouri)	137,000	117	0.20	0.45	<0.001
Alton/ Grafton	Upper Mississippi (Missouri)	171,300	67	0.17	0.42	<0.001

Table 6.3: Missouri River (USACE Records). Drainage areas below Gavins Point Dam are in parenthesis.

Station	Location	Drainage Area	Record Length	R ²	Correlation	Significance Level
Sioux City	Missouri	314,600 (35,120)	100	0.03	-0.17	0.95
Omaha	Missouri	322,820 (43,340)	100	<0.001	-0.01	0.93
Nebraska City	Missouri	414,420 (134,940)	100	0.01	-0.08	0.22
St. Joseph	Missouri	429,340 (149,860)	100	0.05	+0.22	0.01
Kansas City	Missouri	489,162 (209,860)	100	<0.001	-0.02	0.44
Boonville	Lower Missouri	505,710 (226,230)	100	0.01	+0.10	0.16
Hermann	Lower Missouri	528,200 (248,720)	100	0.05	+0.22	0.02

Table 6.4: Upper Mississippi River below Confluence w/ Missouri (USACE Records)

Station	Location	Drainage Area	Record Length	R ²	Correlation	Significance Level
St. Louis	Below Junction of Mississippi and Missouri	697,013 (417,520)	135	0.04	0.19	0.01
Chester	Below Junction of Mississippi and Missouri	708,563 (429,120)	70	0.07	0.26	0.02
Thebes	Below Junction of Mississippi and Missouri	713,200 (433,720)	63	0.10	0.32	0.01

Table 6.5: Missouri River Tributaries (USGS Gage Records)

Station	Confluence	Record Length	R²	Correlation	Significance Level
Nishnabotna River above Hamburg, IA*	Between Nebraska City and St. Joseph	71	0.09	0.29	0.01
Thompson River at Trenton, MO*	Tributary of Grand River (Between Boonville and Hermann)	69	0.08	0.29	0.01
Gasconade River at Jerome, MO*	Between Boonville and Hermann	73	0.02	0.16	0.09

Table 6.6: Mississippi River Tributaries (USGS Gage Records)

Station	Confluence	Record Length	R²	Correlation	Significance Level
Minnesota River near Jordan, MN	At St. Paul	63	0.06	0.24	0.03
St. Croix River St. Croix Falls, WI*	Between St. Paul and Winona	86	0.09	0.30	0.003
Chippewa River at Chippewa Falls, WI	Between St. Paul and Winona	96	<0.001	0.02	0.44
Wisconsin River at Muscoda, WI	Between McGregor and Dubuque	83	0.03	0.16	0.07
Iowa River Wapello, IA	Between Clinton and Keokuk	95	0.01	0.09	0.20
Cedar River near Conesville, IA	Tributary of Iowa River	58	<0.001	0.01	0.47
Des Moines River at Keosauqua, IA	Between Keokuk and Hannibal	86	0.005	0.07	0.27
Illinois River at Meredosia, IL	At Grafton	63	0.10	0.31	0.01
Meremac River near Eureka, MO*	Between St. Louis and Chester	73	0.06	0.27	0.02

*Hydro-Climatic Data Network (HCDN) streamflow gage: average daily values for the entire gage record are relatively unimpaired.

6.2 Other Results Reporting Trends

Several studies have addressed changes in the watershed. For example, Potter (1991) shows that since 1951, flood peaks have decreased in some small agricultural catchments in Wisconsin. One can perhaps see that pattern at the end of the St. Croix record, which otherwise has an increasing trend.

Knox (1983) discusses the likely variation in flood risk at St. Paul from 1860 to 1981. He suggests a period from 1860 to 1895 with high flood risk, and then a period from 1896 - 1949 with significantly depressed flood risk, though the mean flood was thought to have changed very little. Then from 1950 - 1981 flood risks increase to the highest level over the period. Knox (1983, p. 324) provides Table 6.7:

Table 6.7: Variations in Flood Potential with Time reported by Knox (1983)

Climate Episode	2% Chance Exceedance Flood Flow (CMS)
1867-1895	3,100
1896-1919	2,400
1920-1949	2,000
1950-1981	3,200

Knapp (1994) reports an investigation of trends in flood risk over time for the upper Mississippi River. The records used were not corrected for regulation. He observed that the basin has experienced above-average precipitation since 1965 and this has increased streamflows. He concludes: "Tributaries in Minnesota and Illinois have experienced increases in peak discharges and high flows proportional to the increase in average flows, while tributaries in Iowa have not. Most areas in Wisconsin have experienced a reduction in high flows, but not much change in peak discharges." In

addition he states that: "Reforestation in Wisconsin appears to have a mild impact on average flow in the Mississippi River at Clinton Iowa, and flood control reservoirs in the Missouri River watershed appear to produce a 10 percent reduction in the average flood peak and flood volume for the Mississippi River at St. Louis, Missouri." The use of observed flood records (which includes impacts of regulation) by Knapp limits their scope. The record for St. Louis used by the USACE, shown in Figure 6.7, has elevated the magnitude of recent floods to account for regulation. The value of earlier floods has been reduced to correct for velocity/discharge measurement overestimates. It is with these corrections that the St. Louis record has such a statistically significant trend, consistent with other records on the Missouri, upper Mississippi, and Illinois rivers upstream of the confluence before St. Louis.

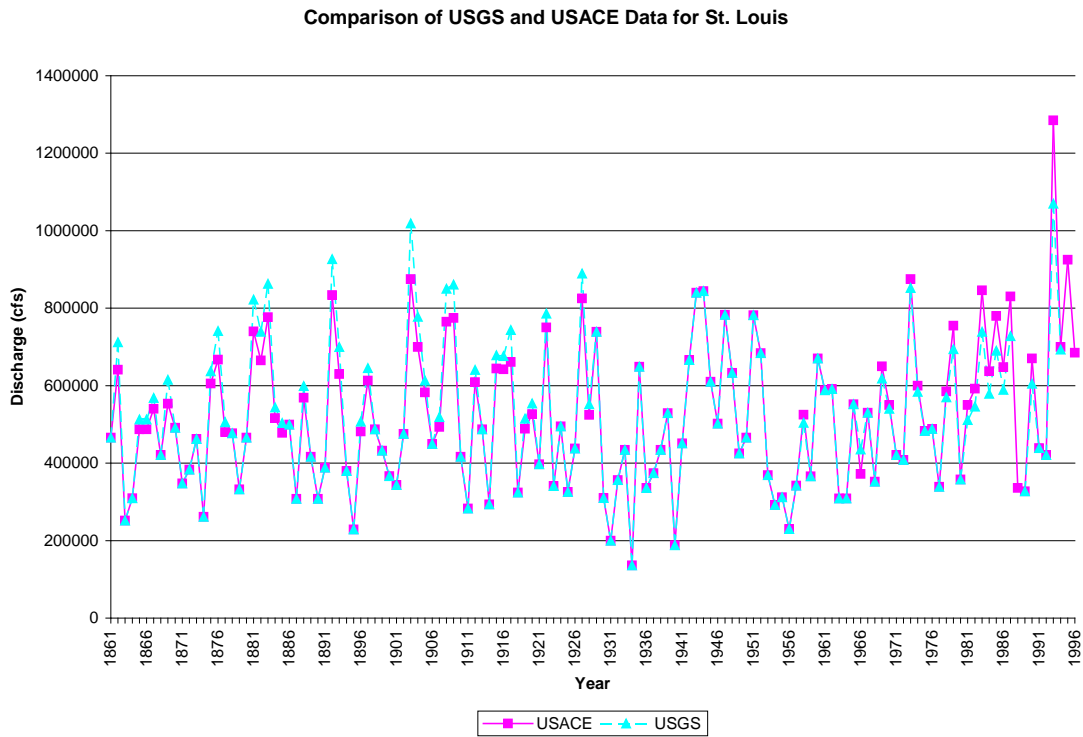


Figure 6.7: Comparison of the U.S. Geological Survey and U.S. Army Corps of Engineers flood records for St. Louis

Baldwin and Lall (1999) record a seasonal shift in the occurrence of annual flood peaks on the upper Mississippi at Clinton and discuss its possible relationship to climatic patterns. They also record a clear variation in the mean annual flow over the 123 year record. Baldwin and Lall (1998) provide an expanded discussion of the likely connection between flows on the Mississippi at Clinton and global climate patterns.

Goldman (1999) looked for trends on several tributaries of the Mississippi and Missouri. The gages selected for the study are unimpaired due to regulation, except for Wapello, Iowa, where the record was adjusted due to regulation of the Coralville Reservoir. Table 6.8 shows the correlation and significance of the linear regression of the annual maximum flood on time for the eight tributaries. Only the Raccoon River in Iowa and the James River in South Dakota show statistically significant trends.

Table 6.8: Statistical significance of trends in annual flood for several tributaries of the Mississippi River (Goldman, 1999).

River	Location	Drainage Area	Period of Record	Significance Level
Cedar River	Conesville, Iowa	7,785	1940-1994	0.41
Iowa River	Wapello, Iowa	12,500	1903-1994	0.38
Skunk River	Augusta, Iowa	4,303	1915-1994	0.19
Des Moines River	Stratford, Iowa	5,452	1968-1994	0.07
Raccoon River	Van Meter, Iowa	3,441	1915-1994	0.01
James River	Scotland, South Dakota	3,898	1929-1994	0.01
Big Sioux River	Brookings, South Dakota	20,653	1954-1994	0.32
Big Blue River	Beatrice, Nebraska	3,901	1902-1994	0.18

The trend pattern in Iowa does not appear to be regionally consistent. The record for the Mississippi River at Clinton, Iowa, did not show a trend over the full record, and the significance level of the trend at Keokuk was only 6%. The tributaries in Iowa do not

show consistent trends in the annual flood. However, the annual floods for basins of the size of these rivers may be relatively short events and could be caused by local storms. Floods on the main stem of the Upper Mississippi River, on the other hand, would be expected to result from longer duration events.

An analysis of trends in the monthly flow of four rivers in Iowa was conducted. The data was derived directly from the Hydro-Climatic Data Network streamflow data set (Slack *et al.*,1993) for monthly flows. These gages are considered to have relatively unimpaired flows. The record for this data set ended in 1988. The months of March, April, May, and June were chosen because most of the floods in this region occur in the spring. The results are shown in Table 6.9. Three of the four stations have a significant trend at the 1% level for average monthly flow in April and in May. The fourth station, the Skunk River, has significant trends at the 1.5% and 7% level for the two months. Only the Des Moines River had a significant trend in June at the 5% level, and none of the stations had a significant trend in March at the 5% level. The increasing trend in flows in April and May appears to be regionally consistent and seems to indicate that the more recent period has had wetter springs.

Table 6.9: Correlation and significance level for trend in average monthly flows for four stations in Iowa.

River Station		March	April	May	June	Period of Record
Cedar River	<i>Correlation</i>	0.061	0.251	0.251	0.146	1903-1988
Cedar Rapids, Iowa	<i>Significance Level</i>	0.290	0.010	0.010	0.090	
Skunk River	<i>Correlation</i>	0.157	0.255	0.172	0.063	1915-1988
Augusta, Iowa	<i>Significance Level</i>	0.090	0.014	0.071	0.297	
Des Moines River	<i>Correlation</i>	0.175	0.319	0.386	0.267	1921-1988
Stratford, Iowa	<i>Significance Level</i>	0.077	0.004	0.001	0.014	
Raccoon River	<i>Correlation</i>	0.174	0.331	0.350	0.119	1916-1988
Van Meter, Iowa	<i>Significance Level</i>	0.070	0.002	0.001	0.158	

6.3 Present-to-Past and Past-to-Present Trend Analysis for Basins

The assessment of trend can be extended by considering its evolution to determine how the trend assessment would have changed over time. A *past-to-present* view is complimented by a *present-to-past* view, i.e. by an assessment of trend considering alternate dates at which the sequence began, where the alternate dates can be taken within the historical time span of the historical flood record. The two views remind us that the future remains unknown, and may eventually contradict the past.

An evolutionary trend assessment was undertaken for annual flood sequences available for sites in the Upper Mississippi and Missouri Basins. The sequences are examined to determine if they are characterized by statistically meaningful trends. Trends are limited to those in the mean defined by the linear regression of flow (annual flood) on time (year). A statistically meaningful trend is taken to be a statistically significant regression at the 5% level and at the 1% level. Each sequence is assessed under this null

hypothesis that the regression coefficient is equal to zero versus it is positive (a one-sided test). In the case of a simple regression, the null hypothesis is equivalent to the null hypothesis that the coefficient of correlation between time and flow is equal to zero.

Tables 6.10 through 6.13 report an evolutionary trend analysis for the gage records at Hermann, Keokuk, Hannibal, and St. Louis. A more detailed description of the past-to-present and present-to-past trend analysis is presented in Appendix C. Results for each gage is also given in this appendix. As one can see, a trend that may not be significant over a period of moderate length may be significant if a longer or a shorter record is employed. A time trend with the Keokuk record ending in 1997 was significant for a record beginning in 1928 to as early as 1888, but was not significant at the 5% level if the period of record was extended back to 1879. For many gages in the basin, such as Hermann and St. Louis, a trend is only significant if the wet 1988-1997 period is included in the analysis. The interpretation of trend analyses such as those in Tables 6.1 through 6.6 should be sensitive to the total record length available, as well as the particular period of record employed for each gage.

Table 6.10: Past-to-present and present-to-past trend analysis for Hermann

Length of Record	Period of Record	Correlation
	<i>Past to Present</i>	
10	(1898-1907)	0.266
20	(1898-1917)	0.179
30	(1898-1927)	0.100
40	(1898-1937)	-0.159
50	(1898-1947)	0.051
60	(1898-1957)	-0.033
70	(1898-1967)	0.002
80	(1898-1977)	-0.005
90	(1898-1987)	0.114
100	(1898-1997)	0.224 *
	<i>Present to Past</i>	
10	(1997-1988)	0.495
20	(1997-1978)	0.374 *
30	(1997-1968)	0.435 **
40	(1997-1958)	0.381 **
50	(1997-1948)	0.372 **
60	(1997-1938)	0.263 *
70	(1997-1928)	0.325 **
80	(1997-1918)	0.296 **
90	(1997-1908)	0.234 *
100	(1997-1898)	0.224 *

* 5% Level of Significance, ** 1% Level of Significance (for a one-sided test).

Table 6.11: Past-to-present and present-to-past trend analysis for Keokuk

Length of Record	Period of Record	Correlation
	<i>Past to Present</i>	
9	(1879-1887)	-0.151
19	(1879-1897)	-0.250
29	(1879-1907)	-0.139
39	(1879-1917)	-0.226
49	(1879-1927)	-0.234
59	(1879-1937)	-0.326 **
69	(1879-1947)	-0.184
79	(1879-1957)	-0.146
89	(1879-1967)	-0.046
99	(1879-1977)	0.044
109	(1879-1987)	0.110
118	(1879-1996)	0.147
	<i>Present to Past</i>	
9	(1996-1988)	0.364
19	(1996-1978)	0.196
29	(1996-1968)	0.104
39	(1996-1958)	0.130
49	(1996-1948)	0.188
59	(1996-1938)	0.202
69	(1996-1928)	0.321 **
79	(1996-1918)	0.309 **
89	(1996-1908)	0.316 **
99	(1996-1898)	0.270 **
109	(1996-1888)	0.223 **
118	(1996-1878)	0.147

* 5% Level of Significance, ** 1% Level of Significance (for a one-sided test).

Table 6.12: Past-to-present and present-to-past trend analysis for Hannibal

Length of Record	Period of Record	Correlation
	<i>Past to Present</i>	
9	(1879-1887)	-0.051
19	(1879-1897)	-0.189
29	(1879-1907)	-0.034
39	(1879-1917)	-0.012
49	(1879-1927)	0.016
59	(1879-1937)	-0.065
69	(1879-1947)	0.123
79	(1879-1957)	0.159
89	(1879-1967)	0.221 *
99	(1879-1977)	0.329 **
109	(1879-1987)	0.425 **
118	(1879-1996)	0.447 **
	<i>Present to Past</i>	
9	(1996-1988)	0.456
19	(1996-1978)	0.228
29	(1996-1968)	0.168
39	(1996-1958)	0.290 *
49	(1996-1948)	0.340 **
59	(1996-1938)	0.341 **
69	(1996-1928)	0.450 **
79	(1996-1918)	0.458 **
89	(1996-1908)	0.475 **
99	(1996-1898)	0.475 **
109	(1996-1888)	0.477 **
118	(1996-1878)	0.447 **

* 5% Level of Significance, ** 1% Level of Significance (for a one-sided test).

Table 6.13: Past-to-present and present-to-past trend analysis for St. Louis

Length of Record	Period of Record	Correlation	
	<i>Past to Present</i>		
7	(1861-1867)	0.087	
17	(1861-1877)	0.146	
27	(1861-1887)	0.228	
37	(1861-1897)	0.112	
47	(1861-1907)	0.152	
57	(1861-1917)	0.202	
67	(1861-1927)	0.134	
77	(1861-1937)	-0.024	
87	(1861-1947)	0.090	
97	(1861-1957)	0.020	
107	(1861-1967)	0.002	
117	(1861-1977)	0.020	
127	(1861-1987)	0.139	
137	(1861-1996)	0.194	*
	<i>Present to Past</i>		
9	(1996-1988)	0.598	*
19	(1996-1978)	0.231	
29	(1996-1968)	0.344	*
39	(1996-1958)	0.393	**
49	(1996-1948)	0.391	**
59	(1996-1938)	0.243	*
69	(1996-1928)	0.325	**
79	(1996-1918)	0.297	**
89	(1996-1908)	0.211	*
99	(1996-1898)	0.185	*
109	(1996-1888)	0.188	*
119	(1996-1878)	0.160	*
129	(1996-1868)	0.179	*
137	(1996-1861)	0.194	*

* 5% Level of Significance, ** 1% Level of Significance

6.4 Possible Causes of Trends

There are several possible causes for the apparent trends on the Upper Mississippi and Lower Missouri Rivers. One possibility is increased precipitation in the more recent period. This climate variability is not clearly associated with global climate indices, which explain only a small fraction of the variability in annual floods. Land use changes and channel modifications may increase flood peaks, but these changes would probably have more effect at the upstream gages that have smaller drainage areas. Measurement errors of flows at stage-only gages such as Hannibal should be investigated. In addition, corrections made by the Corps of Engineers to account for regulation could also have an influence on observed trend. The least likely cause of the trend is anthropogenic climate change associated with increased greenhouse gases. Simulations of the Missouri River basin using General Circulation Model predictions indicate that average monthly runoff may decrease in that basin (Lettenmaier *et al.*, 1996).

6.4.1 Trends in Precipitation

Goldman (1999) looked at precipitation trends in the Keosauqua, Iowa gage, located near the confluence of the Des Moines and Mississippi Rivers. Durations of 1 day to 120 days were analyzed. The results are reproduced in Table 6.14. There is a statistically significant trend for rainfall with a duration of 105 days.

Table 6.14: Precipitation trend analysis for Keosauqua, Iowa.

Duration	R²	Significance Level
1 day	0.000	0.46
15 day	0.022	0.12
30 day	0.013	0.12
60 day	0.014	0.10
90 day	0.016	0.08
105 day	0.019	0.03
120 day	0.022	0.07

A trend analysis was also conducted for monthly precipitation from the United States Historical Climatology Network (U.S. HCN) (Karl *et al.*, 1990). These stations have relatively long records and have experienced few station changes. The average monthly precipitation for five stations in the Iowa River basin and five stations in the Des Moines River basin were analyzed. A linear regression of the average precipitation for March, April, May, and June was performed on time. The results are shown in Tables 6.15 and 6.16. Data for the Iowa River is plotted in Figures 6.8 and 6.9 and the Des Moines River in Figures 6.10 and 6.11. There are statistically significant trends for the average March and April precipitation in both basins. Increases in March and April precipitation indicate wetter springtimes in Iowa which is consistent with the observed trends in annual floods for large drainage areas on the Upper Mississippi.

Table 6.15: Trends in average monthly precipitation of five precipitation gages in the Iowa River basin (1895-1994).

Month	Correlation	Significance Level
March	0.203	<i>0.022</i>
April	0.245	<i>0.007</i>
May	0.067	0.255
June	0.125	0.107

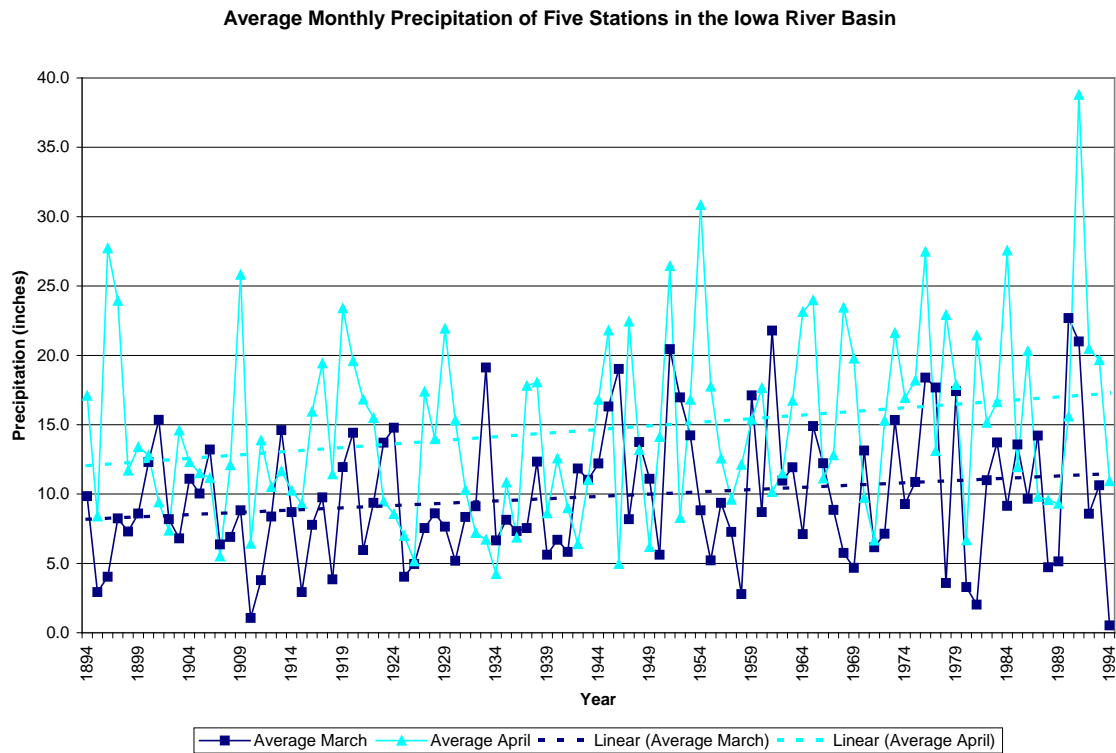


Figure 6.8: The average monthly precipitation for March and April for five stations in the Iowa River basin.

Average Monthly Precipitation of Five Stations in the Iowa River Basin

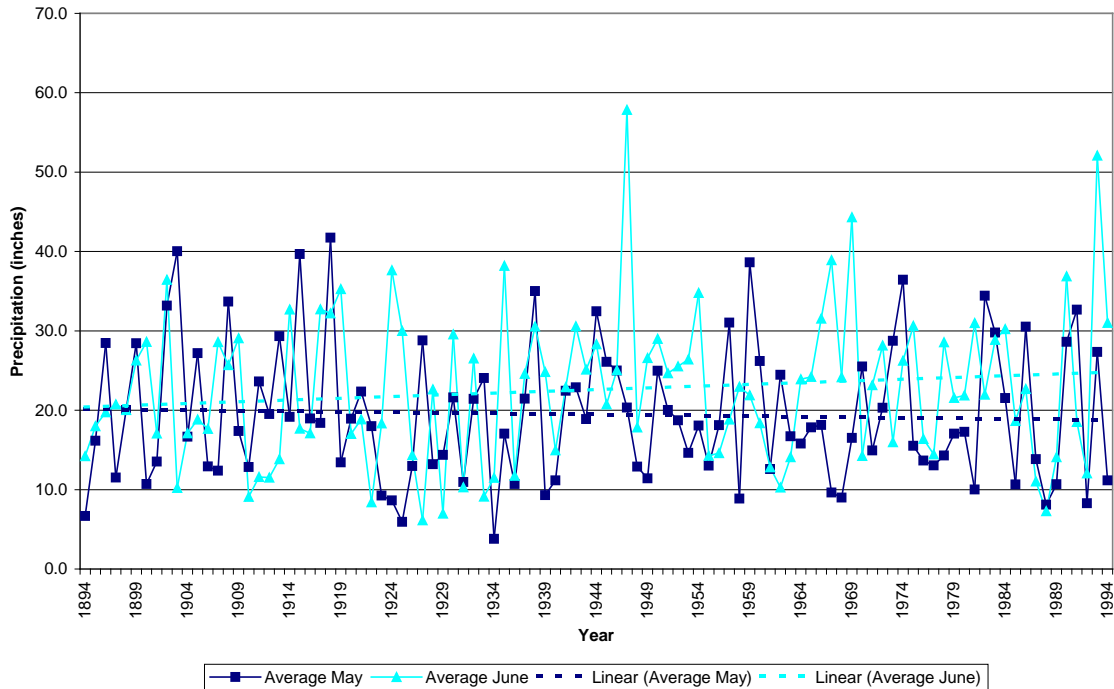


Figure 6.9: The average monthly precipitation for May and June for five stations in the Iowa River basin.

Table 6.16: Trends in average monthly precipitation of five precipitation gages in the Des Moines River basin (1895-1994).

Month	Correlation	Significance Level
March	0.265	0.004
April	0.166	0.049
May	0.038	0.354
June	0.157	0.060

6.5 Summary

This study found trends in the northern part of the Upper Mississippi basin on both the main stem and tributaries. The major floods in this region generally are snowmelt floods. There are also trends in the lower part of the Upper Mississippi basin around St. Louis. The gage records for the Missouri River at Hermann, the Mississippi

River at Hannibal, at Alton/Grafton, and at St. Louis, and the Illinois River at Meredosia all show statistically significant trends at the 5% level. Long duration precipitation over a large area is the cause of major floods in this part of the basin. There is no consistent pattern of trends on the Missouri River. The time period that one uses for trend analysis has a major effect on the size and significance of the trend. For example, major floods in the 1990's have a large influence on the observed trends at St. Louis.

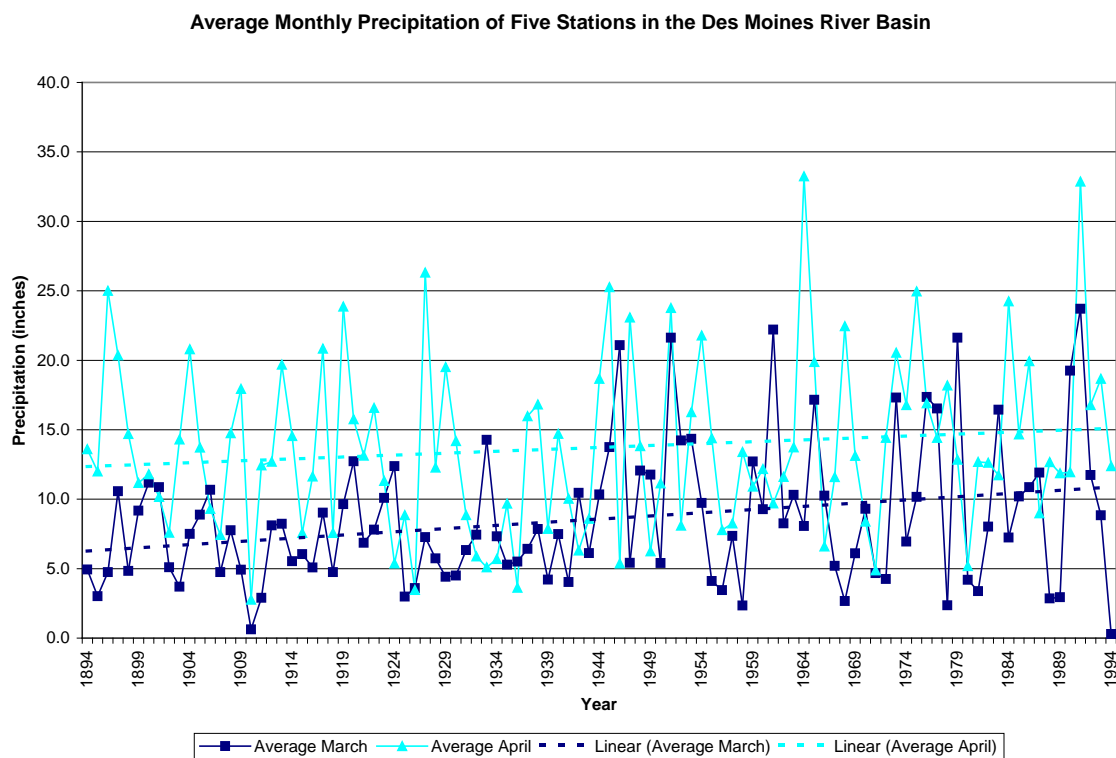


Figure 6.10: The average monthly precipitation for March and April for five stations in the Des Moines River basin.

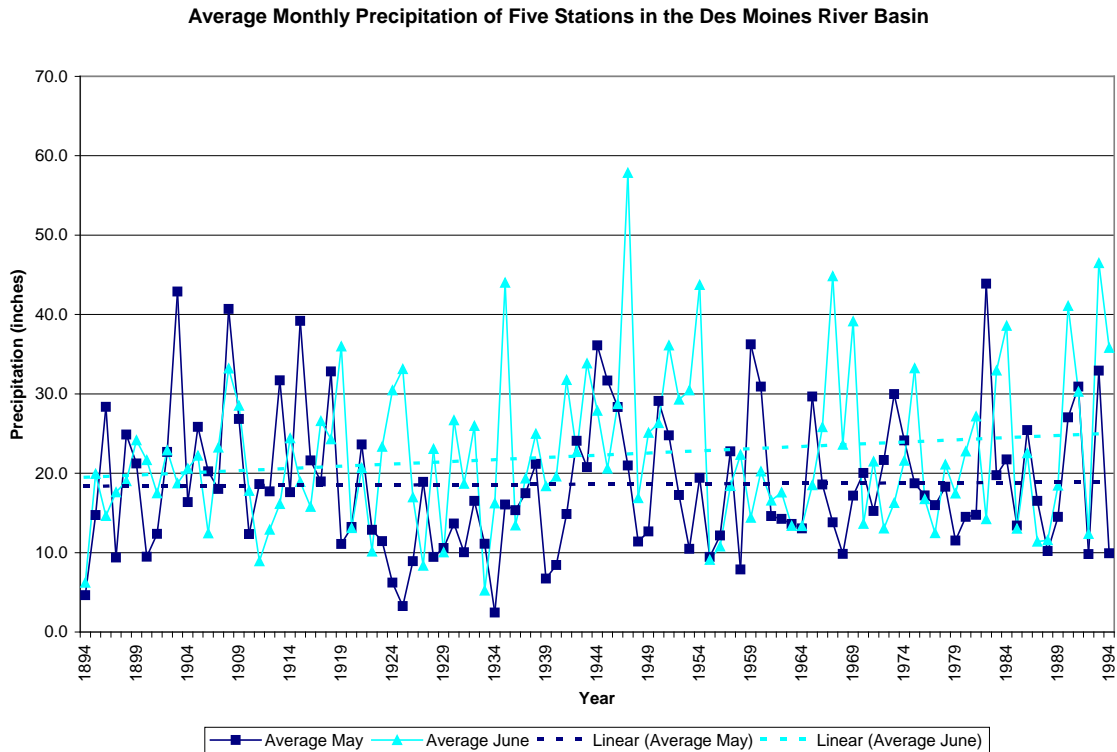


Figure 6.11: The average monthly precipitation for May and June for five stations in the Des Moines River basin.

6.6 References

- Baldwin, C. K., and U. Lall, 1998. Interannual-to-Century Scale Variation and Climatic Teleconnections: The Upper Mississippi River, Utah Water Research Laboratory working paper, Utah State University.
- Baldwin, C. K., and U. Lall, 1999. Seasonality of streamflow: the upper Mississippi River, *Water Resources Research* 35(4), 1143-54, 1999.
- Goldman, D. 1999, Memorandum for Record: 4/23/99. Hydrologic Engineering Center. U.S. Army Corps of Engineers.
- Helsel, D. R. and R.M. Hirsch, 1992. *Statistical Methods in Water Resources*, Elsevier, Amsterdam.
- Karl, T.R., C.N. Williams, Jr., F.T. Quinlan, and T.A. Boden, 1990. United States Historical Climatology Network (HCN) Serial Temperature and Precipitation Data, Environmental Science Division, Publication No. 3404, Carbon Dioxide Information and Analysis Center, Oak Ridge National Laboratory, Oak Ridge, TN.

- Knapp, H. V., 1994. Hydrologic Trends in the Upper Mississippi River Basin, *Water International* 19: 199-206.
- Knox, J.C., 1984. Fluvial responses to small scale climate changes, in *Developments and Applications of Geomorphology*, J.E. Costa and P.J. Fleisher (eds.), Springer-Verlag, Berlin.
- Lettenmaier, D. P., D. Ford, J. P. Hughes, and B. Nijssen, 1996. *Water Management Implications of Global Warming: 5. The Missouri River Basin*, Report to Interstate Commission on the Potomac River Basin and Institute for Water Resources, U.S. Army Corps of Engineers, Seattle, WA: DPL and Associates.
- Potter, K., 1991. Hydrologic Impacts of Changing Land Management Practices in Moderate-sized Agricultural Catchments. *Water Resources Research* 27(5): 845-855.
- Slack, J.R., and J.M. Landwehr, 1992. *Hydro-Climatic Data Network: A U.S. Geological Survey Streamflow Data Set for the Study of Climate Variations, 1874-1988*. U.S. Geological Survey Open-File Report 92-129.
- Slack, J.R., A.M. Lumb, and J.M. Landwehr, 1993. *Hydro-Climatic Data Network (HCDN): Streamflow Data Set, 1874-1988*. U.S. Geological Survey Water-Resources Investigation Report 93-4076.

7 Climate Variability and Flood Frequency Analysis

7.1 Need for Flood Frequency Analysis

Planners and the public require reliable estimates of flood-flow frequency relations to support flood risk management. Designs for flood control works, reservoirs, and other investigations need to reflect the likelihood or probability of large floods which affects the economic justification of such investments. Structural measures (including dams, levees, and channel modifications) can often reduce flood flows or stages and their consequences. Other flood risk management tools that address residual risk or probability of flooding include non-structural actions such as flood-proofing dwellings to mitigate damages, restricting development, and implementing flood warning and response measures. Whatever strategy is adopted, sound planning and system design benefit from accurate estimates of the probability distribution of floods. Such estimates allow a quantitative balancing of flood control efforts and the resultant benefits, and also enhance the credibility of flood plain development restrictions (Stedinger, 1999). In particular, FEMA is concerned with the development of floodplain maps that describe areas with particular probabilities of inundation. Similarly, the USACE is concerned with the economic justification of flood reduction and flood risk management alternatives that require calculation of the expected damages from flooding given alternative action plans. In river basins where human activities and natural processes have not resulted in significant changes in the distribution of floods, statistical procedures are commonly employed to estimate flood risk probabilities.

Early studies attempted to use the flood of record to define the floodplain and the design event for many planning activities. In terms of simplicity, it would be attractive to

use the stage of the largest flood ever observed to define the necessary height of levees and other flood reduction structures. However, the stage in a river for a given flow rate is dependent upon the depth of the channel and any restrictions imposed on the width of the river by levees, buildings, roads, bridges and other restrictions, both above and downstream of a site. Whereas the probability of different flow levels is generally thought not to change much with time, modification of river channels is a regular occurrence due both to man-made structures and natural processes (down cutting of channels, the accumulation of alluvium, changes in vegetation, and shifts in the location of channels and the geometry of bends and meanders). As a result, analysis of flood risk is generally based on historical river flows after adjustments for the effects of impounds such as reservoirs, and not a direct analysis of historical river stages.

One could attempt to base the definition of the floodplain on the largest flood flow of record, but then the implicit risk would depend upon the available record length. As a result, such an analysis would not provide a consistent standard, and would also be highly variable in that it depends upon the single largest event. In the United States, the floodplain for regulatory purposes is defined as that area with a 1% chance of being flooded in any year thereby providing a consistent standard for Federal and local flood risk management planning activities and restrictions on floodplain use across the country. However, most flood records are shorter than 100 years in length and as a result the largest flood of record may not be sufficiently extreme. Many sites do not even have streamflow gages to define the 1% chance exceedance flood. The flood flow defining the floodplain must be computed from some statistical analysis of regional hydrologic and meteorologic information.

To develop consistent and scientifically-justified estimates of various hypothetical floods, the engineering practice is to fit an analytical frequency distribution to the available record of flood flows. Fitting an analytical probability distribution to a flood series has several advantages over attempts to interpolate frequencies within a sample streamflow record. A fitted distribution provides both a compact and smoothed representation of the frequency distribution revealed by the available data which can support a range of engineering and economic computations. The increased precision of flood risk estimates obtained with efficient parameter estimation procedures improves the precision of computed estimates of flood risk. Fitting an analytical frequency distribution provides a systematic algorithm for interpolating within the frequency range provided by the data, and extrapolating to probabilities not represented by the empirical distribution. An agreed upon and reasonable procedure for systematic extrapolation to frequencies beyond the range of the data set is very important in floodplain management given the continuousness of restrictions and requirements placed on floodplain activities.

In the 1970's, the Water Resources Council developed uniform guidelines to be used by U.S. Federal agencies in flood frequency analyses adopting the log-Pearson Type 3 distribution (IACWD, 1982; Thomas, 1985). The log-Pearson type 3 distribution has three parameters: the mean, the standard deviation, and the coefficient of skewness of the logarithms of the flood flows. Several general approaches are available for estimating the parameters of a distribution. A simple approach is the method of moments recommended by Bulletin 17B for use in flood frequency analysis by Federal agencies in the United States. Regional hydrologic experience, as well as at-site historical and paleoflood information can provide additional sources of information about the distribution of floods

(Thomas and Benson, 1970; Tasker and Stedinger, 1986; Stedinger and Baker, 1987; Jin and Stedinger, 1988).

7.2 Climate Variability, Non-Stationarity, and Temporal Dependence

Bulletin 17-B, *Guidelines for Determining Flood Flow Frequency*, observes that traditional flood frequency analysis employs a "stationarity" assumption: "Necessary assumptions for a statistical analysis are that the array of flood information is a reliable and representative time sample of random homogeneous events" (IACWD, 1981, p. 6). The annual maximum peak floods are considered to be a sample of random, independent and identically distributed (iid) events. Thus one implicitly assumes that climatic trends or cycles are not affecting the distribution of flood flows in an important way.

Studies devoted to improving the methodology for flood frequency analysis continue to be based on the iid assumption (NRC, 1999). Current interest in climate change and its potential impacts on hydrology in general and on floods in particular calls into question the iid assumption (NRC, 1998). Whether flood frequency analysis should continue to be pursued employing the iid assumption is presently unresolved. A few studies have addressed the issue of nonstationarity, described as trend in flood flows over time. However, little attention has been given on whether to accept or reject the assumption of temporal independence.

A trend, positive or negative, has a beginning and an end. A sustained positive trend in the mean flood would in time become limited by the carrying capacity of the stream's drainage area and a sustained negative trend would in time render the stream dry. It is reasonable to assume that between these extreme situations, the slope of a positive (negative) trend decreases (increases) as the flood flow distribution approaches a new

regime. For hydrologic sequences, it is unlikely that such episodic behavior would have a fixed period. Trend assessment should be pursued in conjunction with exploration of flood-flow series persistence, which could result in flow series that include statistically significant trends.

Climate is a nonlinear dynamic system. Such nonlinear systems can exhibit apparently periodic behavior over an interannual time scale and/or slowly-varying episodic behavior over decades or centuries (NRC, 1998). Nonlinear systems such as the earth's climate system can follow similar patterns for many years, but these systems are capable of abrupt shifts. In addition to natural climatic variability, man is influencing the climate system by increasing the concentration of carbon dioxide and other greenhouse gases in the atmosphere, as well as changing land cover and associated fluxes of gases, water vapor and energy. This further increases the uncertainty associated with climate variables.

The objective of flood frequency analysis is to estimate the magnitude and probability of floods for approximately the next 30-50 years, which will depend on the prevailing climate during that period. The analysis generally assumes that future climate will be similar to past climate. One response to possible climate variability is to employ only the record for more recent years. In its discussion of such a proposal, a recent National Research Council (NRC) committee observed:

“At this time, given the limited understanding of the low frequency climate-flood connection, the traditional approach to flood frequency estimation entails a tradeoff between potential bias and variance. Bias arises from the use of long periods of record that are more likely to include time periods during which flood risk is different from that during the immediate planning period. On the other hand, longer periods of record allow the construction of risk estimators with less variance due to the larger sample with which the estimators are constructed.” (NRC, 1999)

The most serious problem would be if the nonlinear climate system determining flood risk were nonstationary and thus drifted over time without internal feedbacks that kept the variability from year-to-year within some bounds around a stable regime. In such a case, the past might be a poor guide to the future. A second concern, even if climate is stationary in a statistical sense, is the time scale over which natural variations in climate persist. Does the ebb and flow of climate variation have a short enough memory so that the historical flood distribution observed over the last 100 years is a good guide for the estimation of flood risk over the planning period? From year-to-year, the magnitude of the flood that occurs is highly variable. With modest records it would be very difficult to detect any systematic trend in the mean or the variances of floods from the random variation that might have occurred by chance. In fact, long records are needed to estimate reliably statistical parameters such as the mean and variances of flood flows.

7.3 Trends and Possible Future Flood Risk

The appropriate projection of flood risk across the planning period is complex if the presence of trends is accepted. In particular, one needs to consider how the increasing trend is to be extrapolated over the planning period, or if a constant mean and variance would be employed, implicitly assuming that the trend did not continue. McCuen et al. (1996) discuss several methods for performing flood frequency analysis with records exhibiting trends, including:

- (i) remove the trend in annual peaks and do frequency analysis on the residuals,
- (ii) employ a constant mean in distinct periods and adjust flood series using the relevant mean for each year, and

(iii) adjust peaks using some index of land use change.

With all three of these methods it is necessary to specify how changes in flood risk or land use indices will change over the planning period. Another method often employed on small watersheds is to use a calibrated watershed model with historical precipitation series to construct a homogeneous flood record reflecting future land use. These methods have been developed primarily for changes in land use in the watershed.

The implications of the fitted model of trend can be seen in an analysis of flood risk at the St. Louis gage. Figure 7.1 shows the fitted flood frequency using the whole data set (1861-1996) and from an analysis that modeled the distribution of flood peaks from a trend line. The trend lines describe the increase in the mean of the logarithms with time. The analysis implicitly assumes that the trend is linear and that the coefficient of variation of floods remains constant.

For this nonstationary model, the figure reports the resultant flood distribution for the year 1923 (in the middle of the period of record), for the year 2000 (corresponding to the present period), and for the year 2050 (corresponding to the end of a 50-year planning period). The increasing trend in the upper flood quantiles is apparent. The difference between the quantiles for 1923 and 2000 is about 10% at the 100-year flood level. The difference between the quantiles for the years 2000 and 2050 is another 10%. The standard error of the estimated flood quantile is on the order of 9-12%. Table 7.1 shows the results for the 10%, 1% and 0.2% chance exceedance floods for the estimate using the full data set and the estimates for the years 1923, 2000, 2050. Table 7.2 shows the percentage difference between the estimates correcting for trend. The difference between

the estimate for the year 2000 and the estimate using the entire record is about 7% for the 1% chance exceedance flood and 5.2% for the 0.2% flood.

Another way to deal with variations in flood risk is to fit a distribution using different period of records. Figure 7.2 shows the fitted distributions for the Mississippi River at St. Louis using the full period of record, the first half of the record, and the second half of the record. The parameters for these log Pearson III distributions are derived in a report from the Hydrologic Engineering Center (1998a). If there is an increasing trend at St. Louis, then the second half of the record would have more flood risk than the first. Table 7.2 shows the estimates of the 10%, 1%, and 0.2% chance exceedance floods using the three different data sets. Table 7.4 shows the percentage difference from using half of the record and using the full record. The difference for the 1% exceedance flood between the second half of the record and the entire record is about 8%. The difference between the first and second half of the record is 17%.

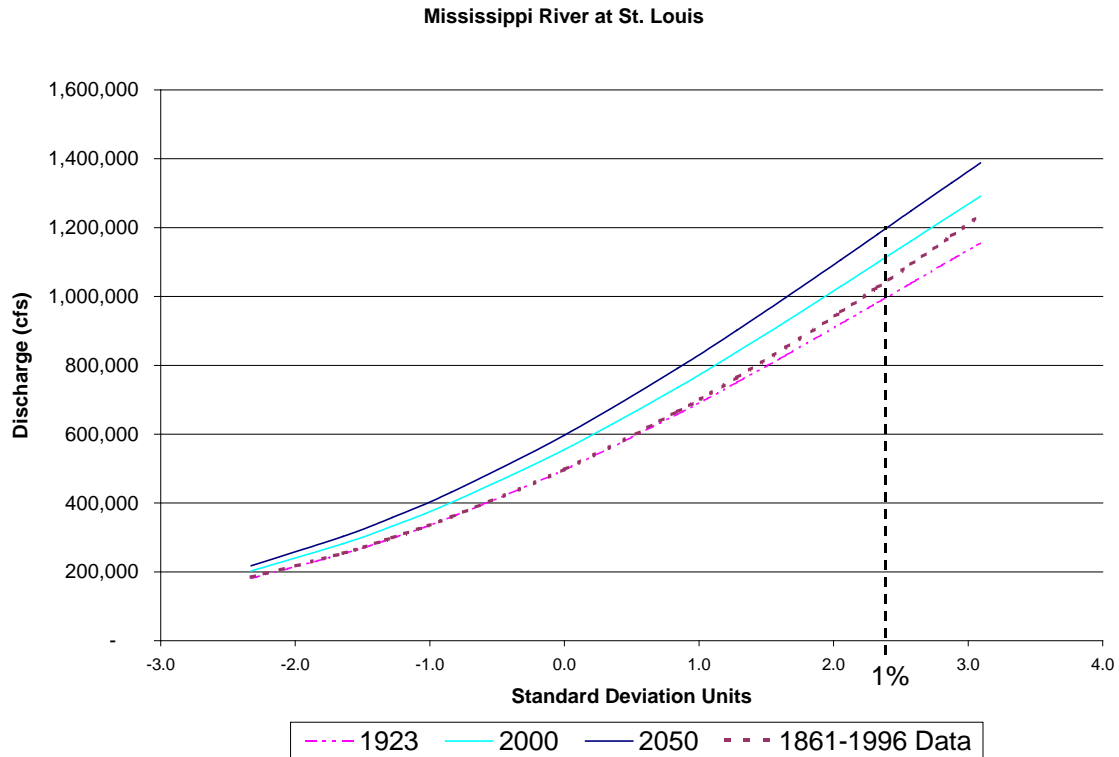


Figure 7.1: Different distributions for flood risk at St. Louis obtained by using the entire 1861-1996 record, and by correcting for trend and then estimating the specific distribution of floods for the years 1923, 2000, and 2050. The dotted vertical line corresponds to the 1 percent chance risk level.

Table 7.1: Estimates of 10%, 1%, and 0.2% chance exceedance flood at St. Louis. [Based upon a LP3 fit to the record using log-space moments. No low-outlier correction was made. At-site skew employed.]

Period	10% Chance Exceedance Flood	1% Chance Exceedance Flood	0.2% Chance Exceedance Flood
<i>1861-1996</i>	765,000	1,026,000	1,176,000
<i>For 1923</i>	750,000	982,000	1,107,000
<i>For 2000</i>	839,000	1,098,000	1,238,000
<i>For 2050</i>	902,000	1,181,000	1,331,000

Table 7.2: The percentage difference between the 10%, 1%, and 0.2% chance exceedance flood for the entire period of record and quantiles corrected for trend and estimated for the years 1923, 2000, and 2050.

Period	10% Chance Exceedance Flood	1% Chance Exceedance Flood	0.2% Chance Exceedance Flood
For 1923	-1.9%	-4.3%	-5.9%
For 2000	9.7%	7.0%	5.2%
For 2050	18%	15%	13%

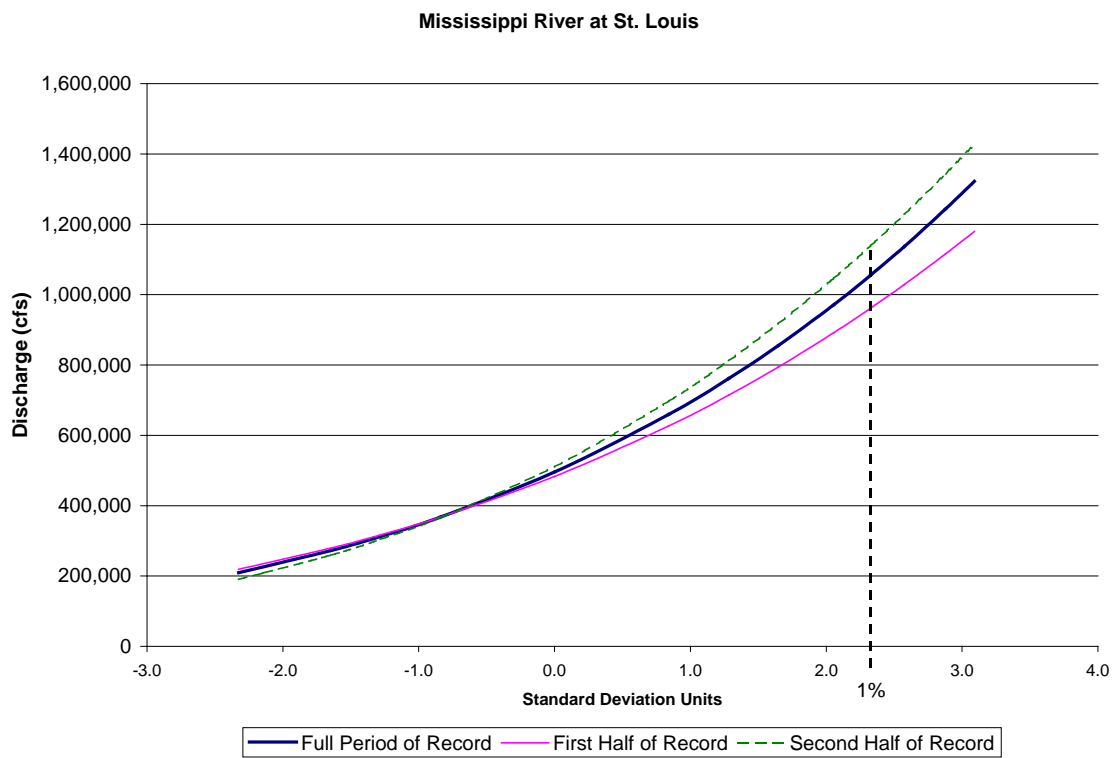


Figure 7.2: A graph showing a log Pearson III (corrected for low outliers) for the Mississippi River at St. Louis using the full period of record, the first half of the record, and the second half of the record.

Table 7.3: Estimates of 10%, 1%, and 0.2% chance exceedance flood at St. Louis using a LP3 (corrected for low outliers) using the full period of record, the first half of the record, and the second half of the record.

	10% Chance Exceedance Flood	1% Chance Exceedance Flood	0.2% Chance Exceedance Flood
<i>Full Period</i>	761,000	1,055,000	1,243,000
<i>First Half of Record</i>	715,000	961,000	1,116,000
<i>Second Half of Record</i>	812,000	1,139,000	1,343,000

Table 7.4: The percentage difference between the estimates of the 10%, 1%, and 0.2% chance exceedance flood using the first and second half of the record and the estimate using the full period of record.

	10% Chance Exceedance Flood	1% Chance Exceedance Flood	0.2% Chance Exceedance Flood
<i>First Half of Record</i>	-6.1%	-8.9%	-10.3%
<i>Second Half of Record</i>	6.7%	8.0%	8.0%

The apparent variation in flood risk over time is one of many factors causing uncertainty in the flood estimates. Table 7.5 shows the 90% confidence intervals for the 10%, 1%, and 0.2% chance exceedance flood at St. Louis using the full period of record. The confidence interval is computed using three different assumptions: (i) the distribution is lognormal; (ii) the distribution is log Pearson III with known skew; (iii) the distribution is log Pearson III with estimated skew (Chowdhury and Stedinger, 1991). For the 1% chance exceedance flood using a log Pearson III with estimated skew, the confidence interval is -11% to +12%. As Goldman (1999) notes, a probability distribution is only an approximate description of the mechanisms causing annual floods. He notes that “the presence of a small trend may make this approximate description less accurate, but still useful given no viable alternative.”

Table 7.5: Uncertainty Analysis for lognormal, log Pearson III with known skew, and log Pearson III with estimated skewness coefficient: percentage deviation from quantile estimator.

	10% Chance Exceedance Flood		1% Chance Exceedance Flood		0.2% Chance Exceedance Flood	
	Lower CI	Upper CI	Lower CI	Upper CI	Lower CI	Upper CI
Lognormal	-6%	7%	-9%	10%	-11%	12%
Log Pearson III Known Skew	-6%	6%	-8%	9%	-10%	11%
Log Pearson III Estimated Skew	-6%	6%	-11%	12%	-15%	18%

7.4 References

Chowdhury, J. U., and J. R. Stedinger 1991. Confidence Interval for Design Floods with Estimated Skew Coefficient, *Journal of Hydrology*, 117(7): 811-829.

Goldman, D. 1999, Memorandum for Record: 4/23/99. Hydrologic Engineering Center. U.S. Army Corps of Engineers.

Hydrologic Engineering Center (HEC), 1998a. "An Investigation of Flood Frequency Estimation Methods for the Upper Mississippi Basin," U.S. Army Corps of Engineers, 4/27/98, Davis, CA.

Hydrologic Engineering Center (HEC), 1998b. "Flood Distribution Selection Upper Mississippi, Lower Missouri, and Illinois River Flow Frequency Study," U.S. Army Corps of Engineers, Status Report November, 1998, Davis, CA.

Interagency Committee on Water Data (IACWD), (Bulletin 17-B of the Hydrology Committee originally published by the Water Resources Council), 1981. *Guidelines for Determining Flood Flow Frequency*, Washington DC: U.S. Government Printing Office.

Jin, M., and J.R. Stedinger, 1989. Flood Frequency Analysis with Regional and Historical Information, *Water Resources Research*, 25(5), 925-936.

McCuen, R.H., W.O. Thomas, Jr., and A.R. Montgomery, 1996. Effects of Watershed Change on Flood Data, manuscript, University of Maryland, College Park, MD.

National Research Council, (NRC), Panel on Climate Variability on Decade-to-Century Time Scales; Board on Atmospheric Sciences and climate; commission on Geosciences, Environment, and Resources, 1998. *Decade-to-Century-Scale*

- Climate Variability and Change A Science Strategy*, Washington, D.C.: National Academy Press.
- National Research Council, (NRC), Committee on American River Flood Frequencies, Water Science and Technology Board, 1999. *Improving American River Flood Frequency Analysis*, Washington, D.C.: National Academy Press.
- Stedinger, J.R. and V.R. Baker, 1987. Surface Water Hydrology: Historical and Paleoflood Information, U.S. National Report to International Union of Geodesy and Geophysics 1983-1987, *Reviews of Geophysics and Space Physics*, 25(2), 119-124.
- Stedinger, J.R., 1999. Flood Frequency Analysis and Statistical Estimation of Flood Risk, Chapter 12, *Inland Flood Hazards: Human, Riparian and Aquatic Communities*, E.E. Wohl (ed.), Cambridge University Press, Stanford, United Kingdom, 1999.
- Stedinger, J.R., and T.A. Cohn, 1986. Flood Frequency Analysis With Historical and Paleoflood Information, *Water Resources Research*, 22(5): 785-793.
- Stedinger, J.R., R.M. Vogel and E. Foufoula-Georgiou, 1993. Frequency Analysis of Extreme Events, Chapter 18, *Handbook of Hydrology*, D. Maidment (ed.), McGraw-Hill, Inc., New York.
- Tasker, G.D., and J.R. Stedinger, 1986. Estimating Generalized Skew With Weighted Least Squares Regression, *Journal of Water Resources Planning and Management*, 112(2), 225-237.
- Thomas, D.M., and M.A. Benson, 1970. Generalization of Streamflow Characteristics from Drainage-Basin Characteristics, U.S. Geological Survey Water-Supply Paper 1975.
- Thomas, W.O., 1985. A uniform technique for flood frequency analysis, *Journal of Water Resources Planning and Management*, 111(3), 321-337.

8 Conclusions

- For the more recent period (1950-1996), El Niño events appear to be associated with larger floods and La Niña events with smaller peak annual floods, but there is relatively little relationship between the two over the longer period (1868-1996). As long as the future frequency and intensity of El Niño events over time resemble the historical pattern, traditional flood frequency analysis will account for this intra-decadal climate variability.
- Further research is needed on the relationship between interdecadal climate signals, and Upper Mississippi and Missouri floods. These patterns or departures from longer-term averages have more effect on uncertainty in flood frequency estimates than interannual variability such as El Niño oscillations. Based on a simple regression analysis with interaction terms, climate indices associated with El Niño/Southern Oscillation, the Pacific Decadal Oscillation and the North Atlantic Oscillation could explain only a small percentage of the variability in the annual maximum floods.
- Simulations using GCM scenarios of future climate with increased carbon dioxide levels generally project lower average monthly flows for the Lower Missouri River. Simulations of Upper Mississippi streamflow using GCM scenarios will be conducted in the next phase of the study. At this time there is little evidence that flood frequencies will increase as a result of global warming. Furthermore, the General Circulation Model projections of future climate are highly uncertain.

- The percentage of total annual precipitation falling as 2 inches or greater one-day rainfall events is increasing in the United States. This amount of rainfall, however, is usually not sufficient to cause increased flooding, since it occurs almost every year. The timing of the increased extreme precipitation is also important. Extreme rainfall in the late summer or autumn has less likelihood of causing flooding due to lower antecedent soil moisture. In addition, average annual temperatures have increased about 0.25°C in the past 40 years. Higher temperatures raise potential evapotranspiration which may lower antecedent soil moisture conditions. Lins and Slack found that the contiguous United States was becoming wetter but less extreme. Only 11 percent of the stations they examined in the United States had a significant trend at the 5% level in the annual maximum flow and the number of uptrends and downtrends was approximately equal.
- There is evidence that flood risk has changed over time for sites where the 1993 flood was the flood of record, particularly at and below Hannibal, Missouri. This increased flood risk challenges the traditional assumption that flood series are independent and identically distributed random variables. This raises concerns that flood risk during the planning period will be underestimated if the entire flood record is used as the basis of projections of future flood risk.
- It is not clear how to accommodate the change in flood risk within traditional flood frequency analysis. In the absence of viable alternatives the use of traditional Bulletin 17B procedures are warranted until better methods are developed.

- Research is needed on how to incorporate interdecadal variation in flood risk into flood frequency analysis so that state and federal water agencies can move to adopt procedures that appropriately reflect such variations when it is documented.

9 Appendix A: Data Sources

Annual Floods: Hydrologic Engineering Center (HEC); Flow Frequency Study Data (unimpaired flow values);

Seasonality of Floods: United States Geological Survey (USGS); direct gage readings:
<http://water.usgs.gov>

Daily Flow: United States Geological Survey (USGS); direct gage readings:
<http://water.usgs.gov>

El Niño Sea Surface Temperature (SST): Japan Meteorological Agency (JMA); available from Center for Ocean-Atmospheric Predictions Studies, Florida State University <http://www.coaps.fsu.edu/research/ENSO.shtml>

North Atlantic Oscillation (NAO): Climate Research Unit, University of East Anglia:
<http://www.cru.uea.ac.uk/cru/data/nao.htm>

Pacific Decadal Oscillation (PDO): International Pacific Halibut Commission, University of Washington:
<http://www.iphc.washington.edu/PAGES/IPHC/Staff/hare/html/decadal/post1977/pdo1.html>

Southern Oscillation Index (SOI): National Oceanographic and Atmospheric Administration Climate Prediction Center (NOAA-CPC):

<http://nic.fb4.noaa.gov:80/data/cddb/cddb/soi>

Other Climate Indices (PNA, PT, NP, etc.): National Oceanographic and Atmospheric Administration Climate Prediction Center (NOAA-CPC):

<http://nic.fb4.noaa.gov:80/data/teledoc/telecontents.html>

10 Appendix B: Abbreviations and Acronyms

2 X CO ₂	Doubling of atmospheric Carbon Dioxide
°C	Degrees Celsius
cfs	Cubic Feet per Second
CH ₄	Methane
cms	Cubic Meters per Second
CNP	Central North Pacific index
CO ₂	Carbon Dioxide
CPC	Climate Prediction Center
ENSO	El Niño/Southern Oscillation
EP	East Pacific pattern
GCM	General Circulation Model
GFDL	Geophysical Fluid Dynamics Laboratory
GFTR	Geophysical Fluid Dynamics Laboratory Transient GCM
HCTR	Hadley Center (UKMO) Transient GCM
HEC	Hydrologic Engineering Center
HP	High Plains region
IA	Iowa
IACWD	Interagency Committee on Water Data
IL	Illinois
IPCC	Intergovernmental Panel on Climate Change
KS	Kansas
LOESS	Locally-weighted least squares regression; a technique for smoothing time series data
LP3	Log Pearson III probability distribution
MCC	Mesoscale Convective Complex
MCC	Midwestern Climate Center
MCS	Mesoscale Convective System
mi ²	Square Miles
mm	Millimeters
MN	Minnesota
MO	Missouri
MPI	Max Planck Institute
MPTR	Max Planck Institute Transient GCM
N ₂ O	Nitrous Oxide
NAO	North Atlantic Oscillation
NB	Nebraska
NIN	An El Niño index based on sea surface temperature
NOAA	National Oceanographic and Atmospheric Administration
NP	North Pacific index
NPPI	North Pacific sea level Pressure Index
NRC	National Research Council
p	Probability of obtaining the test statistic, or one less likely, when the null hypothesis is true

PDO	Pacific Decadal Oscillation
PET	Potential Evapotranspiration
PNA	Pacific/North American pattern
ppmv	Parts Per Million by Volume
PT	Pacific Transition pattern
r	Correlation Coefficient
R ²	Coefficient of determination, or the fraction of the variance explained by regression
SAST	Scientific Assessment and Strategy Team
SOI	Southern Oscillation Index
sq. mi.	Square Miles
SST	Sea Surface Temperature (Refers to sea surface temperatures in the eastern tropical Pacific Ocean)
TNH	Tropical/Northern Hemisphere pattern
UKMO	United Kingdom Meteorological Office
UMRCBS	Upper Mississippi River Comprehensive Basin Study
USACE	U.S. Army Corps of Engineers
USGS	U.S. Geological Survey
VIC-2L	Variable Infiltration Capacity 2-Layer model
WI	Wisconsin
WP	West Pacific oscillation
ρ	Correlation Coefficient
α	Significance level, the probability of incorrectly rejecting the null hypothesis when it is in fact true

11 Appendix C: Nonparametric Trend Analysis at Selected Sites

Jery R. Stedinger

Tables 6.1 through 6.6 report the results of a trend analysis using linear regression. A nonparametric analysis of the frequency of large floods also supports the conclusion that the risk of large floods seems to have been increased. A summary appears in Table C-1 below. The pattern is clearest for Hannibal at the lower end of the Upper Mississippi. In the 56 years from 1941-1996 after the dry 1930's, a threshold of 300,000 cfs was crossed 17 times -- however in the earlier 62 years from 1879-1940, no floods are recorded that exceeded 300,000 cfs. Thus, even though the two periods are of roughly equal length, all 17 floods in excess of 300,000 cfs occurred in the second half of the record. That such a result (all 17 floods occur in the second 56-year period) is due to chance has a probability of less than one-in-a-100,000 (one-sided hypergeometric test).

At Hermann on the lower Missouri, the three largest floods, and the only floods to even approach 1,000,000 cfs, all occurred in the last decade. Overall 12 floods exceeded a threshold of 500,000 cfs in the 57 year period from 1941-1997, whereas only 3 floods exceeded 500,000 cfs in the 43 years from 1898-1940. That such a result (12 or more of the 15 floods in excess of 500,000 cfs fall in the second period) is due to chance has a probability of 5% (one-sided hypergeometric test).

The St. Louis record is unusual. The last decade has the two largest floods of record. And the 1993 event is 20% larger than anything that occurred before. Consider again the division of floods before and after 1940. At St. Louis in the 56 year period from 1941-1996 some 22 floods exceeded a threshold of 600,000 cfs, whereas in the 80 years from 1861-1940, 21 floods exceeded 600,000. That such a result is due to chance has a

probability of 7.8% (one-sided hypergeometric test). In fact, during the recent 20 years from 1977-1996, 11 annual floods exceeded 600,000 cfs, whereas during the 40 years from 1861-1900 that threshold was crossed only 9 times! This result is significant at the 1.4% level (using a one-sided hypergeometric test).

Table C-1: Statistical Analysis of Large Flood Occurrences*

Gage	Threshold (csf)	Floods after 1941	Flood before 1940	Years after 1941	Years before 1940	Significance Level of Test
Hannibal	300,000	17	0	56	62	$< 10^{-5}$
Hermann	500,000	12	3	57	43	0.045
St. Louis	600,000	22	21	56	80	0.078
St. Louis	600,000	11 [#]	9 [#]	20	40	0.014

*The test considered the number of floods above the indicated threshold from 1941 through the end of the record, and from the beginning of the record through 1940. Columns 3 and 4 report the number of floods in each period. Columns 5 and 6 report the number of years in each period. A one-sided significance or P-value for each case is computed using a hypergeometric to determine the probability that a given total number of large floods would by chance be randomly distributed to yield the observed division, or one more extreme.

[#]This special case considers the periods of 1977-1996 versus 1861-1900 to illustrate how different the frequencies of large floods were before the turn of the century and in the last two decades.